INTERSTELLAR REDDENING IN THE GALAXY

by

KASHI NATH NANDY

A Thesis presented for the Degree of
Doctor of Philosophy
of the University of Edinburgh
in the Faculty of Science

ROYAL OBSERVATORY,
EDINBURGH,

August, 1964.

ABSTRACT

Objective prism spectra obtained with the 16/24/60-inch Schmidt telescope have been used for an investigation of the wavelength dependence of interstellar absorption in the spectral range from 8000A to 3450A, in a region of 30 square degrees in Cygnus centred on (20^h15^m, 38^o). Monochromatic magnitude differences have been measured at 24 wavelengths for 28 pairs of stars down to magnitude V = $10^m.0$.

The mean reddening curves derived separately for O- and early B-type stars do not differ by more than 5 per cent. The reddening law in the direction of Cygnus does not change by more than 3 per cent over distances out to 2 - 2.5 kpc. The intrinsic r.m.s. dispersion about the mean reddening curve is less than 3 per cent.

Since there is no significant intrinsic dispersion, no significant distance dependence and no significant difference between the reddening curves for O- and B- stars, all the available observational data in the Cygnus region have been used to give a weighted mean reddening curve with a mean standard error of $\pm$0.8 per cent. Over the observed wavelength range the reddening curve can be represented by two straight lines, intersecting at about 4300A.

C O N T E N T S

CHAPTER IV - RESULTS FOR CYGNUS

LIST OF FIGURES

LIST OF TABLES

INTRODUCTION

The work presented in this thesis is a contribution to our knowledge of interstellar reddening.

For more than a century astronomers suspected the presence of obscuring material in interstellar space, but could not detect it. Around 1930, it became clear that clouds of dust and gas in the plane of the Milky Way absorb and redden the light of distant stars and clusters. As a result of this discovery, the calculated dimensions of the Galaxy had to be reduced. Knowledge of interstellar absorption was thus clearly essential to any investigation of galactic structure.

The basic problems connected with the studies of interstellar absorption are (1) to determine the reddening law, and (2) to study the variation of this law with position in the Galaxy.

Whether or not there is a unique reddening law is of fundamental importance for the study of both galactic structure and properties of the interstellar medium. To determine the absolute value of the total absorption is a difficult matter. If the reddening law is everywhere the same, accurate colour measurements over a short wavelength interval can be used to set the scale of the reddening curve and a ratio of the colouring effect of the medium to the total absorption at some particular

wavelength can be established on the basis of the observed reddening law. This ratio serves a useful measure for correcting distances for interstellar absorption. It is not yet known exactly how uniform the properties of the interstellar medium are, so that a universal reddening law cannot be assumed.

It is now believed that interstellar matter in the form of gas and dust particles constitutes 2% of the total mass of our Galaxy and is being constantly depleted in the process of star formation. As a consequence of nuclear processes occurring within stars, some matter enriched in heavier elements is returned to the interstellar medium. Consequently its mean chemical composition changes with time. The mass of the dust particles which absorb starlight is less than 1 per cent of that of the gas.

The wavelength dependence of interstellar absorption is the basic observational data for the construction of a model of the dust particles. Observed interstellar polarisation and the assumption that polarisation and reddening are produced by the same particles have given rise to a variety of speculations on the models for the particles. The theory which is at present considered to be most likely, predicts that a uniform reddening law cannot be expected.

The published observational results can be

summarised by saying that while spectrophotometric observations indicate a close approach to uniformity of the reddening law, the UBV photometry of galactic O and B stars suggests a general variability of this law.

UBV photometry has been extended to a large number of early type stars mostly between 8th and 10th magnitude; but a serious criticism against broad band filter photometry in connection with studies of the interstellar reddening law is that the effective wavelengths of the filters are not accurately known parameters. Also the derivation of the reddening law from multicolour photometry depends on an accurate knowledge of the intrinsic colours of stars. UBV photometry is therefore not suitable for elucidating the extinction law.

A more direct method of obtaining the reddening law is to compare the spectral energy distributions of reddened and unreddened stars of identical spectral types. Until now, spectrophotometric studies for the investigation of the wavelength dependence of interstellar absorption have been limited to a few bright moderately reddened stars scattered in different parts of the galactic plane. In any given region in space, not enough stars have been studied spectrophotometrically to determine the intrinsic scatter in the derived reddening curve. Study of the variation in the reddening law has

been confined to a limited range of wavelength in the visible and ultraviolet. Moreover, a source of error in the method of deriving the reddening curve from the comparison of a reddened and unreddened star is uncertainty in spectral classification. As a result of an error of ± 1 subclass in spectral type of B stars, the ultraviolet part of the reddening curve derived from a single pair of stars is found to be in error by more than 15 per cent. The error due to uncertainty of spectral types being larger than photometric errors, whether photographic or photo-electric, is predominant and can only be reduced by increasing the number of pairs of stars being compared. Therefore a large number of stars observed photographically gives a more accurate mean reddening curve than a small number observed photo-electrically.

The object of the present work is (1) to extend spectrophotometric observations in the Cygnus region to stars as faint as $11^{m}.0$ in the wavelength range 3400A to 8000A, (2) to improve the accuracy of the mean reddening curve by considering a large number of stars in this region, and (3) to determine the cosmic dispersion in the reddening curve.

Observations have been extended to six regions in different directions and similar investigations are to

follow, the ultimate aim being to make a systematic survey of the reddening law as a function of wavelength and position in the Galaxy.

The programme has been carried out at this Observatory with the 16/24-inch Schmidt telescope in conjunction with a low-dispersion objective prism and grating.

Objective prism spectrophotometry with a Schmidt telescope has the advantage that information can be obtained about a large number of stars over a wide wavelength range in narrow band widths at many accurately determined wavelengths.

Chapter 1 contains a brief review of published works in this field. The observations and the methods of reduction are described in Chapters 2 and 3 respectively. Chapter 4 describes the results of the investigation of stars in the Cygnus region.

As a by-product of this work, relative monochromatic magnitudes at twenty wavelengths between 8000A and 3400A for 218 stars have been derived and are given in the Appendix.

CHAPTER I

LITERATURE REVIEW

1.1 Early History

Around 1920 it was a puzzling problem in Astronomy that the colours of B-type stars were systematically either too red or too blue [Russell (1919), Struve (1926)]. Halm's (1917) suggestion was that the colour-temperature of starlight decreased gradually on its way through space. His results could have been interpreted as a "$\frac{1}{\lambda}$ - law" of interstellar reddening. But the paradox that the interstellar reddening and temperature reddening follow similar laws was not immediately solved through spectrophotometric studies.

The study of galactic star clusters by Trumpler (1930a) played an important part in our understanding of the role of the interstellar medium in our galactic system. He found that the linear sizes of clusters deduced from angular sizes and distances were on the average larger for the more distant galactic clusters than for the nearer ones. He reasoned that the apparently increased size of the distant clusters was not real but was due to the cumulative effect of the dimming of starlight, which caused the distances to be over-estimated. He postulated that in the neighbourhood of the galactic plane there exists a very thin layer of

absorbing matter. Trumpler (1930b) further observed that stars belonging to the same spectral type had colour indices larger than their intrinsic colour indices. This led him to conclude that interstellar absorption is selective with respect to wavelength. His (1930c) spectrophotometric comparison of distant and nearby stars of the same type in a limited wavelength range showed that the absorption does not follow Rayleigh's scattering, but is nearly proportional to wave number. Similar conclusions were reached by Struve, Keenan and Hynek (1934), Rudnick (1936) and Greenstein (1938). Hall (1937) and Stebbins, Huffer and Whitford's (1939) photo-electric work established that as a first approximation absorption is proportional to wave-number over a wide spectral range.

1.2 Observational Terms

Let $A(\lambda)$ be the absorption of the starlight expressed in magnitude, the apparent magnitude $m(\lambda)$ is given by

$$m(\lambda) = M(\lambda) + 5 \log r - 5 + A(\lambda) \qquad (1)$$

where $M(\lambda)$ is the absolute magnitude and r is the distance expressed in parsecs.

For a different wavelength λ^1

$$m(\lambda^1) = M(\lambda^1) + 5 \log r - 5 + A(\lambda^1) \qquad (2)$$

The colour-excess $E(\lambda, \lambda^1)$ is the difference between apparent and intrinsic colour-index. Thus,

$$E(\lambda, \lambda^1) = A(\lambda) - A(\lambda^1) \qquad (3)$$

The ratio of total absorption to selective absorption is then defined as

$$R = \frac{A(\lambda)}{A(\lambda) - A(\lambda^1)} \qquad (4)$$

When a reddened star is compared to a similar unreddened star, $A(\lambda)$ will be given by

$$A(\lambda) = m(\lambda) - m_o(\lambda) - 5 \log \frac{r}{r_o} \qquad (5)$$

where $m_o(\lambda)$ and r_o denote the terms corresponding to the unreddened comparison star.

If there were no absorption, the differences in magnitude of the two stars would have been independent of wavelength. The monochromatic magnitude differences as a function of wavelength are therefore attributed to

the wavelength dependence of interstellar absorption. The curve showing the monochromatic magnitude differences plotted against $1/\lambda$ is usually referred to as the "reddening curve". Each pair of stars gives a different reddening curve, since the absorption varies from one pair to another. For comparison of the reddening curves derived from different pairs, monochromatic magnitude differences are normalised to a certain standard total absorption.

O- and early B-type stars are particularly suitable for the study of interstellar reddening because of (i) their easily defined continua, (ii) their large ultra-violet radiation as compared to A and later type stars, and (iii) the negligible effect of absolute magnitude on their colours. Featureless spectra of these early type stars permit the use of fairly wide band filters.

1.3 Observational Results

1.31 The reddening law from the comparison of pairs of stars

Important progress in the study of the reddening law was made by Stebbins and Whitford (1943) who measured photo-electrically the magnitudes of stars in six fairly broad spectral regions in the wavelength range from 10,300A to 3530A. They derived the reddening curves for 30 pairs of early type stars distributed over different galactic longitudes and studied the deviation from the "$1/\lambda$ -law" of absorption for different pairs of stars. In all cases the direction and magnitudes of deviations from the "$1/\lambda$ -law" were found to be the same. Finally, they concluded that the reddening law is, in general, uniform. Whitford (1948) extended the study to 21,000A by using a lead sulphide photo-conductive cell in his observations of four pairs of stars and Stebbins [Whitford (1948)] obtained measurements at λ = 3200A on the pair of ζ and ϵ Persei. Combining these data with the results of the six-colour photometry, they derived a mean reddening curve. Although the curve follows approximately a "$1/\lambda$ -law" in the red, visible and blue, it shows a continuous change of slope and deviates considerably from the "$1/\lambda$ -law" in the ultra-violet and in the infra-red. The inverse curvature in the infra-red indicates an approach to the "λ^{-4} law".

From objective-prism spectra extending from 6350A to 3900A, Schalén (1952) studied the reddening law in regions in Cygnus and Cepheus. Later the wavelength range was extended to 8500A [Schalén (1957)].

Schalén found that for some stars in the Cepheus region, absorption in the red is abnormally small in comparison with the absorption in the blue and violet regions. However, his general conclusion [Schalén (1959, 1964)] is that there are no certain indications of any significant variation in the reddening law in the directions of Cygnus, Cepheus and Cassiopeia, although minor local variations may exist. But Schalén (1952) found large differences between his results and those by Stebbins and Whitford (1943). Similar deviations from the results of six-colour photometry were also found by van Rhijn (1953) and Borgman (1954). Such differences are attributed to errors in the adopted effective wavelengths of the six-colour photometry.

From spectrophotometric studies in the wavelength range 6100A to 3130A of 20 widely distributed reddened stars in a narrow range of spectral type, Divan (1954) arrived at the conclusion that the reddening law is uniform. But the mean reddening curve which Divan derived from Cygnus stars shows considerable differences from Stebbins and Whitford's (1943, 1948)

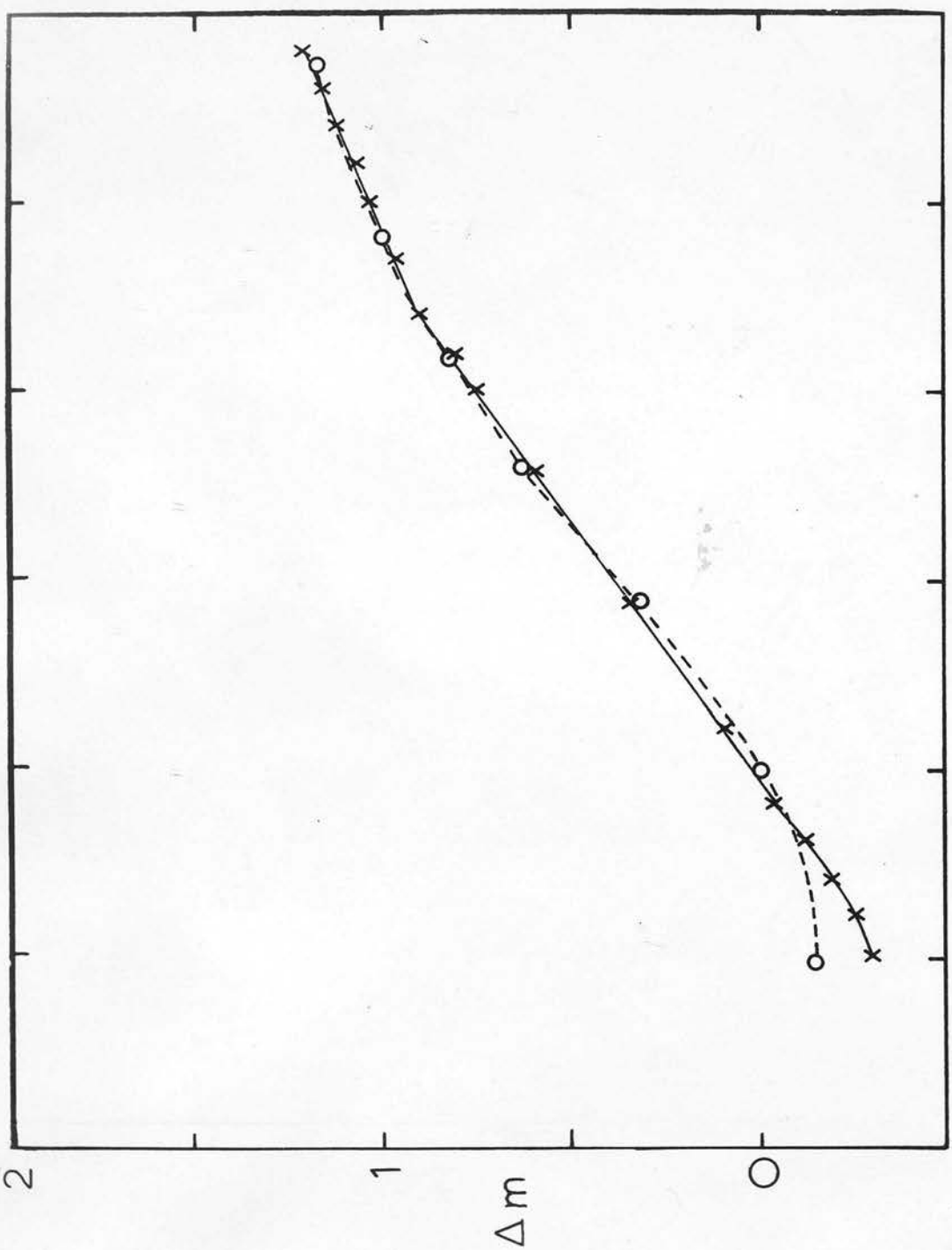

Fig.1 Comparison of Whitford's (1958) result, denoted by crosses, with that of six-colour photometry [Whitford (1948)], denoted by circles.

mean reddening curve. For shorter wavelength Divan's reddening curve is more linear and has a greater slope than Stebbins and Whitford's mean curve. She pointed out that a small difference in the spectral type of a star, a B-star in particular, causes an appreciable variation of the amount of Balmer discontinuity and must be taken into account in the derivation of the ultra-violet part of the reddening curve.

Whitford (1958) has shown that filter corrections, according to King's (1952) method, bring the measures of six-colour photometry into better agreement with the measures derived by other methods. Using a photo-electric spectrum scanner developed by Code (1954) he compared five pairs of stars over the same wavelength range as that of six-colour photometry. From scanner data of three well observed pairs of Cygnus Rift stars, and from observations with a lead sulphide photo-conductive cell of five pairs of stars, he derived a definitive reddening curve over the interval $1/\lambda = .48\,\mu^{-1}$ to $1/\lambda = 3.0\,\mu^{-1}$.

In Fig. 1 Whitford's (1958) curve is reproduced and compared with Stebbins and Whitford's [Whitford (1948)] mean curve. Significant difference exists between these two curves in two respects:

(1) In the wavelength range from 10,300A to 3,530A

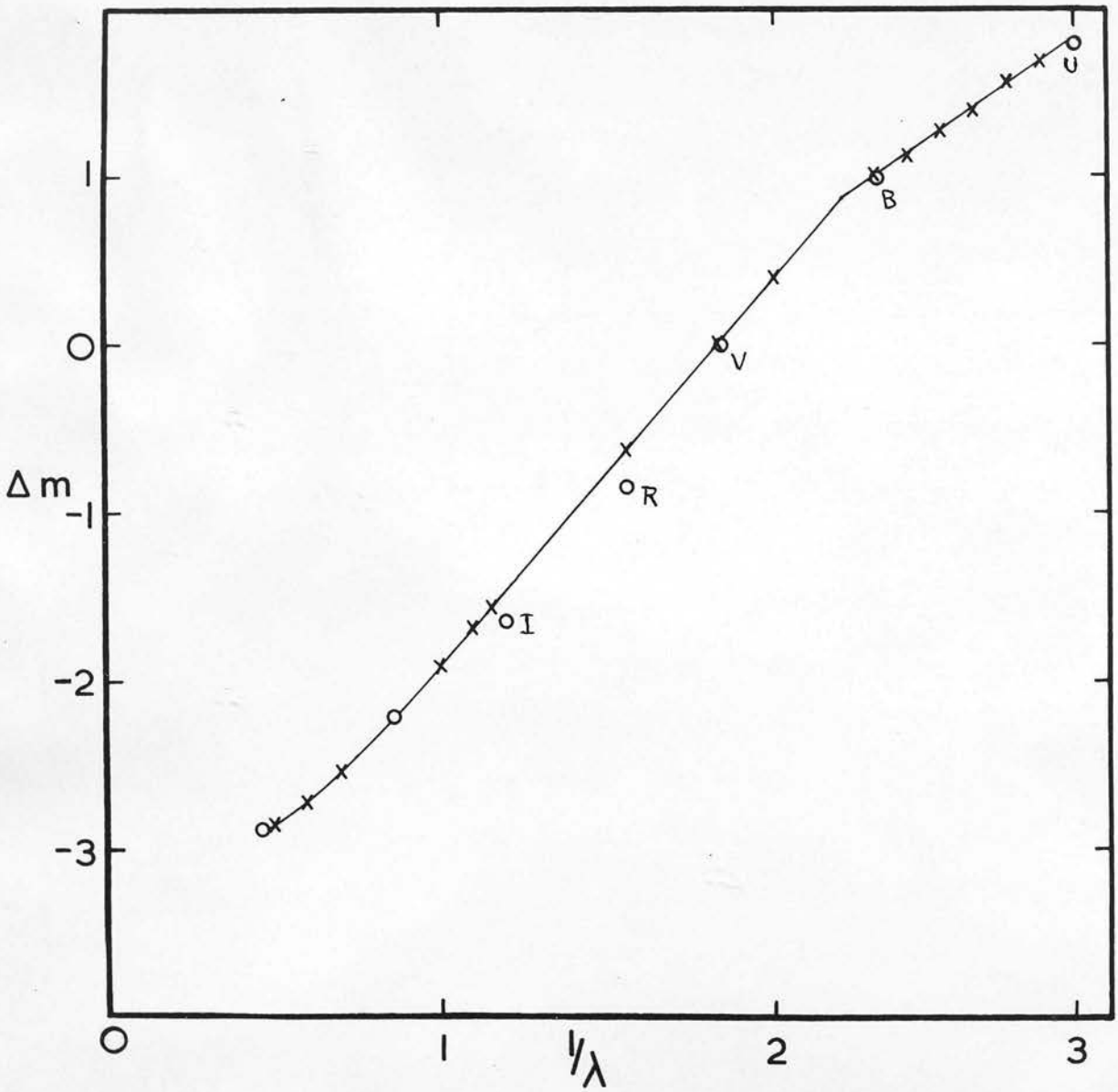

Fig. 2. Whitford's (1958) reddening curve compared with that derived by Johnson and Borgman (1963) for Cygnus stars. Circles represent Johnson and Borgman's measures, and crosses represent Whitford's measures.

Stebbins and Whitford's curve shows a continuously changing slope, whereas Whitford's curve consists of two portions with different slopes, one between $1/\lambda = .8\mu^{-1}$ and $2.2\mu^{-1}$, and the other between $1/\lambda = 2.2\mu^{-1}$ and $3.0\mu^{-1}$.

(2) The rounding off in the infra-red is less in Whitford's curve than that in Stebbins and Whitford's curve.

The difficulty of using broad band filters in the study of the interstellar reddening law can be illustrated by comparing the recently published results of Johnson and Borgman's (1963) wide band photometry with that of Whitford's photo-electric spectrophotometry. Fig. 2 shows the comparison of the reddening curve derived by these authors for Cygnus stars. A smooth curve drawn through the widely spaced points I, R, B, V, U represents a reddening law which is very much different from that represented by Whitford's curve. On the other hand, if the points I and R are plotted against the inverse of the wavelengths of the peak transmission of the filters, the difference between the two curves is much reduced. This indicates that even a small error in the assignment of the effective wavelengths of the filters may change the character of the reddening curve.

A comparison of different spectrophotometric results

shows a significant scatter in the details of the reddening curve. For example, the quantity $\frac{A(\lambda_1) - A(\lambda_2)}{A(\lambda_2) - A(\lambda_3)}$ has been computed for the effective wavelengths of U, B, V filters (Johnson, 1953) from the observed reddening curves for Cygnus stars derived by different authors. The result is shown in the following Table.

TABLE 1

Author	$\frac{A(U) - A(B)}{A(B) - A(V)}$
Whitford (1958)	.84
Divan (1954)	1.00
Rodgers (1961)	.93
Borgman (1961)	1.10

The dispersion about the mean is about 10 per cent. Such a dispersion would suggest either an intrinsic scatter in the space reddening law or a large source of error which is independent of the photometric system. It will be of considerable interest to determine an accurate reddening curve and its intrinsic dispersion for a given region in space from a wide range spectrophotometric study of a large number of reddened stars, and to compare it with the reddening law in other directions.

1.32 Variation of the reddening law

Although Divan (1954) and Whitford (1958) have emphasised the uniformity of the reddening law, there are certain regions of the Galaxy where the reddening curves are found to deviate from Stebbins and Whitford's (1943) mean reddening curve.

An anomalous reddening curve is found for the Trapezium stars in the Orion nebula. This was first pointed out by Baade and Minkowski (1937) and was confirmed by Stebbins and Whitford (1945). The deviation from the "$1/\lambda$ -law" for these stars was found to exceed the mean value by a factor of 2. A similar deviation was also found by Stebbins and Kron (1956), Hallam (1959), Borgman (1961), Johnson and Borgman (1963).

Divan (1954) believes that the reddening law for the Trapezium group of stars is the same as in the other galactic regions and that the observed anomaly is due to the fact that the stars exciting the nebula have, in the ultraviolet, a colour temperature higher than that of other stars of the same spectral type. Stebbins and Kron have suggested that the peculiar reddening curve may be due to the presence of unseen red companions; but the infra-red spectrograms of the Trapezium stars obtained by Sharpless (1956) and Hallam (1959) do not indicate the presence of any red companion.

Johnson and Borgman (1963), on the other hand, have suggested that the different reddening law found for the Orion stars is due to the modification of the properties of the interstellar medium rather than peculiarities of the stars themselves. Such differences in the reddening law may be connected with the association of the interstellar medium with hot stars [Hallam (1959), van de Hulst (1949)].

Any conclusion from the Trapezium stars alone may be misleading since these stars are embedded in the nebulae, and the elimination of the nebulous background effect from photometric measurements is to some extent uncertain. All the four components are known to be peculiar, their spectral types ranging from O6 to B3.

Borgman (1961) from his seven colour narrow band photometry extended from 5900A to 3300A, found that the reddening curves for the stars located in a small area within the association Cygnus 1 (II Cygni) in the Cygnus region and IC 1805 in the Perseus region show systematic deviation from the average reddening law. Borgman's result has not been confirmed by any other spectrophotometric observations.

1.33 Study of the reddening law from UBV photometry

Since thermal reddening does not have the same effect as interstellar reddening on different spectral ranges, a multicolour photometric system provides an independent method of determining some parameters which characterise the space reddening law. Such parameters are (1) ratio of colour excesses, and (2) ratio of total-to-selective absorption.

The ratio E_{U-B}/E_{B-V} on Johnson and Morgan's (1953) U, B, V system, which determines the slope of the reddening trajectory on the (U-B, B-V) diagram of the stars, is essentially a measure of the shape of the extinction curve over the range of wavelength covered by the photometric system. Due to the change of effective wavelengths of the filters with absorption the colour-excess ratio is not constant over a wide range of reddening, thereby producing a curvature in the reddening path (Blanco 1956). Also the ratio depends slightly on spectral type (Lindholm 1957).

The ratio of the total to the selective absorption, R is related to the portion of the reddening curve between 4500A and infinite wavelength.

The study of the variation of the reddening law from the ratio of colour-excesses and the ratio of total-to-selective absorption has become the subject of interest

during recent years, but the conclusions are not free from ambiguity. For example, the (U-B), (B-V) diagram of galactic O-stars [Johnson and Morgan (1955), Hiltner and Johnson (1956)] has been interpreted differently by different authors. The diagram shows that the reddening path of the stars located behind the Great Rift in Cygnus is a straight line with a slope of .83, whereas the reddening path for all the other stars appears to have a curvature and its mean slope is .72. The curvature of the reddening path is in agreement with theoretical prediction. The anomalous reddening path and the large colour-excess ratio of Cygnus stars led Hiltner and Johnson (1956) to conclude that the reddening law in the direction of Cygnus is different from that found elsewhere.

Rozi-Saulgeot (1956) explained the Cygnus anomaly as due to the neglect of the effect of reddening on the filter sensitivity curves.

Rodgers (1961) deduced that the large ultra-violet absorption of Cygnus O-stars as compared to other stars for the same value of E_{B-V} is due to the Cygnus O-stars being intrinsically ultra-violet deficient.

Greenberg and Meltzer (1960) and Wilson (1960) interpreted the difference in the slope of the reddening paths for Cygnus and Perseus stars as an indication of the directional dependence of the reddening law. Another

property of the interstellar medium which is known to vary with galactic longitude is polarisation. They suggested that the dependence of the reddening law on galactic longitude may be connected with the variation of polarisation.

Wampler (1961, 1962) on the other hand, concluded that the curvature of the reddening path is due to the irregularities of the reddening law. By grouping O-stars in the (U-B, B-V) diagram according to their galactic longitude, he has been able to show that the slope of the reddening line in the (U-B, B-V) diagram varies in a sinusoidal manner with galactic longitude. But this variation does not correlate with the variation of the degree of polarisation.

Recently Johnson and Borgman (1963) have extended the wavelength range of UBV photometry of early type stars and have incorporated infra-red colour indices V-I, V-J, V-K and V-L between 5550A and 3.5μ. The effective wavelength of the filters I, J, K and L are 8400A, 1.16μ, 2.14μ and 3.37μ respectively.

Their analysis of the colour excess ratios of O-stars leads them to the following conclusions:-

(1) The variation and galactic longitude dependence of $\frac{E_{U-B}}{E_{B-V}}$ is small. Except for Cygnus stars, the r.m.s. dispersion about the mean value $\frac{E_{U-B}}{E_{B-V}} = .72$ is less than

5 per cent. The mean $\frac{E_{U-B}}{E_{B-V}}$ for the Cygnus region is 20 per cent higher than that found for Perseus stars.

(2) The infra-red colour-excess ratios show a slow variation with galactic longitude. Also at the same galactic longitude these ratios vary over a wide range, depending on whether or not the stars are in bright H II regions.

(3) The variation of infra-red colour-excess ratios is independent of the variation of $\frac{E_{U-B}}{E_{B-V}}$.

Johnson and Borgman have further shown that a direct estimate of R, the ratio of the total to selective absorption on the BV system, is possible from observed values of $\frac{E_{V-I}}{E_{B-V}}$ and $\frac{E_{V-K}}{E_{B-V}}$. They have assumed relations of the form

$$R = f.\frac{E_{V-K}}{E_{B-V}} \text{ , and}$$
$$R = g.\frac{E_{V-I}}{E_{B-V}} \qquad (6)$$

where the factors f and g have been linearly interpolated from a few values of R which are directly derived, on the basis of van de Hulst's (1949) model, from the observed reddening curves extrapolated to $1/\lambda = 0$.

The values of R derived from colour-excess ratios show a considerable range of variation from 2.5 to 9.5, whereas the theoretical value as determined by Blanco

(1956) on the basis of Stebbins and Whitford's curve is 3.0. Stars essentially at the same longitude show high and low values of R, very high values being found for Orion stars. In the direction of Cygnus and Perseus the ratios are found to be the same. However, the value of R does not add any further information to that already given by the ratio of the infra-red colour-indices.

The main problem involved in the study of the reddening law from colour-excesses is to determine the intrinsic colours. Since early-type stars are reddened to some extent because of their distances, a prior knowledge of the reddening law is necessary to derive intrinsic colours from observed colours.

The basic assumptions which Johnson and Borgman have made are:-

(1) The scatter in the colour-colour diagram is due to the variation of the reddening law.

(2) All O-type stars have the same intrinsic colours, and if the colours are plotted against B-V, the reddening lines intersect at (B-V) = -.31, which is the adopted intrinsic (B-V) colour of O-stars.

The accuracy of the conclusions from colour-excess ratios depends primarily on these assumptions.

A significant fact is that the colour-excess ratios for a physical group of stars like the Trapezium Group

and NGC 6530 show a considerable scatter, which cannot be explained by a simple assumption of the variation of the reddening law. It is very unlikely that the reddening law will change across as small a configuration as the Trapezium (Underhill 1964).

It has been mentioned by Hiltner and Johnson (1956) and Wampler (1961) that in the (U-B, B-V) diagram of stars the reddening lines do not intersect at the adopted intrinsic $(U-B)_o$ and $(B-V)_o$ colours of O-stars.

Wampler found that the calculated values of $(U-B)_o$ from the point of intersection of the reddening lines extrapolated to $(B-V)_o = -.31$ range from -1.12 to -1.24 and that the difference between the calculated and the adopted intrinsic $(U-B)_o$ is correlated with the slope of the reddening line. This discrepancy between the calculated values of $(U-B)_o$ may well be due to systematic errors in photometry.

Coincidentally, a difference has been found between the measures of six-colour photometry and those of Johnson and Borgman (1963) of the same pair of stars. Since the zero-point of the colours of six-colour photometry is arbitrary, a constant has to be added to the given magnitude difference in order to find the actual difference. A smooth curve has been drawn through the measures of Stebbins and Whitford and those of Johnson

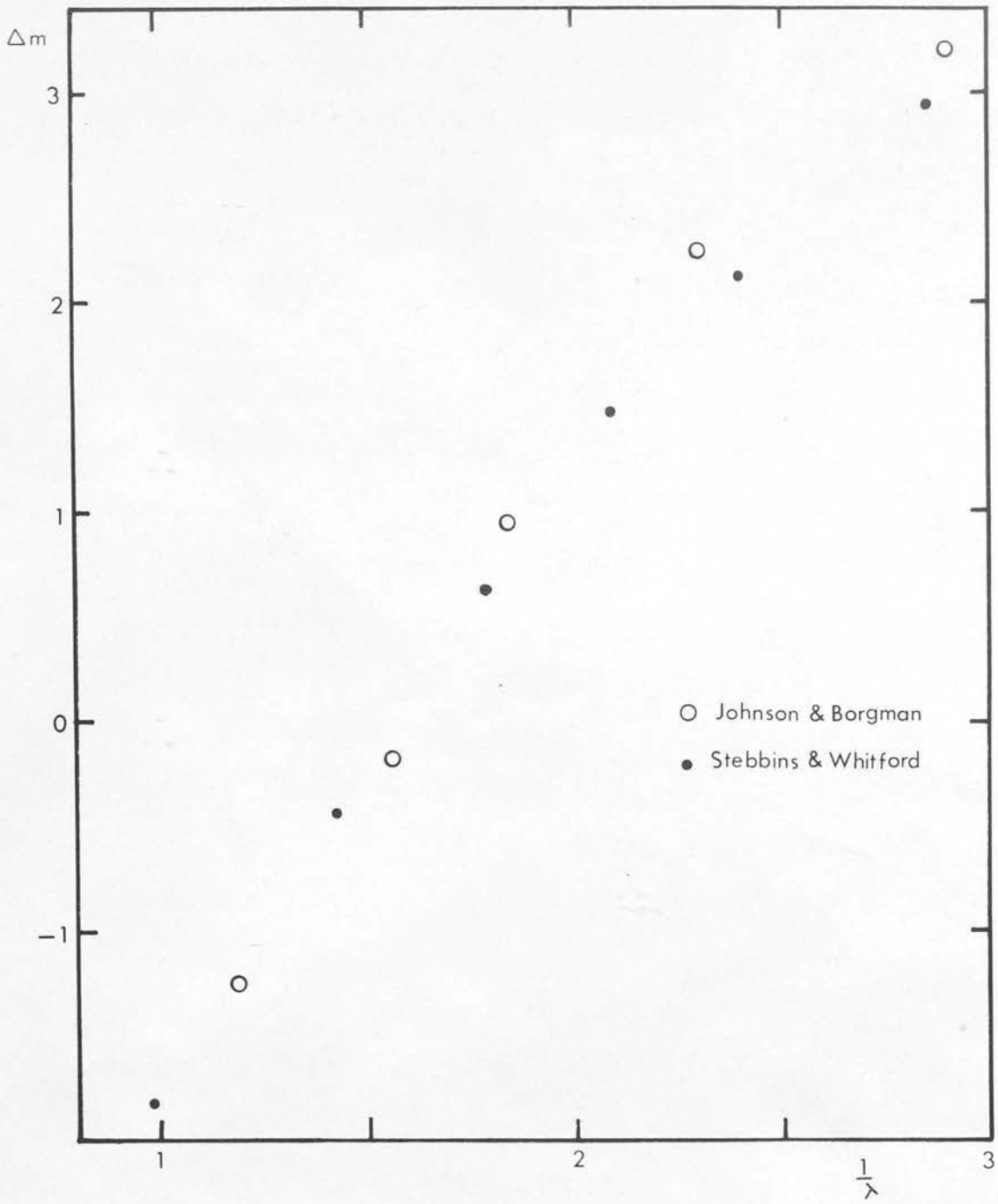

Fig. 3 Comparison between measurements by Stebbins and Whitford (1945) and by Johnson and Borgman (1963) for the pair of stars HD 166734 - HD 14633.

and Borgman, and the constant has been determined by fitting the curves at the effective wavelength of the V filter on UBV system. However, the shape of the curve showing the magnitude differences for a pair of stars as a function of $1/\lambda$ is independent of the zero-point of the magnitude system. Fig. 3 shows that the difference in the shape of the curve for the same pair of stars is not negligible.

It is also found that the reddening lines do not necessarily intersect at Johnson and Borgman's assigned intrinsic colours of O-stars. As shown in Fig. 4 the point of intersection of the reddening lines of Cygnus stars and stars in Perseus double cluster region gives

$$(B-V)_o = -.40 \text{ (assigned value } = -.31)$$

$$(V-I)_o = -.60 \text{ (assigned value } = -.51)$$

Uncertainty in the intrinsic colours derived from the intersection of reddening lines is more than 10 per cent.

Apart from uncertainty in the intrinsic colours, the observed colour-excess may be in error due to probable spectral variations, or the possible presence of unseen red companions.

The resulting error in colour-excess ratios may not be insignificant, especially for stars of little reddening, and this may explain the high scatter in the ratio of the colour-excesses for Orion and NGC 6530, and

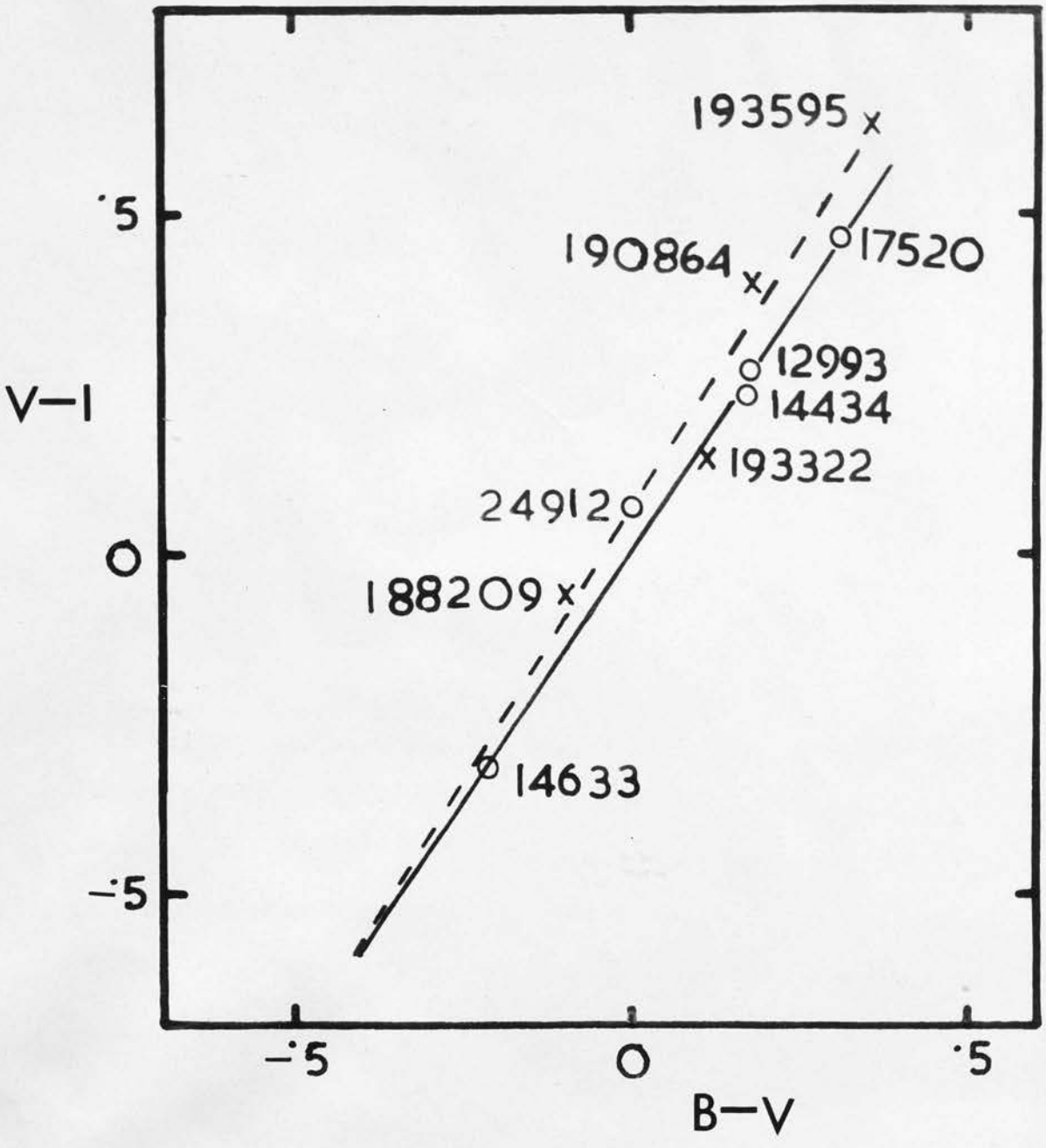

Fig. 4 V - I versus B - V for the O-stars in Cygnus and Perseus regions (data from Johnson and Borgman (1963)).

high values of R as found for stars of small colour-excesses.

In deriving R from the colour-excess ratio, Johnson and Borgman have in fact extrapolated the reddening curves to infinite wavelength by using the factors f and g of equation (6). The accuracy of R is very much limited by uncertainty in extrapolation, in the spectral classification, in the assigned effective wavelengths of the filters, and in the assumed intrinsic colours.

The extrapolation of the reddening curve would not be necessary if clusters or OB-associations showing a range of reddening among their members were considered. For such a group of stars which are assumed to be at the same distance, the apparent distance-moduli would be linearly related to E_{B-V}, with the slope of the line equal to R. Uncertainty in the absolute magnitude determinations is the largest source of error in this method.

Determinations of R have been made in this way by Sharpless (1952), Hiltner and Johnson (1956), Houck (1956), Whitford (1958) and Walker (1962). Whitford summarised the results giving $R = 3.0 \pm .2$. However, a high value of 6 ± 1 was found by Sharpless (1952) for the Orion aggregate.

Walker (1962) argued that for stars nearer than

1.0 kpc, the dependence of reddening on distance has to be considered when R is determined from the slope of the relation between apparent distance-moduli and E_{B-V}. The apparent distance-modulus is given by

$$m - M = 5 \log r - 5 + R. E_{B-V} \qquad (7)$$

Differentiating with respect to E_{B-V} and assuming that R is independent of E_{B-V}, one obtains

$$\frac{d(m-M)}{d E_{B-V}} = 5 r^{-1} . \log e . \left(\frac{dr}{d E_{B-V}}\right) + R \qquad (8)$$

The equation (8) can be approximated to

$$\frac{d(m-M)}{d E_{B-V}} = 5 \log e . \frac{1}{r_o} . \frac{\Delta r}{\Delta E_{B-V}} + R \qquad (9)$$

where r_o = the mean distance of the association,

Δr = the thickness of the association in the line of sight,

ΔE_{B-V} = the variation of E_{B-V} over Δr.

An estimate of the apparent increase in R produced by the distance dependence of reddening made by Walker was found to be 2.9.

The observed value of the slope being 6.0, the equation (9) gives R = 3.1.

For Cygnus Rift stars, Hiltner and Johnson (1956) derived R = 2.1 by assuming that all the O-stars lay at the same distance and were of the same absolute luminosity.

Walker found that the exclusion of the members of the heavily obscured Cygnus II (VI Cygni) association from Cygnus Rift stars would yield a value R = 2.8 $\pm$.2.

Values of R derived for several regions by different authors are shown in the following Table.

TABLE 2

Region	Author	From colour-excess ratios	From apparent modulus — E_{B-V} plot
Cygnus	Hiltner & Johnson (1956)		2.1
	Johnson & Borgman (1963)	3.11	
χ & χ Persei	Hiltner & Johnson (1956)		3.2
	Walker (1962)		3.5
	Johnson & Borgman (1963)	3.16	
Orion	Sharpless (1952)		6.0
	Walker (1962)		3.1
	Johnson & Borgman (1963)	7.37	

The large differences between the values of R obtained from the ratios of the colour-excesses and from the plot of the apparent distance modulus against E_{B-V} illustrate the difficulties in determining this ratio accurately.

To summarise, it is an assumption rather than a conclusion that the variations of colour-excess ratios are of interstellar origin. The strong argument in favour of this assumption is that the variations are independent of E_{B-V}, have longitude-dependence, and also depend on the relative position of stars and absorbing clouds. Spectrophotometric observations, on the other hand, do not indicate any systematic variation of the reddening law. However, the reddening curves derived from spectrophotometric comparisons of a few pairs of stars are not accurate enough to detect small systematic variations.

1.4 Theories of Interstellar Grains

The theoretical problem is to predict the shape, the size-distribution, the optical and the physical properties of the absorbing dust particles, which would produce the observed reddening law and interstellar polarisation. As far as the representation of the reddening curve is concerned, the solution is not unique. Four possible models of the dust particles have been suggested, each of which can satisfy the average absorption law with an appropriate size-distribution. These types of particles can be classified broadly as (1) grains of nearly one micron in diameter, which may be di-electric, metallic or graphite, and interact classically with radiation, (2) unsaturated molecular-type particles about ten angstroms in diameter, which absorb radiation by quantum mechanical processes.

Some hypothesis is necessary concerning the formation and growth of dust particles. Following Lindblad (1935), Oort and van de Hulst (1946) considered the possibility of the formation of the dust particles by condensation from the interstellar gas. Their theory is that large molecules (condensation nuclei) are formed out of the gas and once their nuclei are formed, grains grow by random accretion. Conclusions can be drawn about the composition of the grains from the cosmic abundances of

the elements and from the physical conditions of interstellar space. It has been suggested that the particles are likely to be composed of frozen H_2O, CH_4 and NH_3 together with metallic impurities (van de Hulst, 1955).

Collisions between the grains caused by the occasional encounter of clouds, produce evaporation which check the growth of the grains. On the basis of this hypothesis, Oort and van de Hulst (1946) have determined the resulting equilibrium distribution of grain sizes.

The analytical theory of the scattering of light for smooth spheres of arbitrary size and material was first developed by Mie (1908). The solution involves the parameters

$$x = 2\pi r/\lambda$$

$$m = n + i\,k,$$

where r = radius of the sphere,

λ = wavelength of the incident light,

m = complex refractive index relative to surrounding medium.

For numerical results Mie's formulae are unsuitable, particularly for large values of x. van de Hulst (1949) derived a correct analytical solution for large dielectric spheres whose refractive indices differ little from unity.

Denoting the parameter ϱ by

$$\varrho = 2x\,(m-1)$$

the efficiency factor $E(\varrho)$ for the extinction of a single particle is given by

$$E(\varrho) = 2 - 4/\varrho \ \sin\varrho + 4/\varrho^2\,(1-\cos\varrho) \qquad (10)$$

As $\varrho \rightarrow 0$, $E(\varrho) = 0$.

For other values of m in the range from 1.33 to 1.5 a few points computed accurately from Mie's rigorous formula indicate the nature of the divergence from the curve obtained for $m \rightarrow 1$. A correct extinction curve can be drawn through these computed points for which the curve for $m \rightarrow 1$ serves as a guide. The solution for di-electric spheres is extended to large spheres whose complex refractive index differs little from unity. Since the imaginary part of the refractive index denotes an attenuation factor, a fraction of incident energy will be absorbed and transformed into heat. This absorbed energy is, however, independent of the real part of the refractive index.

The solution which refers to a single particle can be extended to a mixture consisting of particles of various sizes. If the frequency distribution in size is expressed as g(u), the mean value of efficiency factor $\overline{E(\varrho)}$ is given by

$$\overline{E(\varrho)} = \frac{\int_0^\infty E(u, \varrho_0)\ g(u)\ u^2\ du}{\int_0^\infty g(u)\ u^2\ du} \qquad (11)$$

where $\rho_o = 4\pi r_o(m-1)/\lambda$, r_o being the radius of an arbitrary sphere.

By varying the two parameters, viz. the refractive index and the frequency function of the sizes of the particles, van de Hulst (1949) produced a number of theoretical curves. From the choice of the solution (Curve No. 15) giving the best fit to Stebbins and Whitford's [Whitford (1948)] reddening curve for the pair of ζ and ϵ Persei, he inferred that the interstellar particles are di-electric with little metallic impurities having an effective size of 0.8μ. The refractive index and size-distribution of the particles assumed in this solution are consistent with the Oort-van de Hulst (1946) size-distribution function.

Although the gross properties of the reddening curve are reproduced by van de Hulst's solution No. 15, Divan (1954) has pointed out that the ultra-violet part of the theoretical curve deviates from the observed data. Whitford (1958) found that ζ Persei is an anomalous star and that the inverse curvature in the infra-red is less than that predicted by van de Hulst's model.

The theoretical extinction curves are very sensitive to the ratio of the number of large particles relative to that of small particles. The presently observed uniformity of the reddening law implies that the

dispersion in the size-distribution of particles should not generally be more than 5 per cent throughout the regions observed [van de Hulst (1964)]. Proximity of a cloud to hot stars can modify the size-distribution function by increasing the number of large particles. With such modification of size distribution it is possible to explain exceptions such as the different reddening law for Orion stars and stars in H II.

The real difficulty with the model of di-electric spheres is that it cannot explain the observed ratio of polarisation to absorption. The inward curvature of the reddening curve in the infra-red and the high albedo of the scattering particles, as observed by Henyey and Greenstein (1941), suggests a strong argument against the hypothesis of iron particles. Following Schalén (1936, 1939) Güttler (1952) showed that the absorption by a mixture of iron particles with an effective size of .08 could reproduce Stebbins and Whitford's (1943) mean reddening curve. Although the theoretical study of the formation of grains does not favour the formation of pure iron particles, Spitzer and Tukey (1951) suggested a possibility that mutual collision between van de Hulst's particles would produce a total fusion, with a partial evaporation of water and other volatile constituents. Metallic impurities present in the di-electric particles

could be formed into ferromagnetic nuclei which would grow a di-electric skin. These particles would most likely behave optically as ferrites. These ferromagnetic grains would have random shapes and their long axes would orient themselves in the direction of the galactic magnetic field.

The alignment of elongated ferromagnetic grains seems to provide an easy explanation for the observed polarisation. Since the plane of polarisation shows a preference for the galactic plane [Hall (1958), Hiltner (1956)], the long axes of the particles must lie in a direction normal to the galactic plane. Therefore the theory of Spitzer and Tukey requires that the galactic magnetic field is perpendicular to the galactic plane. The field strength necessary to account for the observed polarisation should be of the order of 2.10^{-3} gauss.

The criticisms against the theory of Spitzer and Tukey are:-

(1) It is difficult to explain random orientation and feeble polarisation, as observed in certain regions, unless some depolarising effects are considered.

(2) At present it is believed that the spiral arm structure of our galaxy is bound up with the galactic magnetic field. For the stability of the

spiral arms it has been argued that such a large magnetic field may be force-free, and this may be possible in the case of the magnetic field lying along the spiral arms. This, however, is contrary to the assumption of Spitzer and Tukey, [Davis (1960)].

(3) Considering the balance between gravitational and magnetic forces in the gas, Chandrasekhar and Fermi (1953) estimated the field strength to be of the order of 10^{-6} gauss. The magnetic field required by the theory of Spitzer and Tukey seems to be too high.

The possibility of the formation of elongated ice crystals by ordered accretion has been considered by Kahn (1952). The electric dipole moments of water molecules produce an electrostatic potential which may hold some free hydrogen atoms at the positive end. When an oxygen atom strikes, a water molecule is formed and the crystal grows in one direction. Such crystals may contain sufficient metallic impurities to be paramagnetic. Gold (1952) suggested that if the particles are elongated, collision with a streaming gas cloud might produce a dynamical alignment of the axes of rotation. But Davis (1955) has shown that Gold's mechanism fails under a quantitative examination.

Davis and Greenstein (1951) have developed a theory for the alignment of paramagnetic grains. Their theory suggests that particles are set into a spinning motion by

collisions with the gas atoms. As the grain rotates, its magnetisation lags behind the local galactic magnetic field, the direction of which is along the galactic plane. The out of phase component is given by the ratio $\frac{x_2}{x_1}$ where x_2 and x_1 are the imaginary and the real part of the magnetic susceptibility. This paramagnetic relaxation produces a dissipative torque which tends to make the particle rotate about its short axis and to orient this axis parallel to the direction of this field. Bombardment by the interstellar gas tends to disalign the particles. Solving this non-equilibrium process by using a relaxation time method, Davis and Greenstein (1951) have shown that the magnetic field required to explain the observed polarisation will be of the order of 10^{-5} gauss. The theory has been subsequently generalised to ferromagnetic particles by Henry (1958) who has found that if a sizeable fraction of the grains were ferromagnetic, the required magnetic field could be reduced by a factor of 10. The alignment mechanism of Davis and Greenstein offers a simple explanation for the observed directional dependence of polarisation. In Cygnus where the line of vision is parallel to the spiral arm and therefore to the lines of force, the spinning particles are seen sideways and polarisation should be negligible. On the other hand,

in the direction of Perseus where the spiral arm is viewed perpendicularly, the particles are seen edge on and maximum polarisation should be observed in this direction.

Scattering cross-sections for elongated particles for different orientations have been studied by the micro-wave analogue experiment (Greenberg, Pedersen and Pedersen, 1961). The experimental results indicate a definite dependence of wavelength law of extinction on the orientation of the particles.

Making use of a scalar wave W.K.B. type of approximation, Greenberg (1960) has derived an analytical expression for the total cross-section $\sigma(\chi, b/a, a, n, \lambda)$ for arbitrarily orientated non-spherical particles, where χ is the angle which the axis of symmetry makes with the direction of propagation, b and a are the semi-major and the semi-minor axis respectively, and n is the refractive index.

Assuming that the interstellar dust particles are di-electrics (n = 1.3) having the size distribution as given by Oort-van de Hulst's theory, and the elongation b/a = 2, and that they are perfectly aligned by Davis and Greenstein's mechanism, Greenberg and Meltzer (1960) used the expression for $\sigma(\chi, b/a, a, n, \lambda)$ to obtain the total cross-section for extinction in the direction viewed

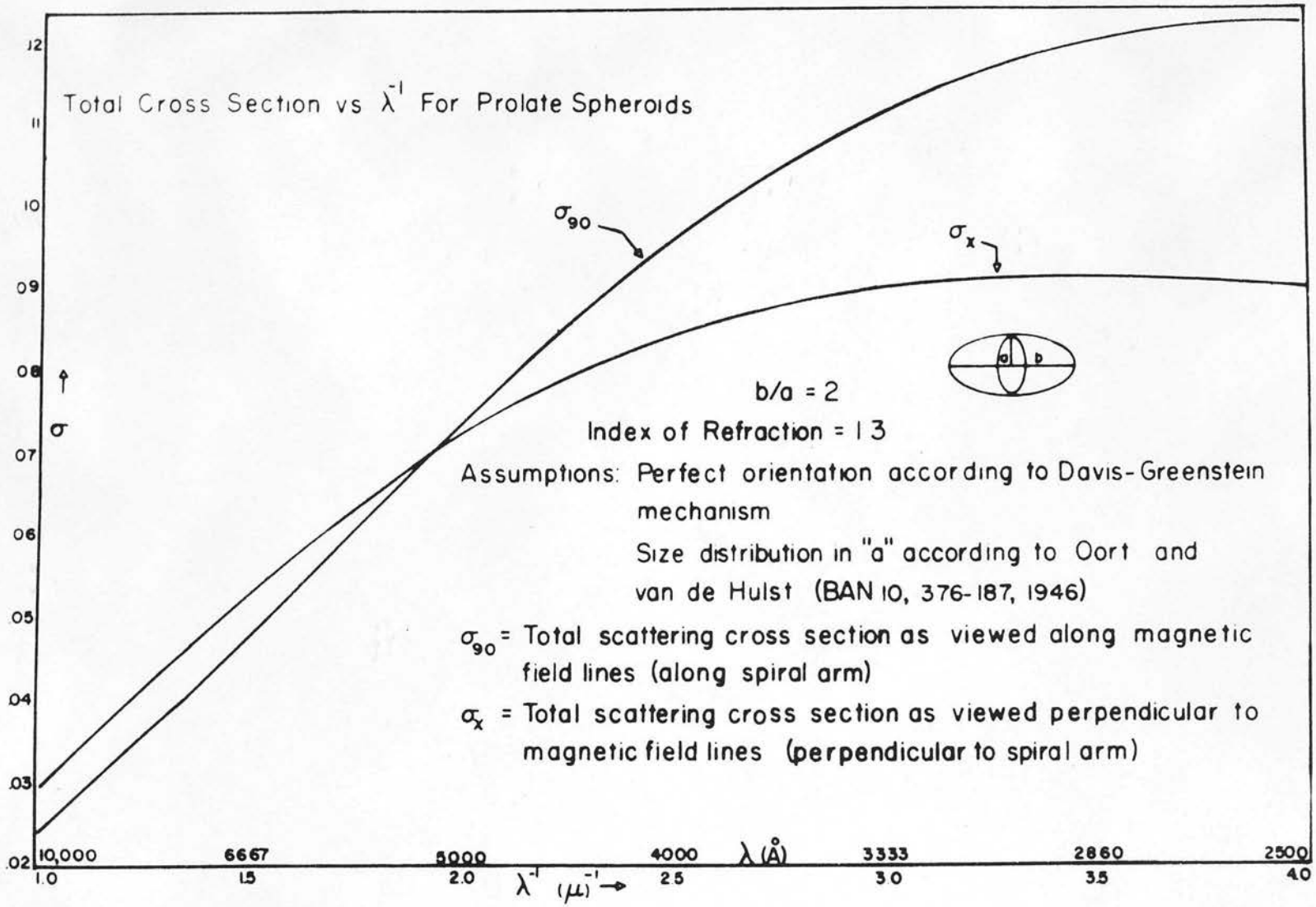

Fig. 5 Wavelength dependence of extinction through clouds of oriented particles as viewed along and perpendicular to the orienting magnetic field direction (after Greenberg (1960).

along and perpendicular to the spiral arm. Their result is shown in Fig. 5 which shows that towards the shorter wavelengths σ_{along} is significantly greater than σ_{across}. The ratio of the slope of the extinction curve in the ultra-violet relative to that in the visible and longer wavelengths is about 50 per cent larger along the spiral arm than across the spiral arm. In reality, the difference may not be as large as 50 per cent since particles may not be perfectly aligned.

Wilson (1960) obtained an approximate solution for an infinite di-electric cylinder for the limiting case of refractive index $m \rightarrow 1$, and computed theoretical extinction curves for different values of polarisibility (polarisation per unit colour-excess) on the assumption that the Davis -Greenstein mechanism for van de Hulst's particles hold. He derived the conclusion that the ratio of ultra-violet colour-excess relative to the visual colour-excess on the U, B, V system will decrease by 30 per cent and that the ratio of total to selective absorption will increase by 60 per cent as the polarisability increases from zero to maximum.

The predictions of Greenberg and Meltzer (1960) and of Wilson (1960) receive a qualitative verification from the results of Borgman (1961) for the stars in Cygnus I (II Cygni) and IC 1805, which are viewed along and

perpendicular to the spiral arm respectively. The larger ratio of the ultra-violet to visual colour-excess for stars in Cygnus as compared to stars in Perseus seems consistent with the prediction. As polarisation implies a fair degree of alignment, it is expected that a systematic variation of the reddening law should be correlated to variation of polarisation. But no such correlation has been found [Wampler (1961), Serkowski (1963)].

A low value of R in Cygnus and a higher value in the Perseus region, as obtained by Hiltner and Johnson (1956) favour the prediction that R increases with increasing polarisation. But Johnson and Borgman (1963) have found the same value of R in these two regions.

The interpretation of polarisation would seem to be easier if the extinction of light could be attributed to small graphite particles [Cayrel and Schatzman (1954)]. Recently Hoyle and Wickramasinghe (1962) have considered the formation of graphite flakes at the surfaces of cool giant stars. They have shown that monatomic carbon vapours would condense into carbon grains in the pulsation cycle of N stars when the temperature falls below 2700°K. These grains have the effect of decreasing the photospheric density as the temperature falls towards 2000°K, and the radiation pressure is sufficient enough to eject

the grains into space if their sizes are of the order of 10^{-5} cm. During the outward journey grains of this size escape evaporation. The calculation of the rate of emission of grains from N stars shows that the 10^4 N stars in the Galaxy would suffice to produce the observed interstellar grain density in a time-scale of 3×10^9 years.

Graphite crystals possess anisotropic conductivity and large anisotropic diamagnetic susceptibility. Taking account of the anisotropic conductivity Wickramasinghe[a] (1962) has shown that a small degree of alignment of only about 2 per cent would be able to explain the observed polarisation. Davis-Greenstein's (1951) theory applied to diamagnetic graphite flakes requires a magnetic field of the order of 10^{-6} gauss. The degree of alignment is so small that the variation in the alignment of grains would not produce any significant effect on the reddening law.

Applying Mie's theory, Wickramasinghe[a] (1963) has derived the extinction cross-sections of graphite spheres of various radii. Rigorous computations lead to the result that the theoretical curves for grains of size $a > .05\mu$ begin to deviate from the observed reddening curve of Whitford (1958). The particles of smaller size represent the observed reddening law better, but their

albedo is lower by 40 per cent than what is required by Henyey and Greenstein's (1941) observations. It is also significant that there is a disagreement between the theoretical reddening curve and the extrapolated portion of Whitford's curve for $\lambda > 2\mu$.

To explain the observed high albedo Wickramasinghe[a] (1963) has considered the possibility of a model of a composite grain consisting of a graphite core surrounded by a concentric shell of ice. Because of the high chemisorbant properties of carbon, the surface of graphite grains would accommodate interstellar atoms and a layer of ice-crystals would eventually grow. The wavelength dependence of extinction in the red and visible is not very sensitive to the amount of ice around the grain, but the slope of the reddening curve in the blue would be slightly increased. Albedo is considerably raised by the presence of ice.

The extent of the condensation of ice on the graphite grains depend on the temperature of the grain and the density of interstellar gas around them. In hot H II regions condensation of ice cannot possibly take place and the particles would be of pure graphite and possess low albedos, while in H I regions grains would be coated with ice. Wickramasinghe[a] has not considered the effect of collisions and subsequent evaporations. It is

likely that there would be a size distribution of composite grains and that the distribution would possibly vary from region to region according to local conditions. A uniform reddening law cannot therefore be expected, but the variation would be confined to blue wavelengths only. In any given direction the average reddening law would show a considerable scatter because the reddening of starlight would be produced by grains in a wide range of sizes.

Since the effect of ice is to increase the slope of the reddening curve in the blue only, the solution which fits in the red and visible gives the size of the graphite core. An upper limit to the grain size can be estimated to be $a \sim .05\mu$, because departure from Whitford's curve is found for sizes $a > .05\mu$. For regions in the vicinity of hot stars where carbon particles are free from contamination, the reddening law would not differ from that predicted for small, pure graphite grains. Such particles, however, cannot reproduce the reddening curve as found for the Trapezium group of stars.

An objection to the hypothesis of carbon particles suggested by Donn(1960) is that because of the overwhelming abundance of hydrogen in space, these particles are likely to be absorbed by atomic hydrogen. In hot H II regions especially small graphite grains may not have a permanent existence.

Donn (1955) has also criticised the hypothesis of growth of large heterogeneous particles by chemical processes involved in the sticking of atoms to the grains. He has emphasised that under the conditions prevailing in the interstellar medium, surface processes cannot be fully understood by extrapolation from the normal laboratory conditions.

Platt and Donn (1956) have considered the formation of molecular type particles by two-body collisions as well as by direct addition of atoms. They have argued that interstellar matter consists primarily of atomic and ionic species and chemical bonding would play an important role for particle growth. This mechanism would result in forming quasi-organic radicals having unfilled energy bonds with linear dimensions about 10 to 50 angstroms.

Platt (1956) has proposed that small molecular-type particles containing free radicals or unfilled energy bonds are efficient absorbers and polarisers. The optical behaviour of these particles can only be predicted by quantum mechanics. On the basis of experimental results and simple quantum mechanical calculations for a rectangular particle containing free electrons, Platt has derived the following conclusions:-

(1) The wavelength of strong allowed absorption is about 400 times the length of the particle. The

absorption cross-section at resonance is of the order of the geometrical cross-section.

(2) The particles are still large enough to have a statistical distribution of sizes to satisfy the average reddening law.

(3) Particles which have unpaired electrons in the system will have a paramagnetic and quasi-metallic character. Due to statistical fluctuations in the random growth process involving small numbers they will tend to be elongated, and to give several per cent polarisation they will require a smaller than usual magnetic field for alignment by the Davis and Greenstein's mechanism.

(4) The particles have high albedo and re-radiate isotropically. On the other hand, Henyey and Greenstein's (1941) observations suggest that the degree of forward scattering is high in interstellar dust.

It does not appear that a sound theory is available which will give a quantitative formula for the wavelength dependence of extinction or polarisation for Platt-type particles. However, if quantum-mechanical particles are dominant, the actual number of particles required to explain the observed extinction would have to be more than that predicted by the Oort-van de Hulst (1946) theory by many orders of magnitude. When such large numbers are involved, small fluctuations in the relative

distribution according to sizes would not produce a significant variation in the wavelength dependence of extinction. Variation of wavelength dependence of total-cross-section for different orientation would be negligible [Greenberg (1960a)]. Therefore, if the particles are always small enough, the law of reddening should be uniform.

CHAPTER II

OBSERVATIONS

2.1 Telescope, Objective Prism and Grating

The 16/24/60-inch Schmidt telescope covers a field of 4^{o} diameter. On a good plate, the diameters of the faintest star images are equal to 20μ corresponding to approximately 3 seconds of arc.

The objective prism of angle $1^{o}.8$, made of Schott LF5 glass, has a high UV transmission. The spectra have a linear dispersion of about 1000A/mm at Hγ and extend from 3200A to 9000A. The spectra were broadened to 0.3 mm. by varying the sidereal rate. Differences in broadening due to differences in declination have been found to be of no significance.

The grating, constructed in the Observatory workshop, is made of threads of nylon which has several advantages over the usual metal wire; in particular it is less affected by changes of temperature. It has 18 threads per inch with a spacing approximately equal to the thickness of the threads.

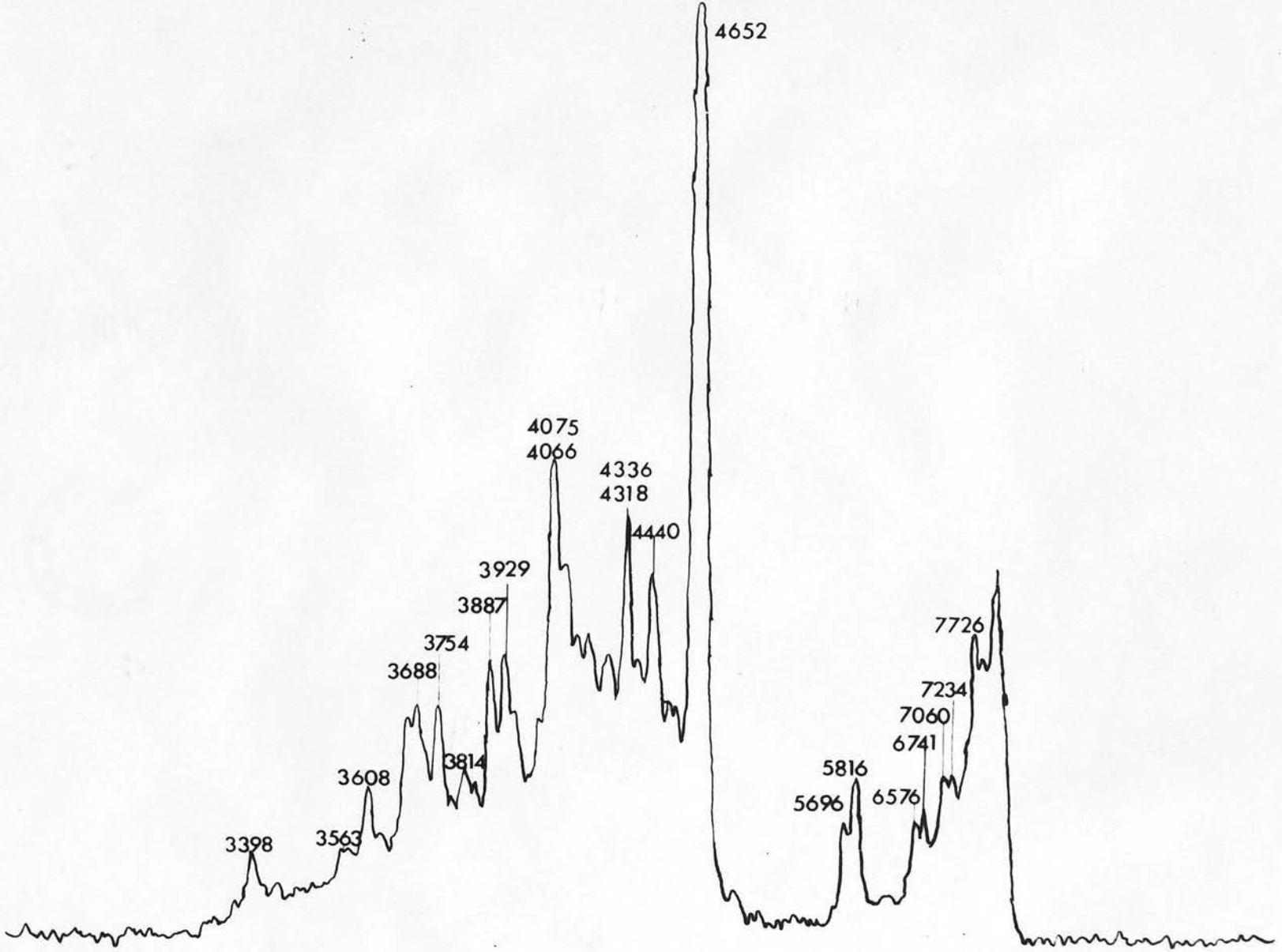

Fig. 6 Microphotometer tracing of the spectrum of the Wolf-Rayet star HD 192103.

2.2 Dispersion Curve of the Prism

The important dispersion curve of the prism was determined by setting a cadmium lamp with collimator in front of the telescope. The constants in Hartman's interpolation formula were found from observations of the 3466A, 4678A and 6438A lines of cadmium. When the distance of the Balmer lines from Hγ (4340.5A) as calculated from the interpolation formula, are compared with their actual measured separations, Table 3(a) results.

The dispersion curve was extended into the infra-red from the spectrum of the Wolf-Rayet star HD 192103, which consists of many broad emission lines covering the range from 3065A to 8666A [Edlén (1956), Underhill (1959)]7.

A microphotometer tracing of the spectrum of this star is shown in Fig. 6. Wavelengths of the emission features have been identified from the lists referred to. The identified wavelengths and contributing spectra are listed in Table 3(b). The width of the lines, however, makes the identification difficult. Where there are two or three lines very close together, their mean wavelength has been taken. Linear distances of these lines on the tracing from the strongest line which occurs at 4652A have been measured on eight plates. Since they are well distributed over the spectrum, they prove sufficient for the purpose of obtaining the dispersion curve.

As shown in Table 3(c) the curve thus derived is in good agreement with that obtained by interpolation from Hartmann's formula.

The error in calibration is $\pm 3\mu$ on the plate which corresponds to ±15A at 7000A, ±5A at 5000A and ±3A at 4000A.

TABLE 3(a)

Dispersion of the Prism
(from the spectrum of Cd)

Balmer Lines	Wavelength	Separation from $H\gamma$ on the plate	
		From Hartmann's formula	Observed
$H\gamma$	4340.5A	0	0
$H\beta$	4861.3	410.8 μ	410 μ
$H\delta$	4101.7	-255.2	-255
$H\varepsilon$	3970	-421.7	-428
$H\zeta$	3889	-535.6	-542

TABLE 3(b)

Wavelengths of Emission Lines in the Spectrum of HD 192103

Wavelength	Mean Wavelength	Contributing Spectra
3384 A		O III, O IV, O V, S III
3399	3398 A	O IV
3410		O IV
3563		C IV, O IV
3608		He I, C III, Al III
3688		C IV
3754		O III
3814		He I, He II, O VI
3887		He I, He II, C III
3929		He II, C II, C IV, S III
4066	4071	C III
4075		C II, Si IV
4318	4327	C II, C III
4336		H, He II, N III, S III
4440		He, C IV
4652		C II, C III, C IV, N III
5696		C III, Al III
5816		C IV, C III
6576		H, He II, C II, C IV
6741		C II, C III
7060		C IV, He I
7234		C II
7726		C IV

TABLE 3(c)

Dispersion of the Prism
(From the Spectrum of HD 192103)

	Separation from H_γ on the Tracing	
	From Hartmann's Formula	Observed for HD 192103
3398 A	-88.3 mm.	-88 mm.
3608	-64.1	-65
3688	-56.4	-56
3929	-37.1	-38
4327	-13.8	-14
5696	+28.3	+29
5816	+30.5	+31
6576	+42.2	+43
6741	+44.2	+45

2.3 Determination of Grating Constant

When the prism is crossed by a coarse grating, each star has fainter first order spectra at both sides of the central spectrum. The magnitude difference between first order spectrum and central spectrum, the Grating Constant is given by

$$m_1 - m_o = -2.5 \log_{10} \frac{\mathrm{Sin}^2 \left(\frac{l}{l+d}\pi\right)}{\left(\frac{l}{l+d}\pi\right)^2} \qquad (12)$$

and

$$\left(\frac{l}{l+d}\right)^2 = \frac{I_o}{I} \qquad (13)$$

where

m_1, m_o denote the magnitude of the first order spectrum and central spectrum at a given wavelength,

d, breadth of threads,

l, spacing between threads,

I_o, I, the intensity of the centre spectrum with and without grating.

The magnitude difference given by (12) is a constant for the grating and is independent of wavelength. For d = l, the theoretical value of the Grating Constant is $0^m.98$.

The determination of the Grating Constant has been done photo-electrically in the laboratory as well as photographically by comparing the quasi-monochromatic

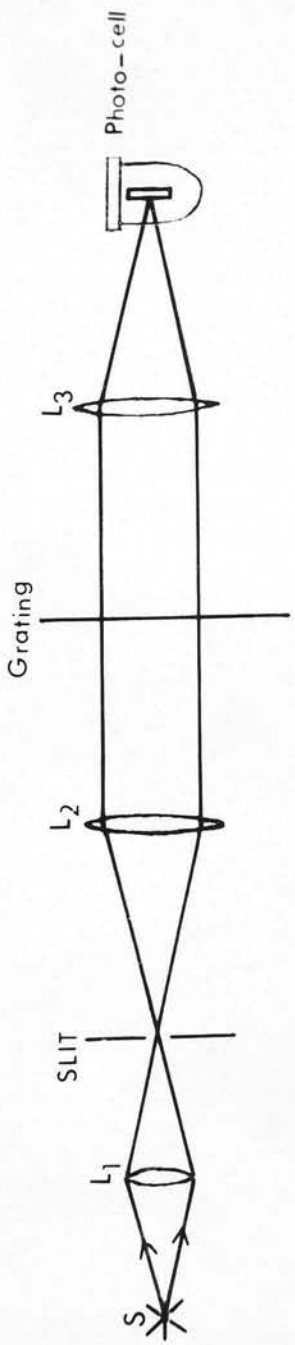

Fig. 7 Optical arrangement for the determination of the Grating Constant.

magnitudes determined for stars in a narrow range of spectral types in the Pleiades with Johnson's photo-electric measures.

The optical arrangement for photo-electric method is shown in Fig. 7.

S is a source of monochromatic light (Mercury lamp). The lens L_1 focusses the beam from S on the slit. The beam is collimated by the lens L_2, passes through the grating and is focussed on the photo-cell by the lens L_3. The grating was fixed to a board and a number of readings were taken for two positions of the grating.

The results are given in Table 4.

The adopted value of the Grating Constant was $0^m.875$.

TABLE 4

Determination of Grating Constant

		G
Photo-electric Method		
I	From centre and side images	
	Upper half of the grating	.888 ± .004
	Lower half of the grating	.871 ± .005
II	From I_o/I [Kienle (1937)]	.872 ± .014
Photographic Method		
	Plate P21	.87 ± .04
	Plate P31	.87 ± .04

2.4 Regions Observed

For the present programme the regions of high obscuration in the Milky Way, given in Table 5, have been chosen. Columns 2, 3, 4 and 5 show respectively the name of the main constellation, equatorial and galactic co-ordinates (galactic pole $\alpha = 12^h49^m$, $\delta = 27.^0$) of the centre of the region and the area of the region of the sky in square degrees.

TABLE 5

	Constellation	α_{1950}	δ_{1950}	l^{II}	b^{II}	Area
I	Vul	19^h46^m	26^o	$62^o.4$	$0^o.30$	20 sq.degs.
II	Cygnus	20^h15^m	38^o	$72^o.5$	$1^o.5$	30 " "
III	Cepheus	22^h36^m	57^o	$105^o.6$	$-1^o.06$	15 " "
IV	Cassiopeia	0^h	63^o	$117^o.5$	$0^o.93$	30 " "
V	Perseus	2^h10^m	58^o	$133^o.5$	$-2^o.9$	40 " "
VI	Orion	5^h36^m	-2^o	$206^o.2$	$-17^o.1$	30 " "

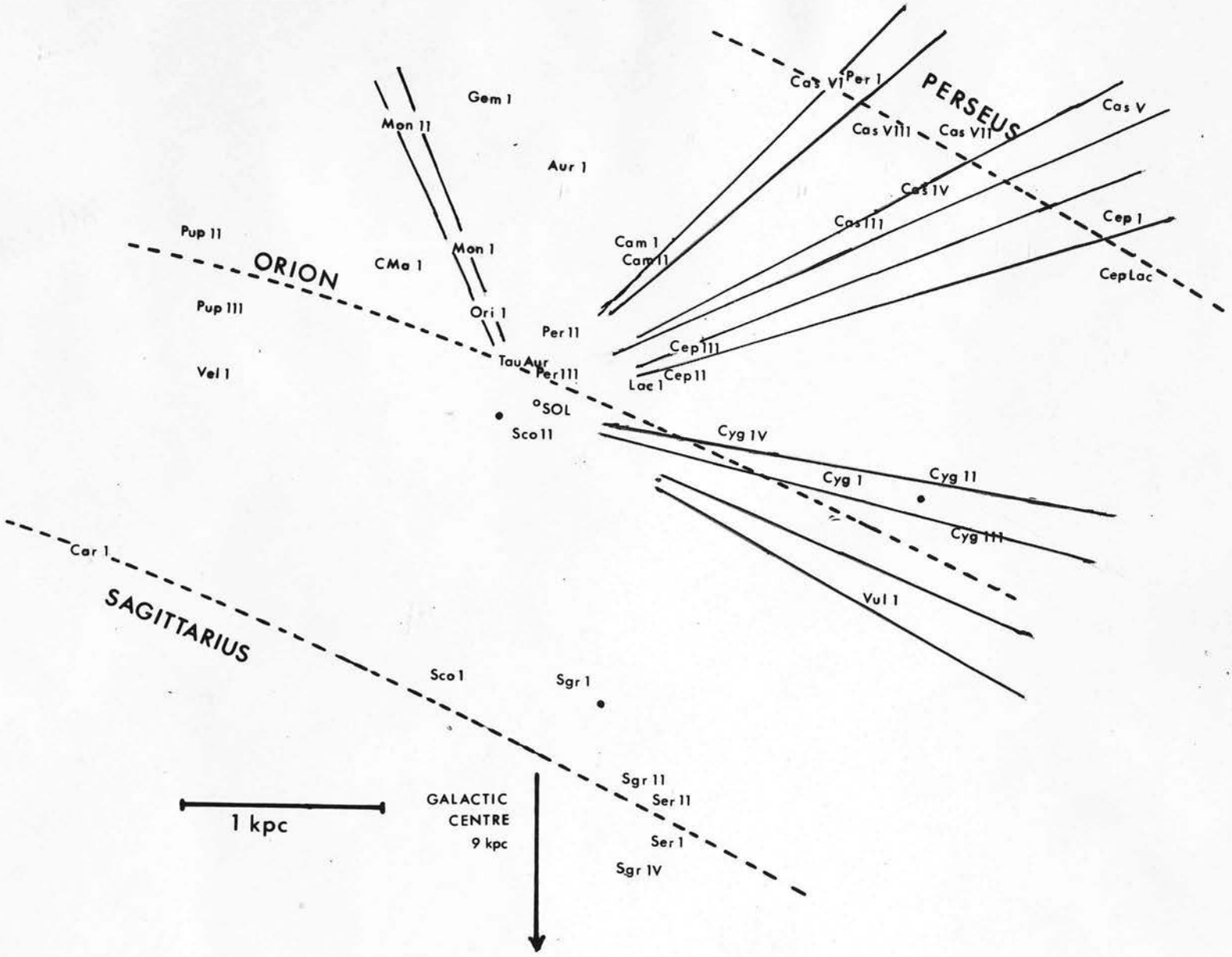

Fig. 8 Space distribution of early type stars. Solid lines represent the regions for which plates have been obtained.

The space distribution of early type stars and O-B associations in the galactic plane is shown schematically in Fig. 8. They delineate the inner arm, local arm and Perseus arm. The Perseus arm is located about 2000 parsecs away from the local arm in the direction of the anticentre.

Region I. Cygnus and Vulpecula provide a cross-section of the local spiral arm in the direction in which it winds into the nucleus of the galaxy. In this region is the association Vul I at a distance of 2 kpc on the inner side of the spiral arm [Morgan (1953), Kopylov (1958)]. Visual absorption averages about 3^m with a maximum of $4^m.5$ (Hiltner 1956). From the three-colour photometry by Serkowski (1963) it appears that the early type stars in this region have ultraviolet excesses compared with other reddened stars.

Region II. At the head of the Great Rift the Cygnus stars form a large complex of neutral and ionized hydrogen, OB stars and associations. The spiral arm is viewed tangentially in this direction. The whole region is rich in early type stars of which the earliest types O-B3 predominate (Serkowski 1963). They are distributed mostly between 1.5 and 2.5 kpc (Hiltner 1956). Absorption values appear to be similar to those for Vulpecula, but in the Cygnus II (VI Cygni) association

several of the bright stars suffer an extinction of 7^m or more and one highly polarised star of more than 10^m [Hiltner (1956), Schulte (1958)].

Region III. In Cepheus we look diagonally through the local arm to Cep I in the outer (Perseus) arm which makes an angle of about 30^o with the line of sight. This region lies a few degrees south of a nearby obscuring cloud but the extinction is everywhere less than 3^m (Hiltner, 1956). The obscuration in this part of the Milky Way is very variable (Risley, 1943).

Region IV. Region IV also covers a section of the local arm and an association (Cas V) in the Perseus arm. Cas V is a ring shaped aggregate of more than 100 bright OB stars (Reddish, 1961); it includes three galactic clusters and a condensation of early type stars around 6 Cas. Colour excesses are low so that the absorption is generally less than $2^m.5$ (Hiltner, 1956).

Region V. This region includes Perseus I, one of the groups tracing the Perseus arm. It is a very young association which forms the densest known concentration of early and late type supergiants, but lacks the dense clouds of obscuring matter found in most groups of this age in the other two spiral arms. In Perseus the line of sight makes an angle of 70^o with the direction of the spiral arm.

Region VI. Ori I, partly because of its nearness, is the most prominent feature on plates of this area. It lies in the local arm opposite to Cygnus at a distance of 500 pc (Morgan, 1953).

Although the nucleus still shows signs of star formation, the average age of the stars of the group is of the same order as in Per I (Herbig, 1958). There exist, however, clouds of gas and dust with masses of the order of 10^5 that of the Sun (Menon, 1958) in a volume no larger than Per I; there are only five supergiants. The greatest extinction occurs for the nuclear cluster ϑ Ori in the Orion nebula where 2^m absorption is observed.

2.5 Plates and Filters

In crowded Milky Way regions overlapping of spectra represents a serious problem. The problem is reduced partly by the low dispersion of the objective prism and greatly by the use of different emulsion-filter combinations to restrict the lengths of spectra.

For measures in the blue and ultra-violet, Ilford SRO (sensitivity 3300A - 4800A) or Kodak II-aO (sensitivity 3300A - 5000A) have been found suitable. For longer wavelengths Kodak IN (sensitivity 3300A - 9000A) has been used in combination with a Schott filter GG 13 which cuts out the blue and ultra-violet. The contrast is high and the sensitivity in the green low. Ilford Astra III (sensitivity 3300A - 6800A) because of its uniform sensitivity has been used to cover the green region in combination with filter GG 13.

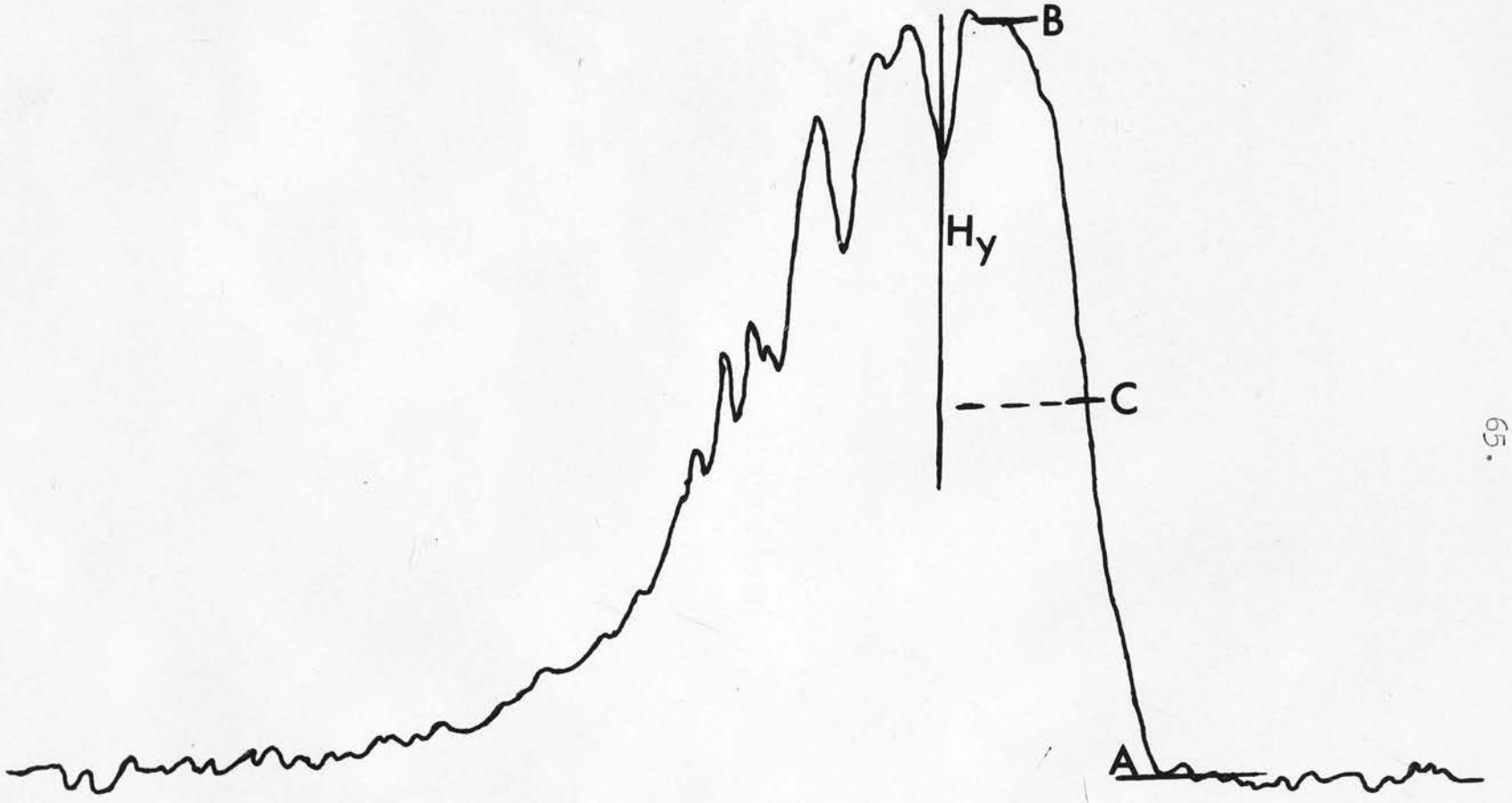

Fig. 9 Identification of wavelength from the tracing (emulsion Ilford SRO)

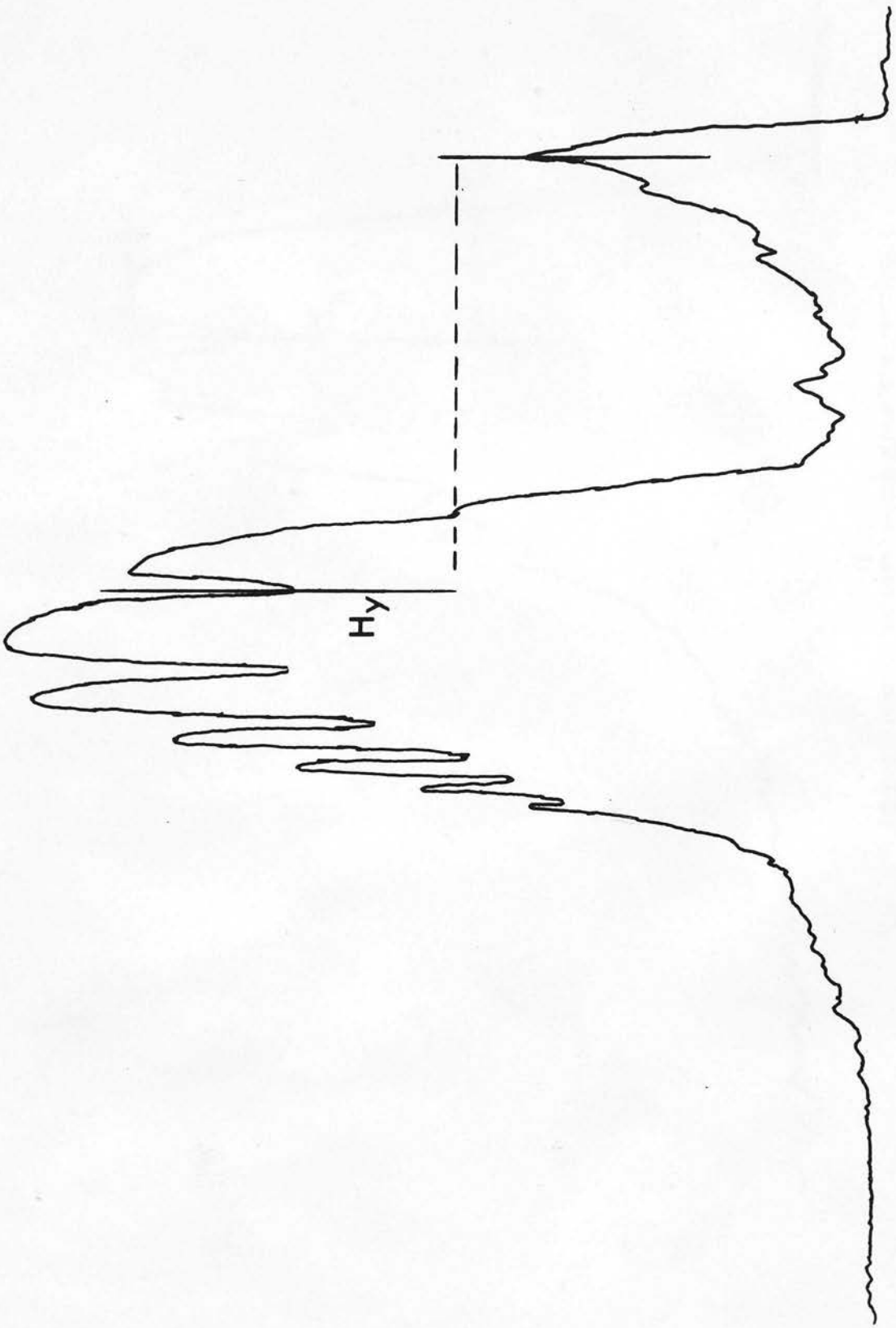

Fig. 10 Identification of wavelength from the tracing (emulsion Kodak IN).

CHAPTER III

MEASUREMENT AND REDUCTION

3.1 Wavelength Identification

The tracings of spectra were obtained with a Joyce Loebl double beam recording microdensitometer in which the tracing table and plate carriage are connected by a rigid lever. The lever ratio being exactly known, the distance between these lines can be accurately determined.

Hydrogen lines provide suitable reference points for wavelength identification for middle and late B-type stars. Difficulties arise when there are no spectral lines, as in the case of O and early B-type stars.

However, the sharp cut-off wavelength of the emulsions and also, on the infra-red plates, the sharp peak at 8000A which is partly due to the low dispersion of the prism at long wavelengths and partly to the high contrast of the IN emulsion, can be used as reference points. To illustrate the method Fig. 9 shows a tracing of a spectrum of a star on a blue sensitive SRO emulsion demonstrating spectral lines. The distance between H_γ and C (the mid-point of A and B) is assumed to be constant. The dispersion is sufficiently low that systematic effects due to differences in spectral types

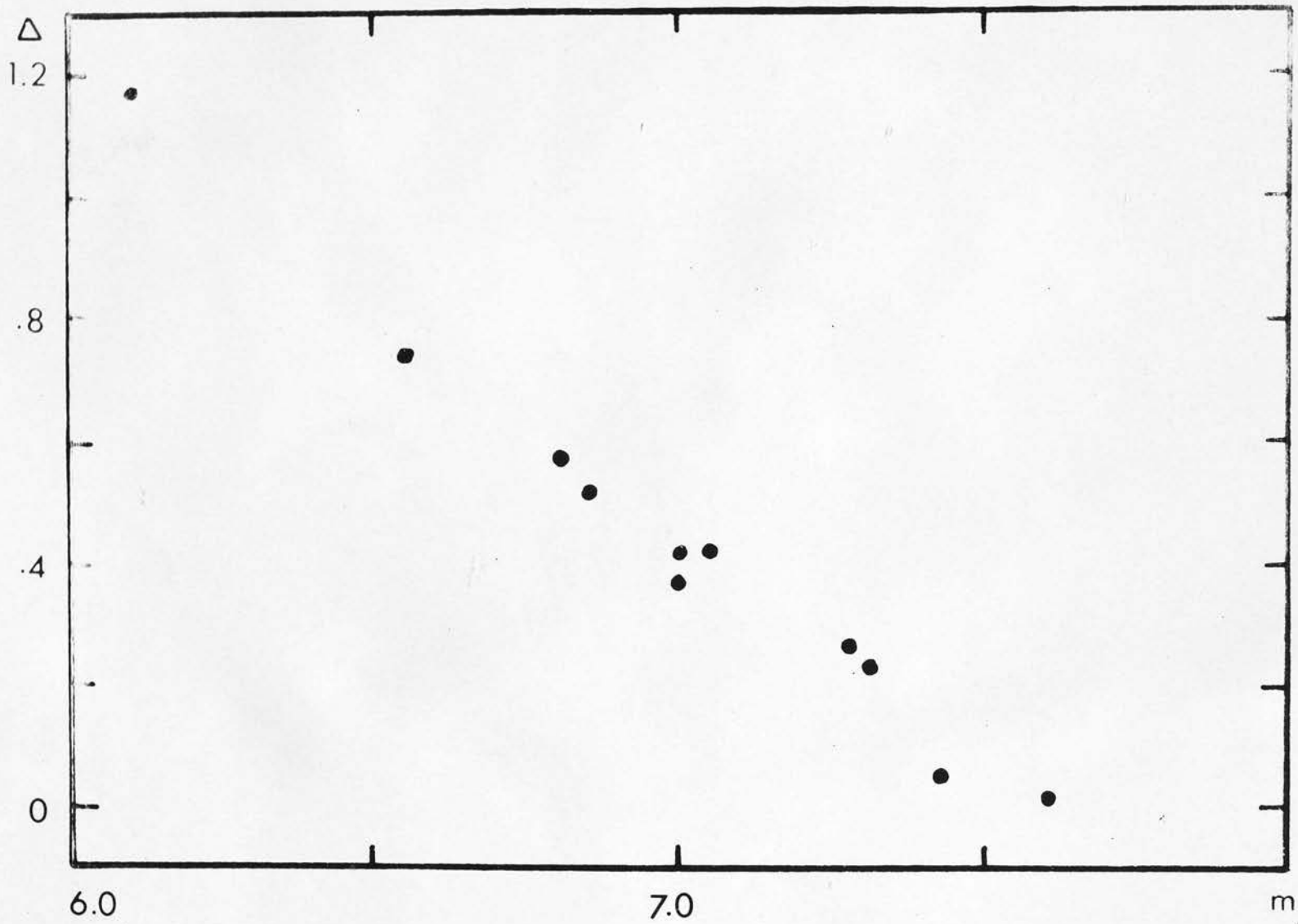

Fig. 11 Relation between "Baker" density, and Johnson's B magnitudes of Pleiades stars in a narrow spectral range.

can be neglected. For each plate the mean distance between H_γ and C is calculated from a number of stars showing hydrogen lines. This gives the position of H_γ with respect to C. The standard error of this mean distance is less than ± 0.5 mm. on the tracing which corresponds to 10A at H_γ. Wavelength identification from the sharp peak at 8000A on infra-red plates is illustrated in Fig. 10.

3.2 Calibration

For the calibration of plates the prism was crossed by the objective grating.

E. A. Baker (1949) has shown that if the blackening of plates is represented by the parameter $\Delta = \log_{10} \frac{1-T}{T}$ where T is the ratio of light through the image to that transmitted by the background, Δ is approximately linearly related to magnitude over a range of T = 0.002 to T = 0.98. This has been verified for Schmidt plates in two ways:-

(a) By plotting Δ's at 4220A against the B-magnitudes of Johnson's photo-electric standards for stars in a narrow range of spectral type in the Pleiades cluster. The plot is shown in Fig. 11.

(b) If $m_\lambda = \phi(\Delta)$ is a linear relation, the relation between the Δ's of centre and side images at

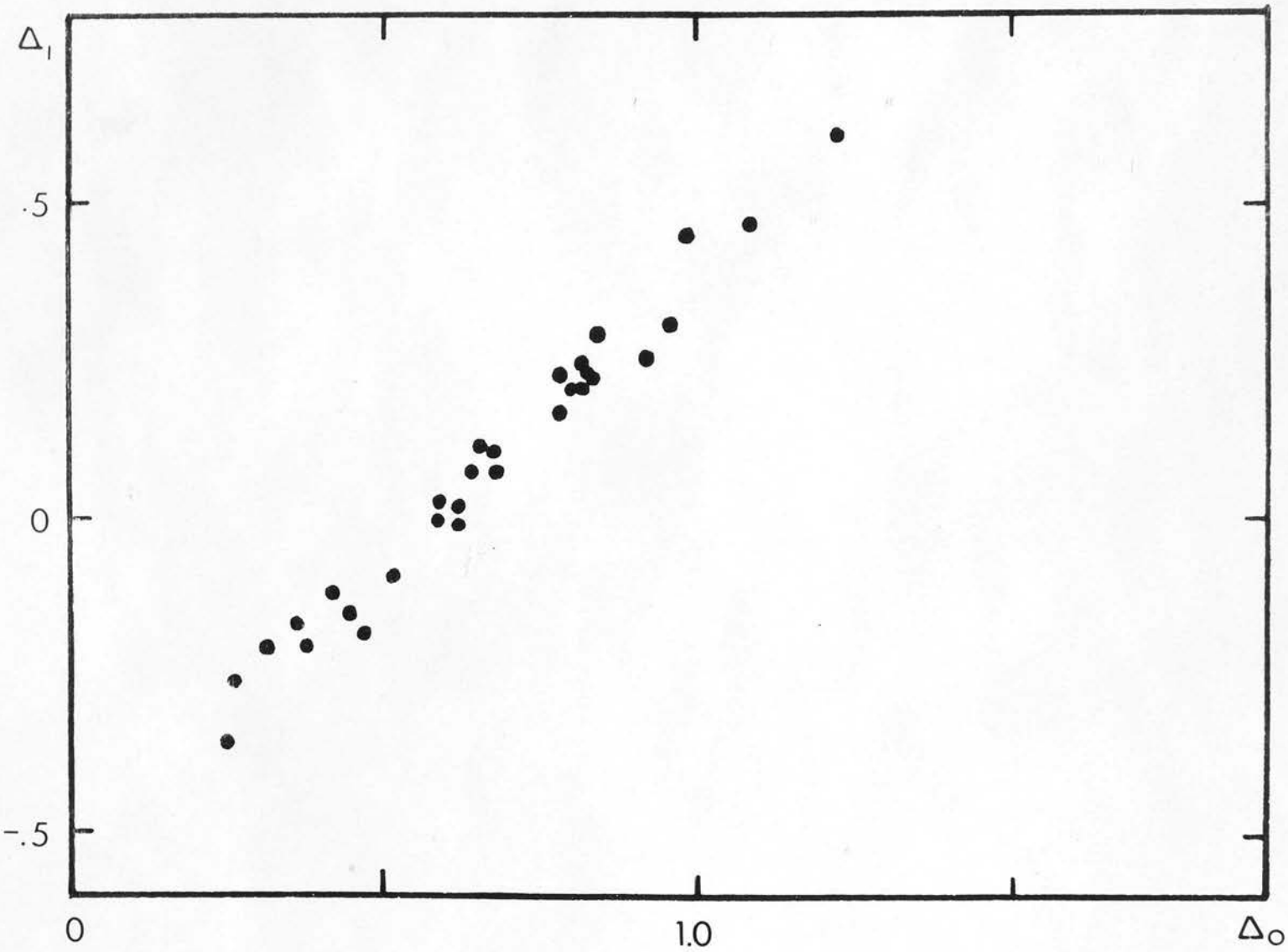

Fig. 12 Baker density of side image versus Baker density of centre image (emulsion Ilford SR0).

a given wavelength should be nearly linear. Fig. 12 shows that the plot of Δ_0 (centre) against Δ_1 (side) is almost a straight line.

The problem of deriving the calibration curve of a prism-crossed-by-grating plate is equivalent to solving the functional equations,

$$\Delta_0 = \psi(\Delta_1) \tag{14}$$

$$m_\lambda = \phi(\Delta) \tag{15}$$

Equation (14) represents a pair of densities such that their difference corresponds to a known magnitude difference equal to the Grating Constant.

Let $\Delta_0 - \Delta_1 = \delta\Delta$ denote the difference in densities of centre and side images, and G denote the Grating Constant. Because of the approximate linearity of (15) it can be assumed that $\frac{G}{\Delta_0 - \Delta_1} = \frac{\delta m}{\delta \Delta}$ represents the slope $\frac{dm}{d\Delta}$ at the middle point of Δ_0 and Δ_1. From (14) values of $\frac{dm}{d\Delta}$ can be obtained corresponding to values of $\frac{1}{2}(\Delta_0 + \Delta_1)$. If the zero of the magnitude scale is chosen so that m = 0 when $\Delta = 0$, the magnitude for a given value of Δ is given by

$$m = -\int_0^{\Delta} \frac{dm}{d\Delta}\, d\Delta \tag{16}$$

If Δ is not very large numerically, with sufficient accuracy

$$m = -\Delta \cdot \left(\frac{dm}{d\Delta}\right)_{\frac{1}{2}\Delta} \tag{17}$$

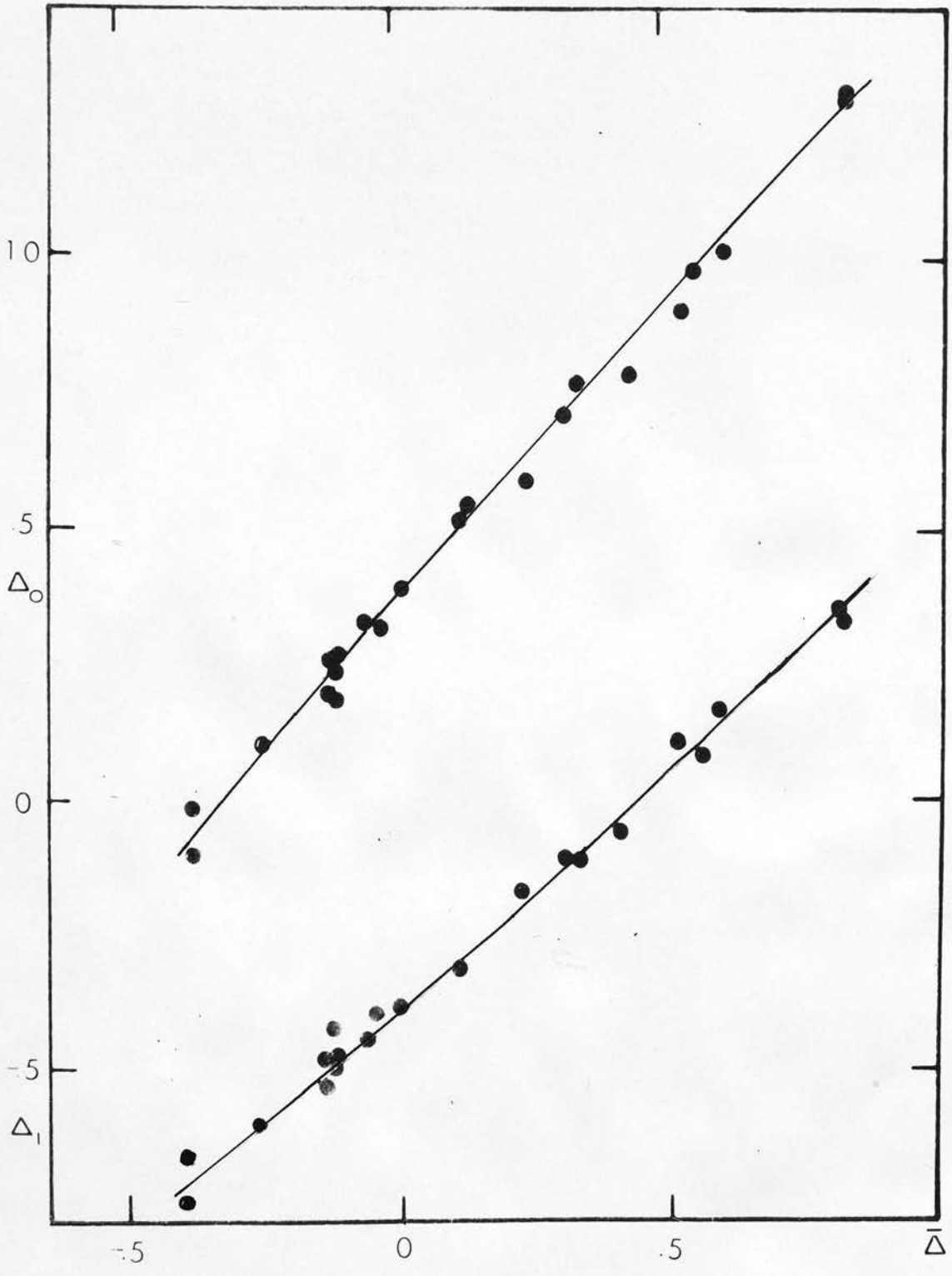

Fig. 13(a)

Baker density of centre images (Δ_0) and side images (Δ_1) versus $\frac{1}{2}(\Delta_0 + \Delta_1) = \bar{\Delta}$.

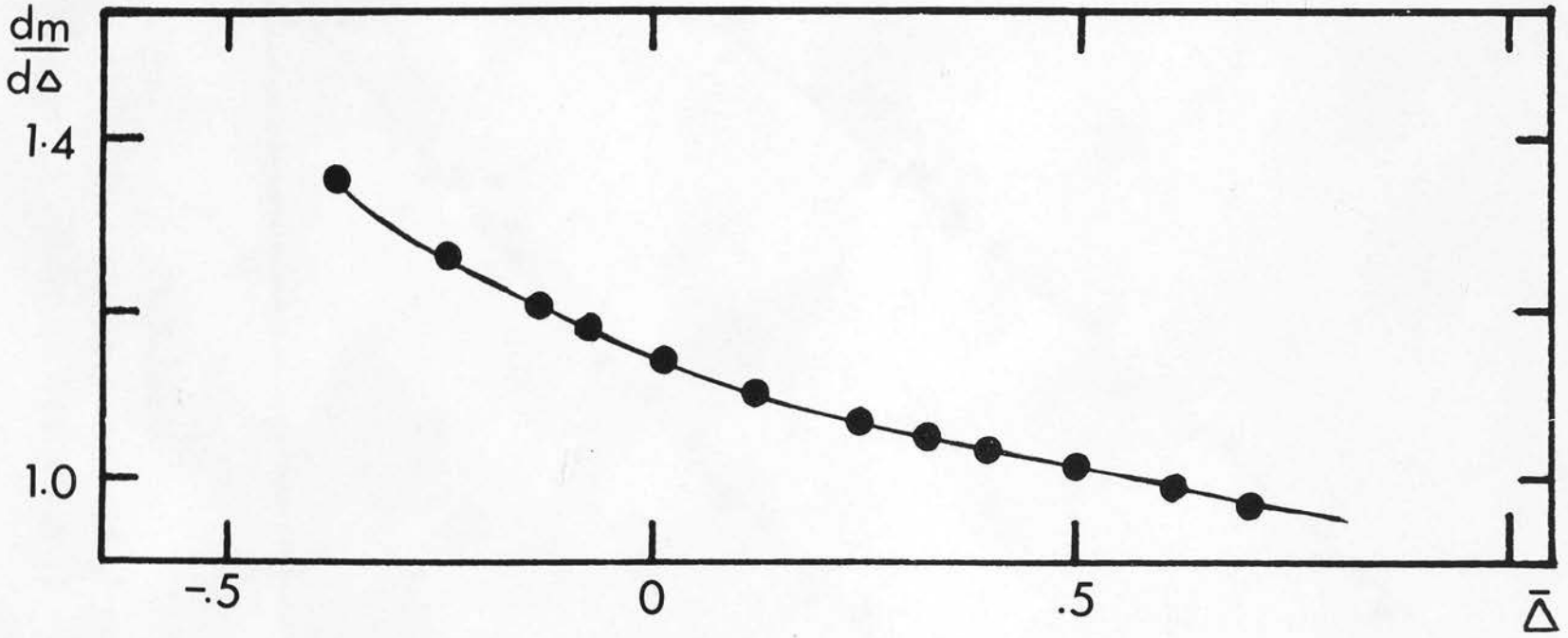

Fig. 13(b) $\frac{\text{Grating const.}}{\Delta_o - \Delta_1} = \frac{dm}{d\Delta}$ versus $\bar{\Delta}$.

Fig. 13(c)

Calibration curve obtained by integrating under the curve of Fig. 13(b).

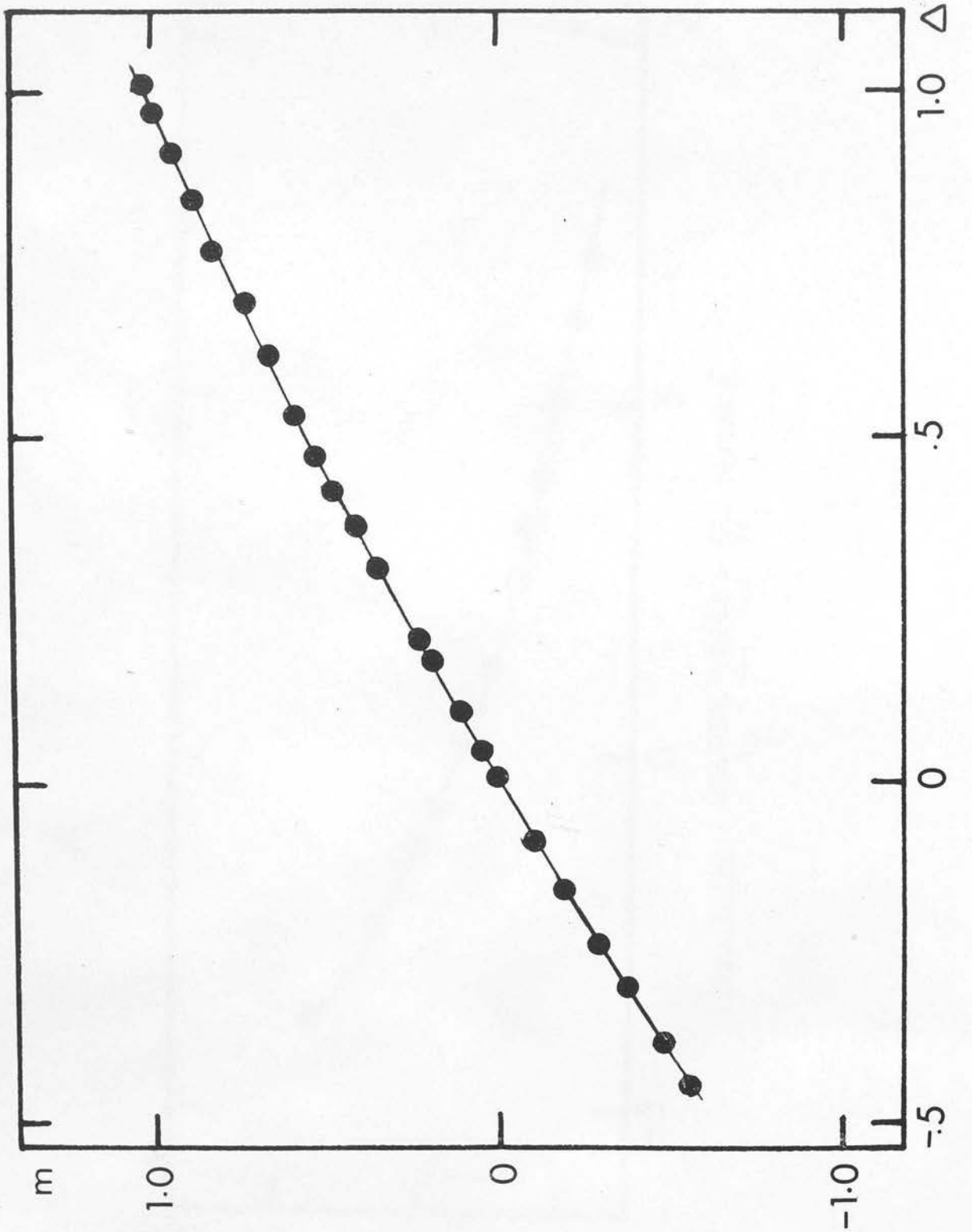

where $\left(\frac{dm}{d\Delta}\right)_{\frac{1}{2}\Delta}$ is the value of slope at $\frac{1}{2}\Delta$.

Having determined magnitudes for a set of values of m by integration of (16), (14) can be used to extend the range of the calibration curve.

This method of calibration may be modified in the following way. Instead of using (14), Δ_o and Δ_1 can be expressed as a function of $\frac{1}{2}(\Delta_o + \Delta_1)$ so that one can write,

$$\Delta_o = f_1(\overline{\Delta}) \qquad (18)$$

$$\Delta_1 = f_2(\overline{\Delta}) \qquad (19)$$

where $\overline{\Delta}$ is the mid-point of Δ_o and Δ_1.

From (18) and (19) one can obtain,

$$(\Delta_o - \Delta_1) = F(\overline{\Delta}) \qquad (20)$$

Therefore, $\therefore m = -G \int_0^{\Delta} \frac{1}{F(\bar{\Delta})}\, d\bar{\Delta}$ (21)

If (18), (19) and (20) are approximated by suitable polynomials, the integration can be performed analytically. This method has advantages for computer programming.

The modified method is illustrated in Fig. 13(a), 13(b) and 13(c).

The advantage of the integration method over the usual one is that the calibration curve can be derived from a large number of points.

3.3 Effect of Fog

It is not possible to obtain plates entirely free from sky fog. In addition, the surface brightness of a nebulous region may contribute to the fog level. Let I_f and I_s be the intensities of sky-light and star-light respectively and Δ_f and Δ_s the corresponding densities relative to the chemical fog level.

Let Δ be the observed density at any point of a star's spectrum which will correspond to the sum of the intensities of superimposed sky-light and star-light.

One can write,

$$\Delta_f = \phi(I_f) \qquad (22)$$

$$\Delta_s = \phi(I_s) \qquad (23)$$

$$\Delta = \phi(I) \text{ where } I = I_f + I_s \qquad (24)$$

Now

$$\phi(I) \neq \phi(I_f) + \phi(I_s)$$

but can be approximated to

$$\phi(I) = \phi(I_f) + \phi(I_s) + \psi(I_f, I_s) \qquad (25)$$

where ψ is an unknown function.

(22) to (25) give

$$\Delta = \Delta_f + \Delta_s + \psi$$

$$\text{or } (\Delta - \Delta_f) = \Delta_s + \psi \qquad (26)$$

If the density of the star's image be measured with respect to the fog level in the neighbourhood of the

star's image for centre and side spectra of the star, one obtains

$$\Delta_o = \phi(I_{so}) + \psi(I_{so}, I_f)$$

$$\Delta_1 = \phi(I_{s1}) + \psi(I_{s1}, I_f) \qquad (27)$$

where the subscripts 0 and 1 denote the quantities corresponding to the centre and side spectrum respectively.

The process of calibration consists in determining a function of $(\Delta_o - \Delta_1)$ so that

$$F(\Delta_o - \Delta_1) = G \qquad (28)$$

where $G = -2.5 (\log I_{so} - \log I_{s1})$.

The unknown function $\psi(I_s, I_f)$ is empirically determined and included in (28).

Thus relation (28) represents the calibration curve of the plate for a given fog level which is in practice the mean of fog levels in the neighbourhood of the star-images used for calibration.

If in any part of the plate the background fog level f^1 differs from the mean fog level $\bar{f}$, the calibration function for that part will be slightly different from (28) and can be written as

$$F\left\{ (\Delta_o - \Delta_1)_{f^1} + \delta\Delta \right\} = G \qquad (29)$$

where $\delta\Delta$ is a correction term. In other words, if

the densities of centre and side spectra of star images relative to the neighbouring fog level are converted to magnitudes from (28) the difference between the two magnitudes should be equal to the adopted value of G. Any deviation from this value of G indicates an error introduced by graininess and variation in fog level. This gives an objective way of determining the error of the calibration curve. If ε_1 and ε_2 be errors in the magnitudes of the centre and side spectra derived from the calibration curve, then assuming $\varepsilon_1 = \varepsilon_2$ the error of the calibration curve is given by

$$\varepsilon = \pm \sqrt{\frac{(\Delta G)^2}{2n}} \qquad (30)$$

where ΔG = (observed value of G) - (adopted value of G)

n = number of stars.

The mean error is found to be $\pm 0^m.04$.

3.4 Determination of Monochromatic Magnitude Differences

The microdensitometer records density ($D = \log_{10} 1/T$) directly and linearly within the density range of the instrument. An absolute density scale was constructed from the known densities of three neutral filters. Resolution depends on the width of the slit while integration of graininess depends on the area of the slit. By increasing the height of the slit as far as possible

the width of the slit can be adjusted until optimum conditions are obtained. However, for a given height tracings taken with the slit width of 30μ to 60μ do not show any significant difference. In general, the width of the slit along the length of the spectrum was 40μ on the plate and the height across the spectrum was 0.2 mm. The width corresponded therefore to about 200A at 8000A, 70A at 5000A and 16A at 3500A.

Absolute density values were converted to "Baker" densities ($\Delta = \log_{10} \frac{1-T}{T}$). Monochromatic magnitudes derived from Δ have different zero-points for different wavelengths. However, the monochromatic magnitude-difference at a given wavelength for a pair of stars on the same plate is independent of the zero-point of the magnitude scale. If the magnitudes have to be compared among stars which appear on two different plates, it is necessary that the two plates have a region in common. Comparing the magnitudes of stars common to both plates, a transformation equation of the kind

$$x_\lambda - y_\lambda = K_\lambda \qquad (31)$$

where x_λ and y_λ are the magnitudes of the same star on the plates X and Y respectively and K_λ is a constant, can be obtained for each wavelength.

Since the plates have not been taken at the same

zenith distance, the magnitudes of the stars common to both plates which are used to determine the transformation equation (31) are subject to corrections for atmospheric extinction, and K_λ is therefore numerically equal to the sum of the difference in zero-points of magnitude scale and the difference in atmospheric extinction for wavelength λ .

The difference of monochromatic magnitude for a pair of stars is corrected for atmospheric extinction by the formula

$$\delta m_\lambda = a_\lambda (\text{Sec } Z_1 - \text{Sec } Z_2) \qquad (32)$$

where δm_λ = difference in atmospheric extinction for wavelength λ

a_λ = extinction co-efficient for vertical transmission

Z_1, Z_2 = the zenith distances of stars.

For the present work a_λ has been computed from Washington observations (1908) as well as from Chalonge's (1952) formula. The mean value has been adopted. The numerical value of δ(Sec Z) being small generally less than 0.05 error due to uncertainty in the value of a_λ is negligible.

However, in future a_λ will be determined from Schmidt plates thus:

The plates on the same region having been taken at

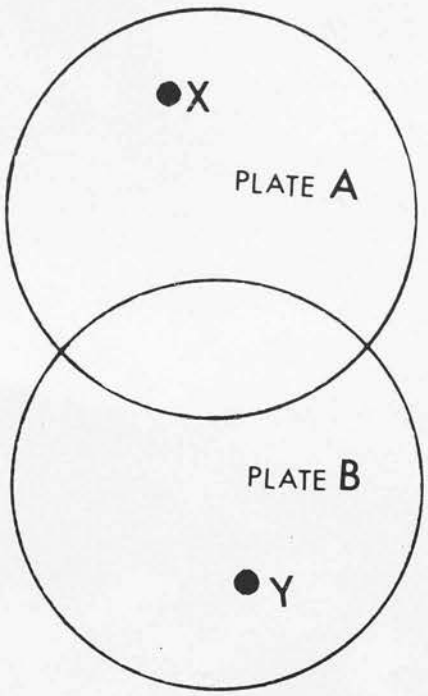

Fig. 14

Two plates having a region in common.

different zenith distances from the observed magnitude differences of the two stars most widely separated on the plate one can obtain a set of equations of the form

$$(\Delta m_\lambda)_{true} - (\Delta m_\lambda)_{obs.} = a_\lambda . \delta(\text{Sec } Z) \qquad (33)$$

where

Δm_λ = monochromatic magnitude-difference

$\delta(\text{Sec } Z)$ = difference in values of Sec Z.

A least squares solution of (33) gives the value of a_λ. Reliable values of a_λ can be obtained from the reduction of a large number of plates taken over a period of six months.

When the reddened and comparison star do not appear on the same plate, the magnitude difference for the pair is corrected for atmospheric extinction in the following way:-

Let m_λ and $m_\lambda{}^1$ be the monochromatic magnitudes of X, a reddened star on plate A, and of Y, a comparison star on plate B, respectively (Fig. 14).

Let Z_X, $\bar{Z}_A$ be the zenith distances of X and the centre of the overlapping region on plate A; and Z_y, $\bar{Z}_B$ zenith distances of Y and the centre of the overlapping region on plate B.

$(\Delta m)_{\lambda obs} = m_\lambda - (m_\lambda{}^1 + K_\lambda)$, K_λ being given by (31).

The correction for atmospheric extinction is

$$\delta m_\lambda = a_\lambda (\text{Sec } Z_x - \text{Sec } Z_y)$$
$$= a_\lambda \left\{ (\text{Sec } Z_x - \text{Sec } \bar{Z}_A) + (\text{Sec } \bar{Z}_A - \text{Sec } \bar{Z}_B) + (\text{Sec } \bar{Z}_B - \text{Sec } Z_y) \right\}$$

But K_λ = difference in zero-point of magnitude scale for wavelength λ + a_λ (Sec $\bar{Z}_A$ - Sec $\bar{Z}_B$)

Therefore,

$$(\Delta m_\lambda)_{true} = (\Delta m_\lambda)_{obs.} + a_\lambda \left\{ (\text{Sec } Z_x - \text{Sec } \bar{Z}_A) + (\text{Sec } \bar{Z}_B - \text{Sec } Z_y) \right\} \quad (34)$$

3.5 Normalisation of Reddening Curves

The monochromatic magnitude difference between a reddened and a comparison star consists of two parts: an intrinsic magnitude difference depending on absolute magnitudes and the difference in the effects of interstellar absorption on these two stars. Thus,

$$\Delta m_\lambda = dm + (A_\lambda - a_\lambda) \quad (35)$$

where dm = intrinsic magnitude difference,

A_λ, a_λ = absorption at λ for a reddened and a comparison star respectively.

If (i) the spectral energy distribution of the two stars is identical, and (ii) a_λ is small in comparison with A_λ, by plotting Δm_λ against $1/\lambda$, a function of the form

$$A_\lambda = f(1/\lambda) + \text{constant} \quad (36)$$

is derived which with suitable normalisation gives the

extinction law

$$A_\lambda = \phi\,(1/\lambda) \qquad (37)$$

The method of normalisation adopted for the present work is as follows:-

Two regions are chosen, one between $1/\lambda = 1.25\,\mu^{-1}$ and $1.43\,\mu^{-1}$, and the other between $1/\lambda = 2.22\,\mu^{-1}$ and $2.37\,\mu^{-1}$. A smooth curve is drawn through the observed points in each of these regions. The mean points correspond to Δm_λ at $1/\lambda = 1.34\,\mu^{-1}$ in the red and $1/\lambda = 2.28\,\mu^{-1}$ in the blue. The normalising factor is the reciprocal of the slope of the line joining these two mean points. All observed magnitude-differences have been multiplied by this factor. The zero-point of Δm_λ has been adjusted by making Δm_λ at $1/\lambda = 2.22\,\mu^{-1}$ read off from the smooth curve equal to unity.

Condition (i) of equation (36) is approximately fulfilled by considering a pair of stars of the same spectral type and luminosity class which are situated in the same region of the galaxy. The comparison of pairs of stars can be made in two steps:

In the first step highly reddened stars are compared with neighbouring moderately reddened stars of the same spectral type;

In the second step the moderately reddened stars are compared with similar nearby unreddened or slightly

reddened stars.

If the reddening curves derived in these two steps are identical, reddening effects for both groups of stars must be the same, and the derived function must represent the extinction by the interstellar matter which is distributed over the distance at which the observed stars are situated.

On the other hand, if the reddening curves are systematically different no immediate conclusion can be reached. Such a difference may be due either to a difference in the effects of interstellar absorption or to peculiarities in the stars themselves. The latter case may be investigated further by comparing reddening curves obtained from O-stars with those derived from B-stars.

3.6 Sources of Error

The main sources of error are (a) graininess, (b) overlapping, (c) uncertainty in wavelength identification, and (d) uncertainty in spectral types.

(a) The standard error of a single measurement of monochromatic magnitude at any given wavelength due to graininess is given in Table 8, Section 4.2, and is about $\pm 0^m.05$.

(b) Errors due to overlapping of spectra are

somewhat uncertain. No spectra have been measured which were obviously disturbed by overlapping. In order to estimate the effect on spectra of overlapping by faint other spectra, long and short exposure plates have been compared. These show that errors in monochromatic magnitude on account of overlapping should not exceed ± 0.02 magnitudes.

(c) Errors arising from uncertainty in wavelength identification depend on the slope of the tracings of the spectra. The tracing in the blue and visible part of the spectrum is reasonably flat for the emulsions which have been used and this error is negligible. The tracing has a steep slope in the red and ultraviolet, and monochromatic magnitudes may be in error by $\pm 0^m.05$ in the red and $\pm 0^m.03$ in the ultraviolet.

(d) Error resulting from uncertainty in the spectral types of stars is inherent in the method of comparison of two stars. The wavelength dependence of the mean error in the magnitude difference for a pair of stars due to error in spectral types reduced to unit normalising factor, is shown in Table 6(a).

Combining all the errors, the standard error in the monochromatic magnitude-difference for a given wavelength from a pair of stars is given by

$$\varepsilon_{\Delta m_\lambda} = \pm\sqrt{\frac{1}{n_\lambda}} \cdot \sqrt{2\varepsilon_a^2 + 2\varepsilon_b^2 + 2\varepsilon_c^2 + \varepsilon_d^2} \qquad (38)$$

where n_λ = the number of measures for the given pair at wavelength λ.

Taking $n_\lambda = 2$ and assuming that the error in spectral type is ± 1 subclass (which is the uncertainty in the MK classifications used) values of ε_λ have been calculated for different spectral ranges and are given in Table 6(b).

Large errors in the blue and ultraviolet are mainly due to errors arising from uncertainty of spectral types which are greater than any photometric errors whether photographic or photo-electric. The accuracy of the results could be greatly improved if one could increase the accuracy of spectral classification. Alternatively, if the reddening law is uniform in the region investigated, the effect of errors in spectral classification may be reduced by obtaining a mean reddening curve from measurements of many stars.

TABLE 6(a)

Error in Δm_λ due to Uncertainty in Spectral Type

$\frac{1}{\lambda}$ (μ^{-1})	Error in monochromatic mag. diff. from one pair of stars due to error of ±1 subclass in spectral type	$\frac{1}{\lambda}$ (μ^{-1})	Error in monochromatic mag. diff. from one pair of stars due to error of ± subclass in spectral type
1.25	0	2.26	±.01
1.35	±.01	2.37	.01
1.43	.01	2.41	.02
1.54	.01	2.48	.05
1.67	.02	2.54	.06
1.75	.02	2.59	.08
1.82	.02	2.62	.10
1.92	.03	2.67	.10
2.0	.03	2.72	.10
2.04	.03	2.78	.15
2.20	.03	2.82	.15
2.22	0	2.86	.15
		2.91	.16

TABLE 6(b)

Standard Error in Δm_λ

λ	8000	7000	5000	4500	4220	4030	3858	3670	3450
ε_a	±.04	±.04	±.06	±.04	±.05	±.06	±.05	±.05	±.05
ε_b	.02	.02	.02	.02	.02	.02	.02	.02	.02
ε_c	0	.05	0	0	0	0	.03	.03	.03
ε_d	0	0	.02	0	.01	.04	.06	.08	.16
$\varepsilon_{\Delta m_\lambda}$	±.05	±.07	±.06	±.05	±.06	±.07	±.08	±.08	±.13

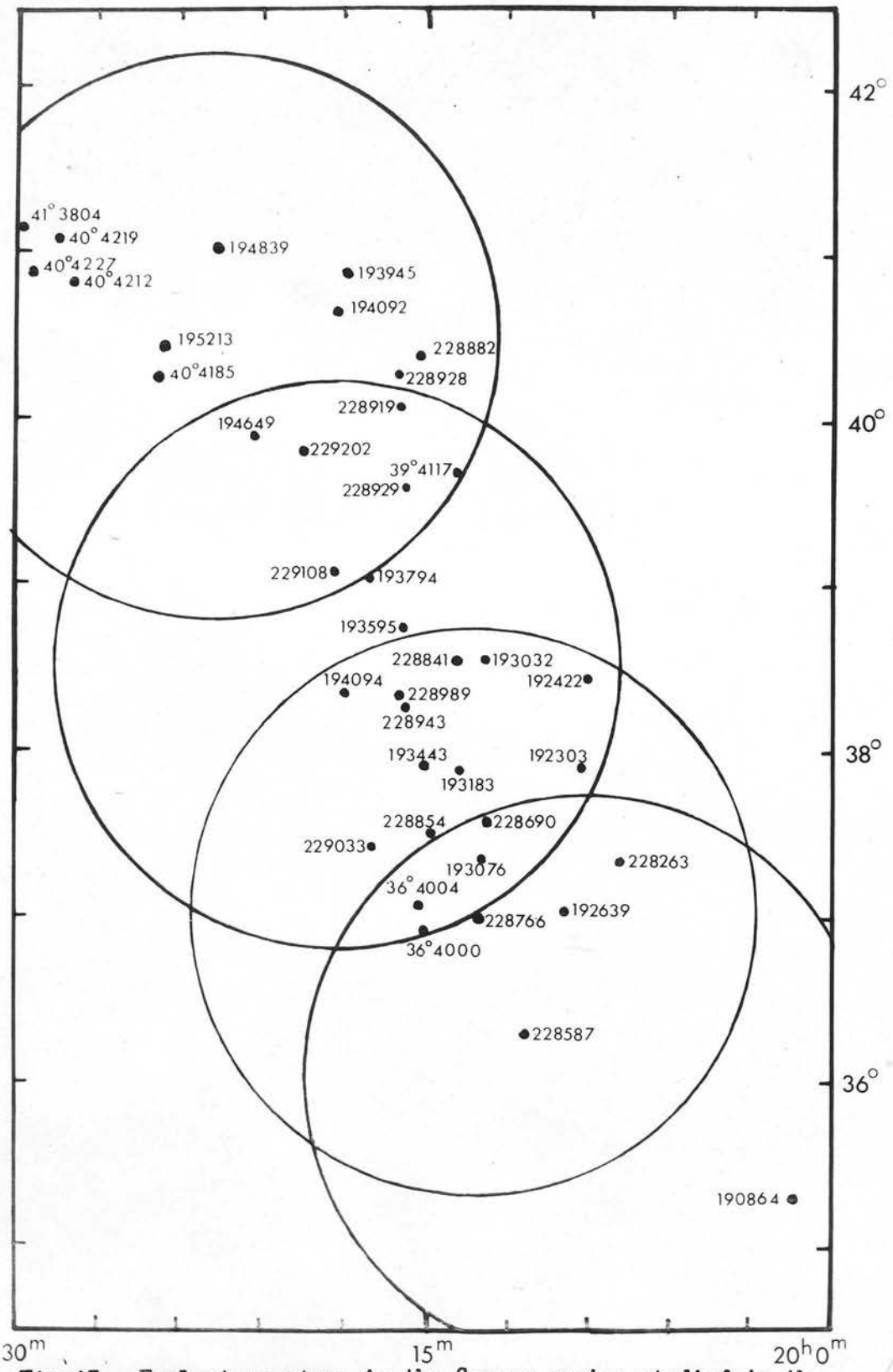

Fig.15. Early type stars in the Cygnus region studied in the present work for the wavelength dependence of interstellar absorption. Circles denote the areas covered by the plates.

CHAPTER IV

RESULTS FOR CYGNUS

4.1 Details of plates

A region of 30 square degrees centred on (20^h15^m,38°) has been covered by four sets of plates. The positions of the areas observed are shown in Fig. 15. The plates were taken during the winters of 1962 and 1963. For each position two series of plates were taken, one series with prism crossed-by-grating, and the other series with prism only to reach fainter magnitudes. Details of the plates are given in Table 7.

Having calibrated "Prism + Grating" plates by means of grating images, relative monochromatic magnitudes at a number of wavelengths were obtained for a large number of stars. These relative magnitudes were then used to calibrate prism plates taken without grating.

For IN-emulsions, no systematic variations in the shape of the calibration curves were found for wavelengths ranging from 8000A to 6000A and from 4500A to 3650A. This feature of the IN-emulsion has already been found by Schalén (1961). For SRO-emulsions the shape of the calibration curves did not change with wavelength over the range from 4500A to 3600A.

For this reason, a single calibration curve has been used for each IN- or SRO- plate for all wavelengths to derive magnitudes from densities.

TABLE 7

RA 1950	Dec. 1950	Series	Emulsion and Filter	Total No.	Exposures
20^h12^m	$35^\circ\ 30'$	Prism & Grating	IN	2	9^m, 9^m
	"	"	Astra III	1	15^m
		Prism	IN + 2CC 50Y	1	15^m
20^h14^m	$37^\circ\ 30'$	Prism & Grating	IN + GG 13	1	30^m
		"	SRO	2	15^m, 20^m
		"	Astra III + GG 13	1	20^m
		Prism	IN	2	$5\frac{1}{2}^m$, 14^m
		"	SRO	2	8^m, 20^m
		"	Astra III + GG 13	2	16^m, 25^m
20^h18^m	$39^\circ\ 30'$	Prism & Grating	IN	1	12^m
		"	Astra III	1	40^m
		Prism	IN	2	$5^m.5$, 14^m
		"	SRO	1	9^m
		"	Astra III + GG 13	2	25^m, 35^m
20^h20^m	41°	Prism & Grating	IN	1	10^m
		"	Astra III + GG 13	2	45^m, 60^m
		Prism	IN	2	$5^m.5$, $5^m.5$
		"	SRO	2	8^m, 15^m

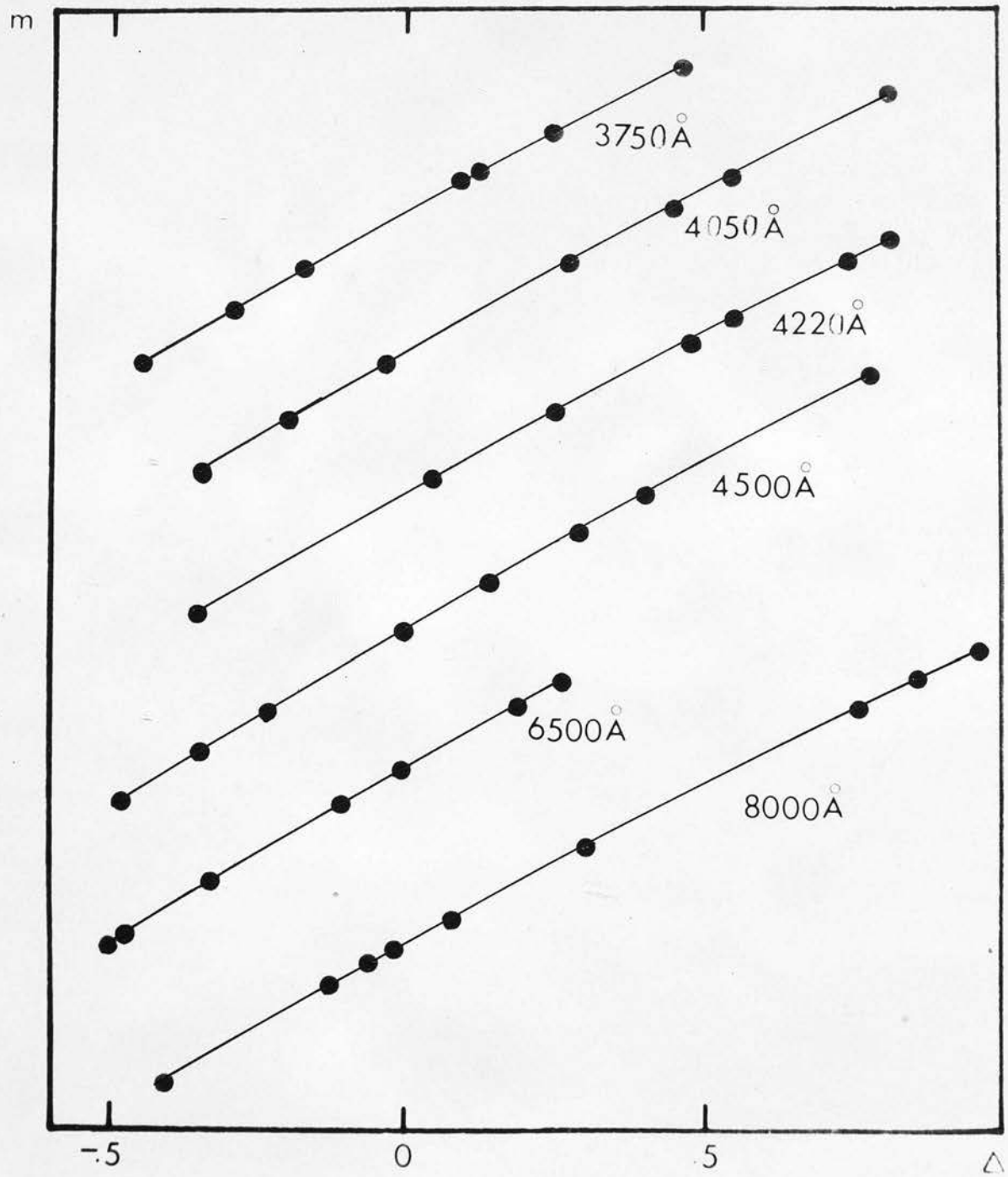

Fig. 16(a) Calibration curves of a Kodak IN- emulsion at different wavelengths. Abscissa: Baker density (Δ); Ordinate: magnitude (m).

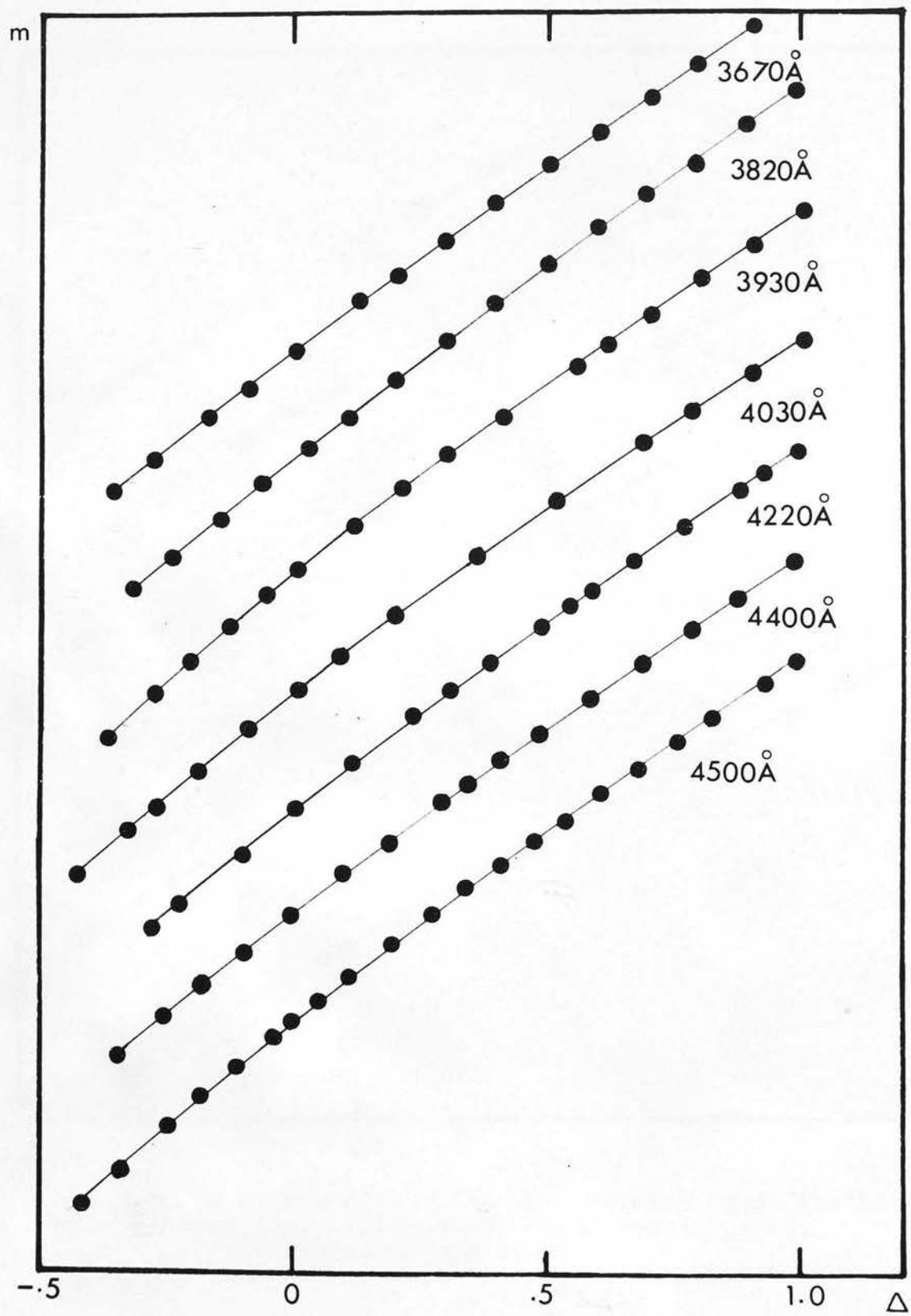

Fig.16(b) Calibration curves of an Ilford SRO- emulsion at different wavelengths. Abscissa: Baker density (Δ); Ordinate: magnitude (m).

Fig. 16(a) and 16(b) show the calibration curves at several wavelengths for IN- and SRO- plates.

For Ilford Astra III a systematic change in the slope of the calibration curves was found even for the wavelength from 6000A to 4500A. Separate calibration curves have been used therefore for extending each wavelength at which magnitudes had been measured on Astra III plates.

4.2 Photometric Errors and Comparison with Photo-Electric Work

The average standard error in a single measurement of monochromatic magnitude has been calculated from the formula

$$\varepsilon = \pm\sqrt{\frac{1}{n}\sum\frac{v^2}{m}} \qquad (39)$$

where n = number of stars, each star appearing on m plates,

$\frac{v^2}{m}$ = mean square deviation of the mean magnitude of each star.

Table 8 shows the average standard errors in a single measurement of monochromatic magnitude at different wavelengths. This and other sources of error have been discussed in Section 3.5.

TABLE 8

Average Standard Error of a Single Measurement of Monochromatic Magnitude

λ	8000A	5000A	4500A	4220A	4030A	3858A	3670A
ε	±0.04	±0.06	±0.04	±0.05	±0.06	±0.05	±0.05

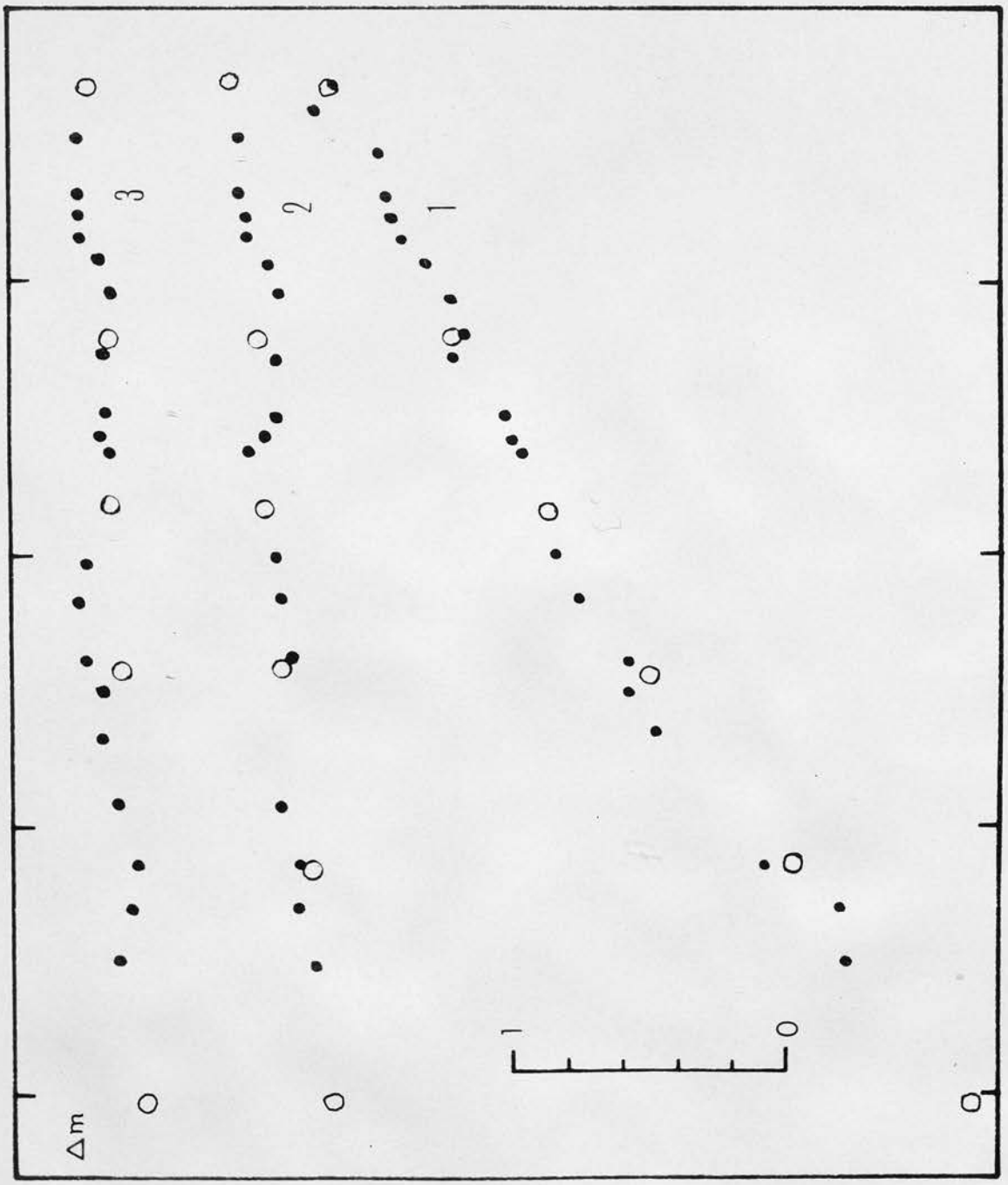

Fig.17. Comparison between Edinburgh measures and Stebbins and Whitford's measures. Open circles denote Stebbins and Whitford's measures, filled circles denote Edinburgh measures.

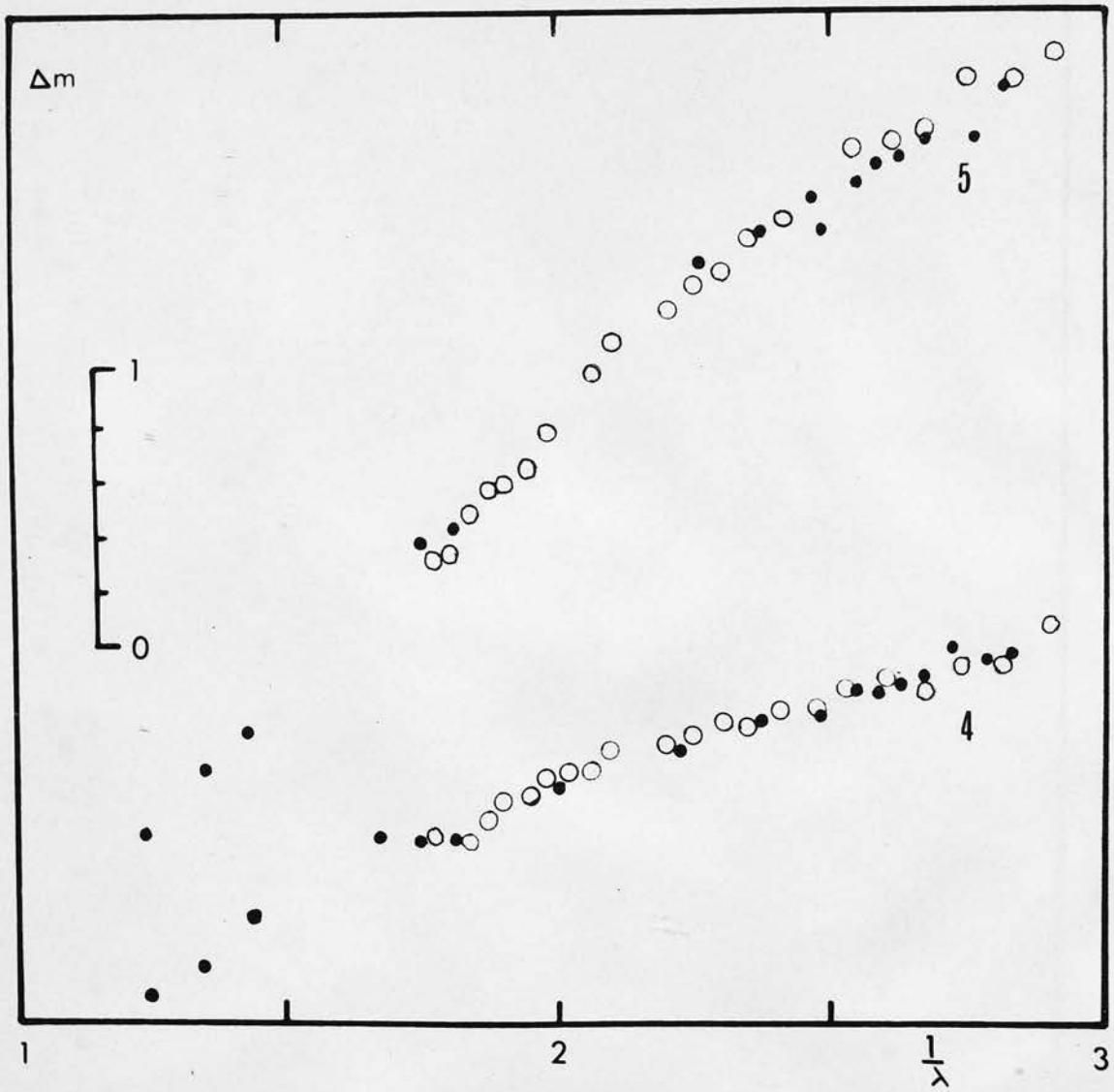

Fig.18 Comparison between Edinburgh measures and Rodgers' measures.

4. HD 228854 - HD 193595
5. BD 40°4227- HD 193595

Open circles denote Rodgers' measures and filled circles denote Edinburgh measures.

Fig. 19

Comparison between Edinburgh measures and Johnson and Borgman's measures.

6. HD 195213 - HD 193682
7. HD 195213 - HD 193595
8. HD 193682 - HD 193514
9. HD 193595 - HD 193514

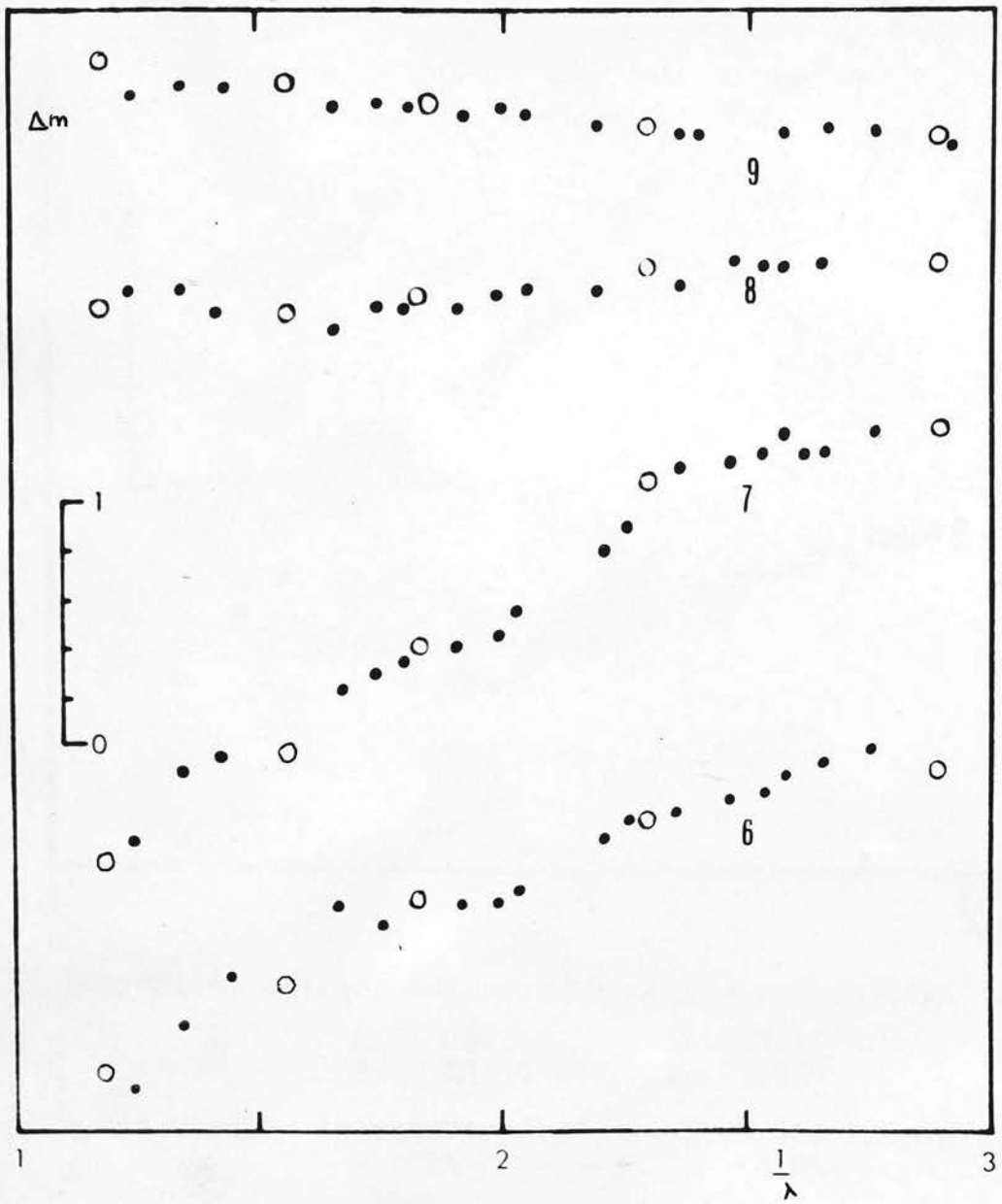

Open circles denote Johnson and Borgman's measures and filled circles denote Edinburgh measures.

Magnitude differences for the following pairs of stars of the same spectral type have been compared with Stebbins and Whitford's (1943, 1945) measures

HD 194839 - HD 193443

HD 190919 - HD 191201

HD 193443 - HD 192639

The comparison is shown in Fig. 17. The effective wavelengths of the filter of the six-colour photometry have been adopted from Whitford's (1958) paper. Since Stebbins and Whitford have reduced the magnitudes relative to a mean value for the B-, G- and R- filters the magnitude differences for the pairs of stars derived from their measures differ by a constant from the actual differences. However, no constant has been added to Stebbins and Whitford's measures to derive Fig. 17.

In Fig. 18 reddening curves from two pairs of stars are compared with the curves derived from Rodger's (1961) data on the same pairs of stars.

Comparison with Johnson and Borgman's (1964) measures of the following pairs of stars is shown in Fig.19.

HD 195213 - HD 193682

HD 195213 - HD 193595

HD 193682 - HD 193514

HD 193595 - HD 193514

As shown in Figs. 17-19 the agreement with photo-electric measures is satisfactory.

TABLE 9

O-stars

Reddened Star

(Pairs of stars compared)

Serial No.	HD	BD	RA_{1900}	Dec_{1900}	Sp. Type	V	E_{B-V}	m-M
1	228766	$36^{\circ}3991$	$20^{h}13^{m}.8$	$37^{\circ}00'$	06f or WR	9.14	.97	-
2	228841	$38^{\circ}4000$	$20^{h}14^{m}.8$	$38^{\circ}34'$	07.5p	8.93	.89	11.4
3	228854	$35^{\circ}4062$	$20^{h}15^{m}.0$	$36^{\circ}02'$	08:	8.93	1.02	11.0
4	228989	$38^{\circ}4025$	$20^{h}16^{m}.7$	$38^{\circ}23'$	08Vnn	9.72	1.08	11.1
5	194094	$38^{\circ}4043$	$20^{h}18^{m}.7$	$38^{\circ}24'$	09 III	9.02	.90	12.02
6	229202	$30^{\circ}4162$	$20^{h}19^{m}.8$	$39^{\circ}50'$	08V:	9.53	1.17	11.1
7(i)	229232	$38^{\circ}4070$	$20^{h}20^{m}.3$	$38^{\circ}47'$	05f	9.53	1.14	11.7
(ii)	"	"	"	"	"	"	"	"
8	194649	$39^{\circ}4177$	$20^{h}21^{m}.7$	$39^{\circ}54'$	06.5	9.0	1.27	10.5
9(i)	195213	$40^{\circ}4187$	$20^{h}24^{m}.9$	$40^{\circ}28'$	07	8.74	1.17	10.4
(ii)	"	"	"	"	"	"	"	"
10		$40^{\circ}4212$	$20^{h}28^{m}.0$	$40^{\circ}52'$	09	10.29	1.94	9.1
11		$40^{\circ}4219$	$20^{h}28^{m}.6$	$41^{\circ}06'$	08	10.22	1.50	10.8
12(i)		$40^{\circ}4227$	$20^{h}29^{m}.6$	$40^{\circ}48'$	06f	9.05	1.59	9.7
(ii)		"	"	"	"	"	"	"
13(i)		$41^{\circ}3804$	$20^{h}30^{m}.2$	$40^{\circ}12'$	09.5Ia	9.89	1.83	10.6
(ii)		"	"	"	"	"	"	"

TABLE 9

Comparison Star

	HD	BD	RA_{1900}	Dec_{1900}	Sp. Type		E_{B-V}	m-M
	193595	$38^{\circ}4012$	$20^{h}15^{m}.9$	$38^{\circ}44'$	07	8.73	.67	12.1
	193595	$38^{\circ}4012$	$20^{h}15^{m}.9$	$38^{\circ}44'$	07	8.73	.67	12.1
	193595	$38^{\circ}4012$	$20^{h}15^{m}.9$	$38^{\circ}44'$	07	8.73	.67	12.1
	193595	$38^{\circ}4012$	$20^{h}15^{m}.9$	$38^{\circ}44'$	07	8.73	.67	12.1
	193595	$38^{\circ}4012$	$20^{h}15^{m}.9$	$38^{\circ}44'$	07	8.73	.67	12.1
	192639	$36^{\circ}3958$	$20^{h}10^{m}.8$	$37^{\circ}03'$	08f	7.11	.66	-
(i)	190864	$35^{\circ}3949$	$20^{h}01^{m}.9$	$35^{\circ}19'$	06	7.76	.52	11.6
(ii)	193595	$38^{\circ}4012$	$20^{h}15^{m}.9$	$38^{\circ}44'$	07	8.73	.67	12.1
	193595	$38^{\circ}4012$	$20^{h}15^{m}.9$	$38^{\circ}44'$	07	8.73	.67	12.1
(i)	193595	$38^{\circ}4012$	$20^{h}15^{m}.9$	$38^{\circ}44'$	07	8.73	.67	12.1
(ii)	193682	$37^{\circ}3894$	$20^{h}16^{m}.5$	$37^{\circ}30'$	05	-	.81	-
	193595	$38^{\circ}4012$	$20^{h}15^{m}.9$	$38^{\circ}44'$	07	8.73	.67	12.1
	193595	$38^{\circ}4012$	$20^{h}15^{m}.9$	$38^{\circ}44'$	07	8.73	.67	12.1
(i)	190864	$35^{\circ}3949$	$20^{h}01^{m}.9$	$35^{\circ}19'$	06	7.76	.52	11.6
(ii)	193595	$38^{\circ}4012$	$20^{h}15^{m}.9$	$38^{\circ}44'$	07	8.73	.67	12.1
(i)	192639	$36^{\circ}3958$	$20^{h}10^{m}.8$	$37^{\circ}03'$	08f	7.11	.66	-
(ii)	193595	$38^{\circ}4012$			07	8.73	.67	12.1

TABLE 9 (Contd.)

Reddened Star

B-stars

Serial No.	HD	BD	RA_{1900}	Dec_{1900}	Sp. Type	V	E_{B-V}	m-M
14	228587	$36^{\circ}3966$	$20^{h}11^{m}.7$	$36^{\circ}19'$	B1 II	10.07	1.06	11.89
15		$39^{\circ}4117$	$20^{h}14^{m}.2$	$39^{\circ}43'$	B1 II	9.92	1.13	11.53
16		$36^{\circ}4000$	$20^{h}15^{m}.1$	$36^{\circ}56'$	B05 Ia	9.63	1.09	12.8
17		$36^{\circ}4004$	$20^{h}15^{m}.4$	$37^{\circ}05'$	B05 III	9.63	1.18	10.8
18(i)	228882	$40^{\circ}4113$	$20^{h}15^{m}.4$	$40^{\circ}23'$	B05 Ia	9.21	1.43	11.3
18(ii)	"	"	"	"	"	"	"	"
19	228919	$39^{\circ}4135$	$20^{h}15^{m}.9$	$40^{\circ}08'$	B1 IV	9.68	.89	11.01
20	228928	$40^{\circ}4117$	$20^{h}16^{m}.0$	$40^{\circ}20'$	B2 Ib:nn	9.69	1.13	12.0
21(i)	228929	$39^{\circ}4136$	$20^{h}16^{m}.0$	$39^{\circ}36'$	B0.5 Ib	9.63	1.43	11.2
(ii)	"	"	"	"	"	"	"	"
22	228943	$38^{\circ}4016$	$20^{h}16^{m}.1$	$38^{\circ}17'$	B0 II	9.29	1.21	11.06
23	193794	$38^{\circ}4028$	$20^{h}17^{m}.1$	$39^{\circ}2'$	B0 V			
24	229033	$37^{\circ}3898$	$20^{h}17^{m}.2$	$37^{\circ}25'$	B0II-III	8.77	1.02	10.7
25	193945	$40^{\circ}4132$	$20^{h}17^{m}.9$	$40^{\circ}52'$	B0 Vnn			
26	229108	$38^{\circ}4038$	$20^{h}18^{m}.3$	$39^{\circ}08'$	B0.5 Ib	9.48	1.09	13.31
27(i)	194839	$40^{\circ}4165$	$20^{h}22^{m}.8$	$41^{\circ}03'$	B0.5 Ia	7.49	1.28	10.35
(ii)	"	"	"	"	"	"	"	"
28(i)		$40^{\circ}4185$	$20^{h}24^{m}.7$	$40^{\circ}18'$	B0 V	9.82	1.14	10.6
(ii)		"	"	"	"	"	"	"

TABLE 9

Comparison Star

B-stars

	HD	BD	RA_{1900}	Dec_{1900}	Sp. Type	V	E_{B-V}	m-M
	192303	$37^{\circ}3828$	$20^{h}9^{m}.1$	$37^{\circ}56'$	B1 III	8.96	.56	11.5
	194092	$40^{\circ}4137$	$20^{h}18^{m}.6$	$40^{\circ}39'$	B05 III	8.26	.41	11.73
	193076	$37^{\circ}3866$	$20^{h}13^{m}.3$	$37^{\circ}22'$	B05 II	7.62	.61	11.0
	193032	$38^{\circ}3980$	$20^{h}13^{m}.0$	$38^{\circ}35'$	B0 III	8.32	.65	11.37
(i)	192422	$38^{\circ}3956$	$20^{h}09^{m}.7$	$38^{\circ}28'$	B05 Ib	7.09	.78	10.55
(ii)	193443	$37^{\circ}3879$	$20^{h}15^{m}.2$	$37^{\circ}57'$	09 III	7.24	.72	11.18
	192303	$37^{\circ}3828$	$20^{h}9^{m}.1$	$37^{\circ}56'$	B1 III	8.96	.56	11.5
	193183	$37^{\circ}3867$	$20^{h}13^{m}.8$	$37^{\circ}55'$	B1.5 Ib	7.12	.67	12.81
(i)	192422	$38^{\circ}3956$	$20^{h}09^{m}.7$	$38^{\circ}28'$	B05 Ib	7.09	.78	10.55
(ii)	193443	$37^{\circ}3879$	$20^{h}15^{m}.2$	$37^{\circ}57'$	09 III	7.24	.72	11.18
	193076	$37^{\circ}3866$	$20^{h}13^{m}.3$	$37^{\circ}22'$	B05 II	7.62	.61	11.0
	228263	$37^{\circ}3819$	$20^{h}08^{m}.4$	$37^{\circ}21'$	B1 V	9.42	.42	11.66
	192303	$37^{\circ}3828$	$20^{h}9^{m}.1$	$37^{\circ}56'$	B1 III	8.96	.56	11.5
	228263	$37^{\circ}3819$	$20^{h}08^{m}.4$	$37^{\circ}21'$	B1 V	9.42	.42	11.66
	193076	$37^{\circ}3866$	$20^{h}13^{m}.3$	$37^{\circ}22'$	B05 II	7.62	.61	11.0
(i)	192422	$38^{\circ}3956$	$20^{h}09^{m}.7$	$38^{\circ}28'$	B05 Ib	7.09	.78	10.55
(ii)	193443	$37^{\circ}3879$	$20^{h}15^{m}.2$	$37^{\circ}57'$	09 III	7.24	.72	11.18
(i)	228263	$37^{\circ}3819$	$20^{h}08^{m}.4$	$37^{\circ}21'$	B1 V	9.42	.42	11.66
(ii)	228690	$37^{\circ}3861$	$20^{h}12^{m}.8$	$37^{\circ}37'$	B05 V	9.25	.55	11.4

TABLE 10

Normalised magnitude differences between reddened and comparison stars.

Serial No.	f	$\frac{1}{\lambda}$ k	1.25 Δm_λ	1.35 Δm_λ	1.43 Δm_λ	1.34 Δm_λ	1.67 Δm_λ	1.75 Δm_λ	1.82 Δm_λ	1.92 Δm_λ	2.0 Δm_λ	2.04 Δm_λ	2.20 Δm_λ
1	.82	-.15	0	.10	.25			.56	.60		.76	.83	
2	.34	.03	-.03	.15	.26	.38	.56	.56	.65	.65	.73	.71	
3	.89	-.65	.04	.12	.39			.63	.63	-	.81	.76	
4	.90	-.39	.03	.21	.15	.33	.46	.52	.61	.52	.70	.68	.86
5	.44	.09	-.04	.14	.23	-	.41	.55	.64	.71	.80	.82	
6	1.39	.96	.04	.09	.10	.38	.57	.61	-	.80	.78	.88	.98
7(i)	1.44	.56	.04	.16									
(ii)	.92	.13	-.01	.16	.14	.28	.52	.52	.67	.69	.76	.80	
8	1.08	-.48	.02	.15	.08	.33							
9(i)	1.16	-.60	-.08	.19	.24		.51	.49	.57	.63	.73		
(ii)	.92	-.35	-.14	.18	.42		-	.61	.69	.71	.69	.76	
10	2.79	-.20	.05	.19	.23								
11	1.48	.12	.06	.12									
12(i)	2.3	-.24	.03	.17									
(ii)	1.93	-.64	.02	.14	.21			.58	.59	.70			
13(i)	2.36	.38	.03	.13	.22								
(ii)	2.04	-.22	.02	.08	.21								
14	1.05	.59	.02	.15	.37	.23		.38	.45	.51			

TABLE 10

$\frac{1}{\lambda}$	2.22	2.26	2.37	2.41	2.48	2.54	2.59	2.62	2.67	2.72	2.78	2.82	2.86	2.91
	Δm_λ	Δm_λ	Δm_λ	Δm_λ	Δm_λ	Δm_λ	Δm_λ	Δm_λ	Δm_λ	Δm_λ	Δm_λ	Δm_λ	Δm_λ	Δm_λ
	1.0	1.04	1.08	1.16	1.16	1.19	1.20	1.23		1.34				
	1.0	1.0	1.15	1.29	1.12	1.21	1.24	1.27	1.27	1.35				
	1.0	1.05	1.14		1.14	1.23	1.25	1.27	1.31	1.44	1.35	1.36		
	1.09	-	1.11	-	1.21	1.26	1.37	1.31						
	1.0	1.0	1.14	-	1.10	1.19	1.26	1.26	1.44	1.52				
	1.08	1.10	1.14	-	1.20	1.20	1.24	1.32	-	1.33	1.36	1.32		
	.97	1.09	1.16	1.19	1.20	1.27	1.33	1.32						
	.93	1.04	1.17	-	1.30	1.29	1.38	1.28	1.29	1.40	1.43	1.33		
	1.07	1.09	1.16	1.24	1.10	1.29	1.24	1.21	1.28	1.23	1.24	1.24		1.28
	.94	1.03	1.18	-	1.23	1.28	1.29	1.28	1.31	1.35				
	1.0	1.10	1.15	-	1.18	1.20	1.34	1.42	1.39	1.47				
	1.0	1.08	1.15		1.14									
	1.0	1.05	1.17	1.22	1.20	1.29	1.28	1.34	1.37					
	1.0	-	1.21	1.18	1.20	1.25	1.27	1.30	1.31	1.38	1.38			
	1.0	1.10	1.15	1.18	1.13	1.22	1.25	1.28	1.31	1.30	-	1.44		
	1.07	1.12	1.13		1.13									
	1.06	1.08	1.10		1.11									
	1.07	1.03	1.18		1.21	1.22	1.21		1.27	1.27	1.32	1.34		

TABLE 10 (Contd.)

Serial No.		$\frac{1}{\lambda}$	1.25	1.35	1.43	1.34	1.67	1.75	1.82	1.92	2.0	2.04	2.20
	f	k	Δm_λ	Δm_λ	Δm_λ	Δm_λ	Δm_λ	Δm_λ	Δm_λ	Δm_λ	Δm_λ	Δm_λ	Δm_λ
15	1.79	.23	.01	.14	.24			.54	.62	.61	.73	.70	
16	1.23	1.02	0	.14	.20	-	.46	.50	.50	.70	-	.86	
17	1.07	.63	.02	.08	.08	.34	.43	.44	.46	-	.71	.76	
18(i)	1.52	.64	.03	.14	.22	.30			.61	.60	.81	.79	.96
(ii)	1.81	.38	.02	.14	.19	.28			.62	.68	.80		.96
19	.54	.84	.01	.18	.31	.50	.46	-	.61	.58	.82	.92	.97
20	1.20	1.53	.03	.11	.14	.22	.51	.63	.67	.65	.80	.86	
21(i)	1.61	.76	.11	.14	.23	.27			.61	.65	.75	.74	
(ii)	1.78	.56	.07	.13	.18	.23	.54	.61	.63	.68			
22	1.20	.75	-.02	.12	.23	.17	.51	.54	.50	.67	.72	.83	
23	.86	-1.08	.01	.14	.25	.48	.41	.45	.56	.81	.82	.92	
24	.74	-.53	-.01	.07	.25	.36	-	.42	.49	.71	.72	.76	.94
25	1.02	-1.53	.02	.11			.43	.46	.53	.72	.71		.92
26	1.40	.58	.11	.13	.21	.37	.60	.61	.62	.72	.91	.91	
27(i)	1.10	-.45	.15	.09	.30				.67	.80	.89		.91
(ii)	1.24	-.56	.06	.05	.26	-	.62	.68	.68	.82	.89		.97
28(i)	1.28	-.34	-.04	.15			.44	.47	.59	.61	.71	.81	
(ii)	.97	-.11	-.07	.19			.44	.47	.65	.60	.76	.79	

TABLE 10 (Contd.)

2.22	2.26	2.37	2.41	2.48	2.54	2.59	2.62	2.67	2.72	2.78	2.82	2.86	2.91
Δm_λ	Δm_λ	Δm_λ	Δm_λ	Δm_λ	Δm_λ	Δm_λ	Δm_λ	Δm_λ	Δm_λ	Δm_λ	Δm_λ	Δm_λ	Δm_λ
.99	1.11	1.16	1.22	1.23	1.24	1.27	1.26	1.36					
1.04	1.07	1.07	1.09	1.11	1.17	1.21	1.16	1.26	-	1.25	1.32		
1.05	1.09	1.26		1.20	1.25	1.36	1.20	1.24	1.38	1.30			
1.07	1.09	1.22		1.23	-	1.30	1.25	1.26	1.31				
1.08	1.10	1.16	1.17	1.28	1.25	1.32	1.25	1.25	1.32				
.92	.92	1.14	1.20	1.24	1.24	1.27	1.14	1.53	1.56	1.35	1.46	1.64	
1.03	1.10	1.13	-	1.17	1.13			1.07					
1.06	1.13	1.15	1.13	1.16	1.18	1.18	1.23	1.19	1.19				
1.13	1.16	1.16	1.16	1.29	1.24	1.24	1.23	1.21	1.21				
1.07	1.01	1.15	-	1.20	-	1.31	-	1.28	1.33	1.34	1.45		
1.0	1.0	1.16	1.15	1.27	1.30	1.38	1.23	1.25	1.45	1.41	1.45	1.39	1.59
1.0	1.0	1.08	1.0	1.12	1.31	1.28	1.31	1.35	1.33	1.28	1.45	1.43	1.41
1.0	1.05	1.02	1.16	1.15	1.25	1.31	1.24	1.20	1.40	1.38	1.50		1.62
1.0	1.08	1.11	1.19	1.19	1.23								
1.0	1.03	1.20	1.15	1.26	1.21	1.32	1.37	1.34	1.40	-	1.45	1.50	
1.0	1.02	1.19	1.14	1.20	1.27	1.33	1.37	1.37	1.40		1.48	1.45	
1.0	1.06	1.09	1.10	1.18	1.22	1.26	1.23	1.32	1.32				
1.0	1.02	1.21	1.05	1.21	1.27	1.21	1.31	1.32	1.25				

TABLE 11

Deviation from "$1/\lambda$ -law"

Ser. No.	$1/\lambda$	1.25	1.35	1.43	1.54	1.67	1.75	1.82	1.92	2.0	2.04	2.20
1		.03	.03	-.04			-.03	0	-	.02	-.01	
2		.06	-.02	-.05	-.06	-.11	-.03	-.05	.05	.05	.11	
3		-.01	.01	-.18			.06	-.03	-	-.03	.06	
4		0	-.08	.06	-.01	.01	.01	-.01	.18	.08	.14	.12
5		.07	-.01	-.02	-	.04	-.02	-.04	-.01	.02	0	
6		-.01	.04	.11	-.06	-.12	-.08	-	-.10	0	-.06	0
7		0	-.03	.07	.04	-.07	.01	-.07	.01	-.02	.02	
8		.01	-.02	.13	-.01					0	-.03	
9		.08	-.06	-.12		.06	.02	-.03	.05	.12	.07	
10		-.02	-.06	-.02								
11		-.03	.01									
12		0	-.03	0			-.05	.01	0			
13		0	.03	-.01								
14		.01	-.02	-.16	.09		.15	.15	.19			
15		.02	-.01	-.03			-.01	-.02	.09	.05	.12	
16		.03	-.01	-.01	-	-.01	.03	.10	0	-	-.04	
17		.01	.05	.13	-.02	.02	.09	.14	-	.07	.06	
18		0	-.01	0	.03			-.02	.06	-.03	.03	.02
19		.02	-.05	-.10	-.28	-.01		-.01	.12	.04	-.10	.01
20		0	.02	.07	.10	-.06	.10	.05	-.07	-.02	-.04	
21		-.06	-.01	0	.06	-.09	-.08	-.02	.03	.03	.08	
22		.05	..01	-.02	.15	-.06	-.01	.10	.03	.06	-.01	
23		.02	-.01	-.04	-.16	.04	.08	.04	-.11	-.04	-.10	
24		.04	.06	.04	.04		.11	.11	-.01	.06	.06	.04
25		.01	.02			.02	.07	.07	-.02	.07		.06
26		-.08	0	0	-.05	-.15	-.08	-.02	-.02	-.13	-.09	
27		-.07	.06	-.07	-	-.17	-.15	-.08	-.11	-.11		.04
28		.08	-.04			.01	.06	-.02	.09	.04	.02	

TABLE 11

2.26	2.37	2.41	2.48	2.54	2.59	2.62	2.67	2.72	2.78	2.82	2.86	2.91
0	.07	.03	.10	.13	.17	.17	-	.16				
.04	0	-.10	.14	.13	.13	.13	.18	.15				
-.01	.01		.12	.09	.12	.13	.14	.6	.21	.24		
-	.04	-	.05	.06	0	.09						
.04	.01	-	.16	.13	.11	.14	.01	.02				
-.06	.01	-	.06	.12	.13	.08	-	.17	.20	.28		
-.02	-.02	0	.01	.04	.02	.10	.16	.10	.13	.27		
-.05	-.01	-.05	.16	.03	.13	.19	.17	.27	.32	.36		.41
-.03	-.01		.06	.08	.05	.05	.10	.09				
-.04	0		.12									
-.01	-.02	-.03	.06	.03	.09	.06	.08					
-.06	-.02	.01	.10	.07	.11	.11	.14	.16	.18	.16		
-.06	.04		.14									
.01	-.03		.05	.10	.16		.18	.23	.24	.26		
.07	-.01	.03	.03	.08	.10	.14	.09					
-.03	.08	.10	.15	.15	.16	.24	.19		.31	.28		
-.05	-.11		.06	.07	.01	.20	.21	.12	.26			
-.06	.03	.02	.01	.07	.06	.15	.20	.19				
.12	.01	-.01	.02	.08	.10	.26	-.08	-.06	.21	.14	0	
-.06	.02	-	.09	.19	.30							
.11	.01	.03	.04	.10	.15	.17	.25	.30				
.03	0		.06		.06		.17	.17	.22	.15		
.04	.01	.04	.01	.02	-.01	.17	.20	.05	.15	.15	.25	.10
.04	.07	.19	.14	.01	-.09	.09	.10	.17	.28	.15	.21	.25
-.01	.13	.03	.11	.07	.06	.16	.25	.10	.18	.10	-	.07
.04	.04	0	.07	.09								
.01	-.05	.04	.03	.08	.04	.03	.10	.10	-	.14	.17	
0	0	.11	.06	.07	.14	.13	.13	.21				

4.3 Reddening Law in Cygnus

4.31 Results of present investigation

The reddening curves have been derived for 28 pairs of highly and moderately reddened O- and early B- type stars down to magnitude V = $10^m.0$, for which spectral types are available in the literature. Spectral types of stars fainter than $11^m.0$ are not accurately known and therefore they have not been considered.

Stars investigated are plotted in Fig. 15 and the necessary data for the pairs of stars compared are given in Table 9. V is the apparent visual magnitude and E_{B-V} is the colour excess on Johnson's (1953) system. These columns have been obtained from Hiltner's (1956) catalogue. (m - M) is the true distance modulus which has been determined from the spectral type-luminosity relation given by Schmidt-Kaler (1962). The average error in distance-modulus is about $\pm 1^m.0$. The spectral types on the two-dimensional MK system have been taken from the following sources:-

1. Hiltner (1956)
2. Morgan et al (1955)
3. Barbier (1962)

A comparison between the spectral types determined by Barbier and those determined by Morgan shows that the standard error in spectral types is $\pm$.07 subclass.

Stars later than type B3 have not been measured. For the pairs No. 7, 9, 12, 13, 18, 21, 27 and 28 two stars have been used as comparison stars.

Normalised magnitude differences for each pair of stars are given in Table 10. The values in the table can be converted to observed magnitude differences by the following equation,

$$(\Delta m_\lambda)_{obs.} = f \cdot (\Delta m_\lambda)_{normalised} + k \qquad (40)$$

Column 1 gives the serial number which corresponds to the stars of the same serial number of Table 9. Values of f and k are given in columns 2 and 3. Deviations from the straight line which passes through ($\Delta m_\lambda = 1^m.0$, $1/\lambda = 1.22\mu^{-1}$) and whose slope is unity, are given in Table 11.

4.32 Continuum anomalies

The anomaly that O-stars in Cygnus have a higher ratio of (U-B)-colour excess to (B-V)-colour excess than is found elsewhere was noted by Rodger (1961); he suggested that the effect is due to intrinsic ultra-violet deficiency in these stars. In this case the reddening effect for O-stars should be different from that for B-stars. The differences

$$(\overline{\Delta m}_\lambda)_{O\text{-stars}} - (\overline{\Delta m}_\lambda)_{B\text{-stars}}$$

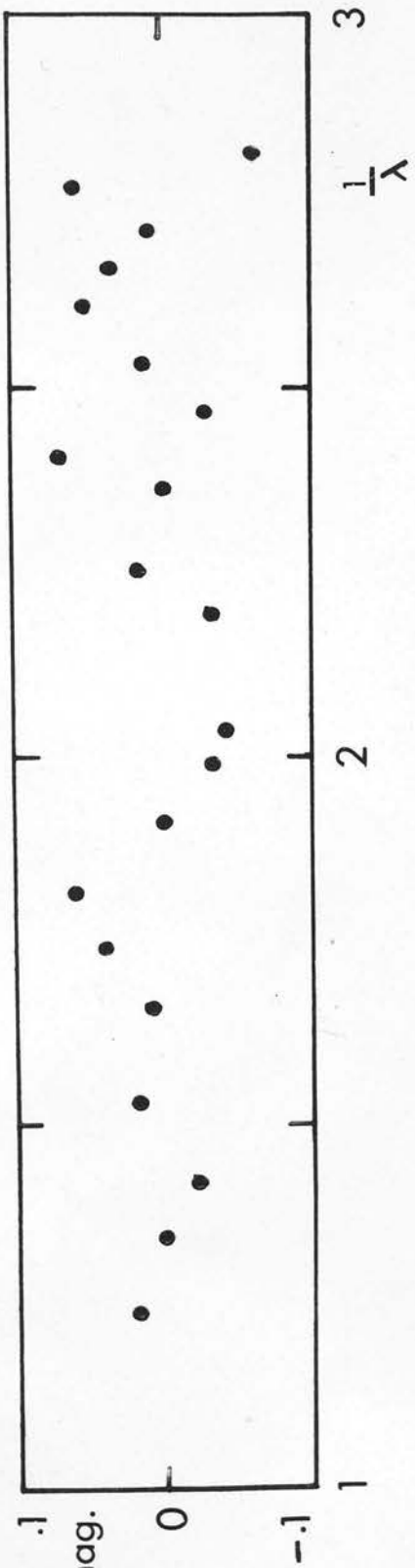

Fig. 20

$\{(\Delta m_\lambda)_{O\text{-stars}} - (\Delta m_\lambda)_{B\text{-stars}}\}$ versus $\frac{1}{\lambda}$

have been plotted against $1/\lambda$ in Fig. 20. They are within the r.m.s. dispersion about the mean and have therefore no significance.

4.33 Intrinsic dispersion of reddening curves

Table 12 compares the total error of observations, as described in section 3.5, with the r.m.s. dispersion about the mean of the magnitude-differences from all pairs of stars measured in the present work.

The table shows that the dispersion in the reddening curves can be explained solely in terms of error of classification and measurement. An upper limit of 3 per cent can be placed on any intrinsic r.m.s. dispersion of the reddening curves, having regard to uncertainties in the measured dispersion and errors.

4.34 Dependence of the reddening law on distance

The patchiness of interstellar absorption in the region of Cygnus is illustrated in Fig. 21 in which colour-excesses of the stars investigated in the present work (denoted by filled circles) and by other authors (denoted by circles) have been plotted against distance moduli [Lawrence and Reddish (1964)].

For a comparison with results derived by different authors as well as for an investigation of whether or

not there is any variation in the reddening law with distance, the stars in Fig. 21 are divided into two groups, A and B, each containing approximately an equal number of stars. The average distance modulus of the stars of Group A is $10^m.8$ and of Group B $12^m.0$. The moderately reddened stars are separated from the highly reddened ones by a dotted line. Normalised magnitude differences have been calculated for pairs of highly and moderately reddened stars belonging to the same group. Since the stars are situated in the same region in space irregularities in the properties of stars due to local galactic conditions, if any, will probably be the same for reddened and comparison stars. The curves are normalised in the manner described earlier. Where observations are limited to the spectral range from 6000A to 3400A, the curves are normalised so that the slope of the line between $\frac{1}{\lambda} = 1.70\,\mu^{-1}$ and $\frac{1}{\lambda} = 2.28\,\mu^{-1}$ is unity and

$$\Delta m_\lambda = 1^m.0 \text{ at } \frac{1}{\lambda} = 2.22\,\mu^{-1}$$

For each group of stars a mean reddening curve has been derived separately from the results of the present work and from the published data of Stebbins and Whitford (1943), Schalén (1959, 1961), Divan (1954), Rodgers (1961), Johnson and Borgman (1963). The results are summarised in Table 13 and the comparison with the

reddening curves derived from the data of different sources is shown in Figs. 22 and 23.

Deviations from the $\frac{1}{\lambda}$ law fitted at $\frac{1}{\lambda} = 1.22\mu^{-1}$ and $\frac{1}{\lambda} = 2.22\mu^{-1}$ averaged over $\frac{1}{\lambda} = 2.26\mu^{-1}$ to $2.90\mu^{-1}$ are plotted against distance as well as colour-excess in Figs. 24(a) and 24(b). No correlation has been found. A smooth curve has been drawn through the plotted points of Figs. 22 and 23. The difference in mean reddening curves derived from the stars of Group A and Group B does not exceed $0^m.03$.

It is now necessary to investigate whether the reddening law for moderately reddened stars obtained by comparing them with nearby slightly reddened stars is the same as that found for the pairs of highly and moderately reddened stars. This study is not possible from our objective prism plates as the nearby stars are too wide apart. However, from Stebbins and Whitford's and from Johnson and Borgman's photometries the moderately reddened stars have been compared with the following nearby stars:

Sp. type	Reference Stars
O	HD 47839 (15 Mon)
	HD 14633
	HD 66811 (ζ Pup)
	HD 214680 (10 Lac)
B0 V	HD 36512 (υ Ori)
B1 Ib	HD 91316 (ρ Leo)

Mean Δm_{λ}'s for different groups of stars at the respective inverse effective wavelengths of the filters have been compared in Table 14 which shows that within the errors of observation the reddening effect of highly reddened stars is the same as for moderately reddened stars with respect to nearby stars.

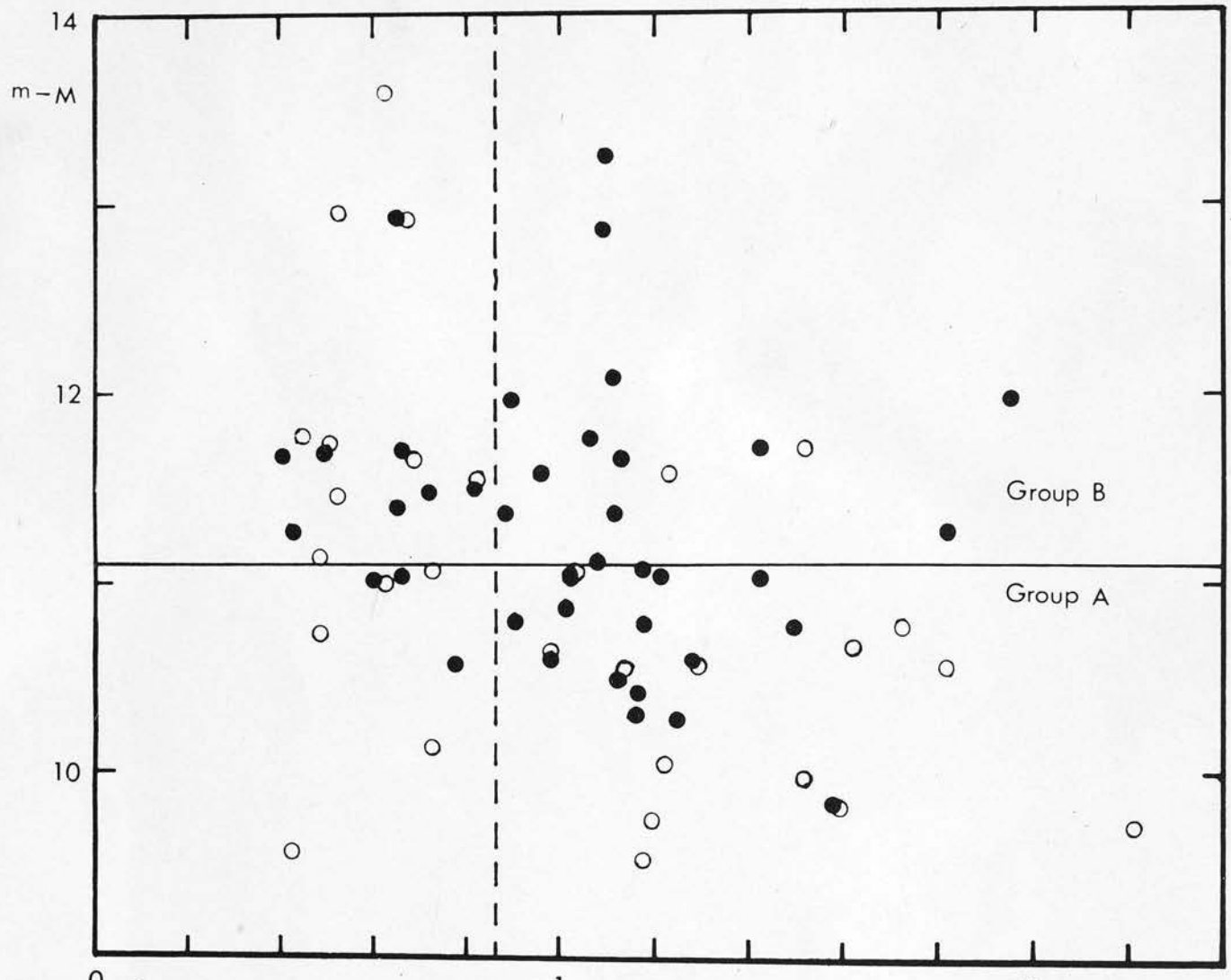

Fig.21 Distance modulus versus colour-excess. The solid line divides the stars into Group A and B. The dashed lines divide the stars into moderately reddened and highly reddened stars. Open circles represent stars studied by other authors and filled circles denote stars studied in the present work.

Comparison between Edinburgh results and results of other authors derived from the stars of Group A of Fig. 21

Fig. 22.

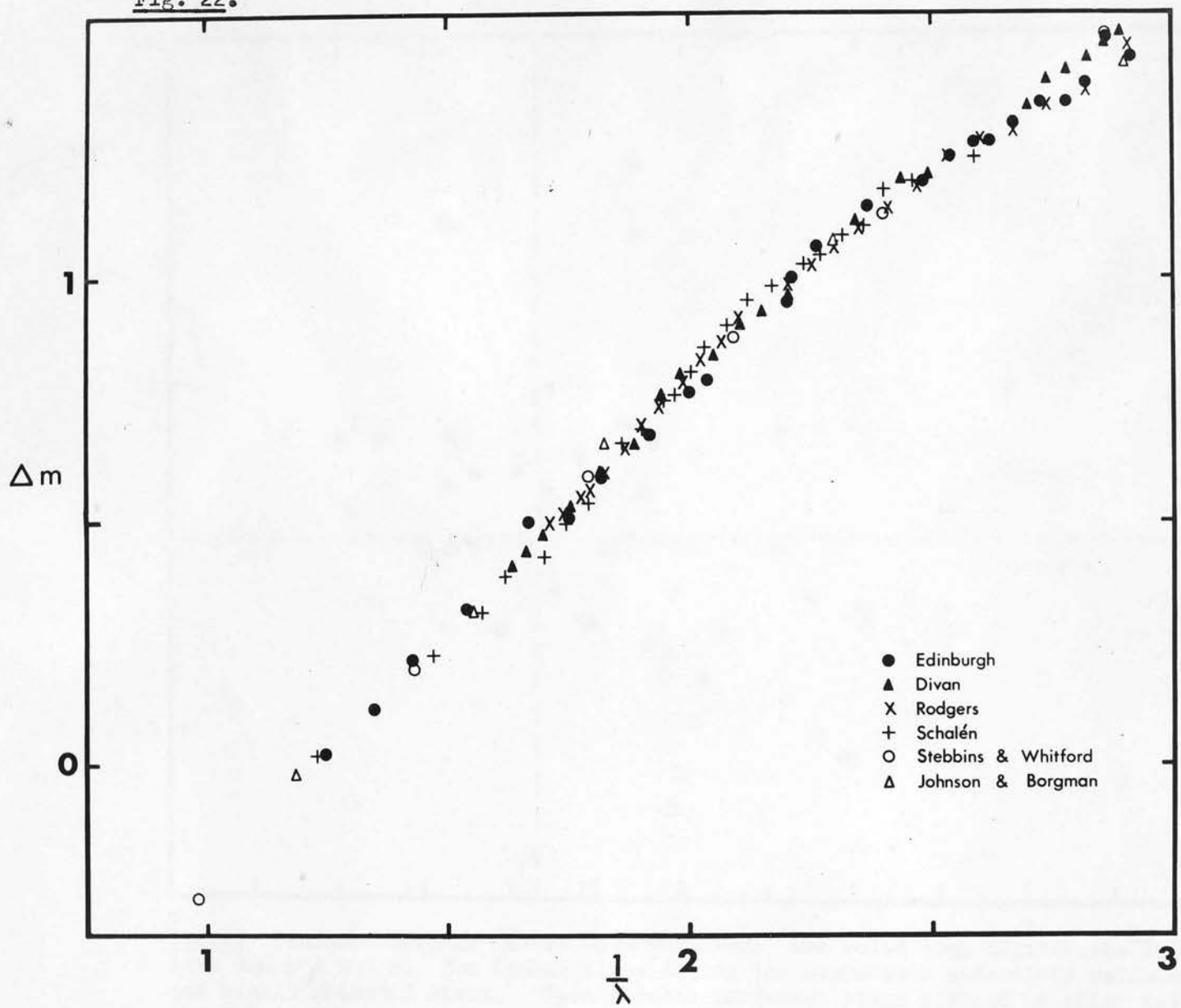

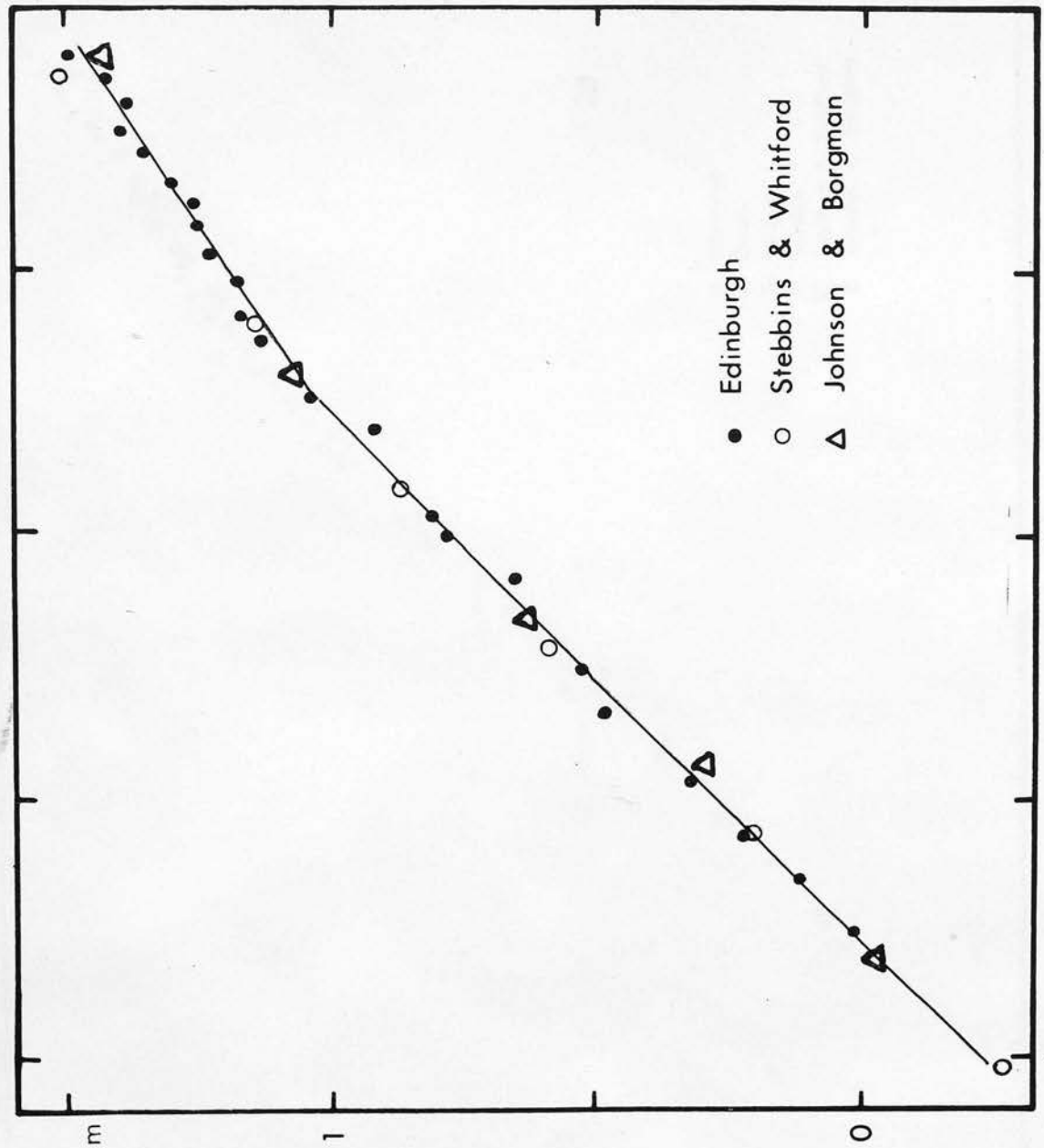

Fig. 23 Comparison between Edinburgh results and results of other authors derived from the stars of Group B of Fig. 21. Solid line represents the mean curve drawn through the plotted points of Fig. 22.

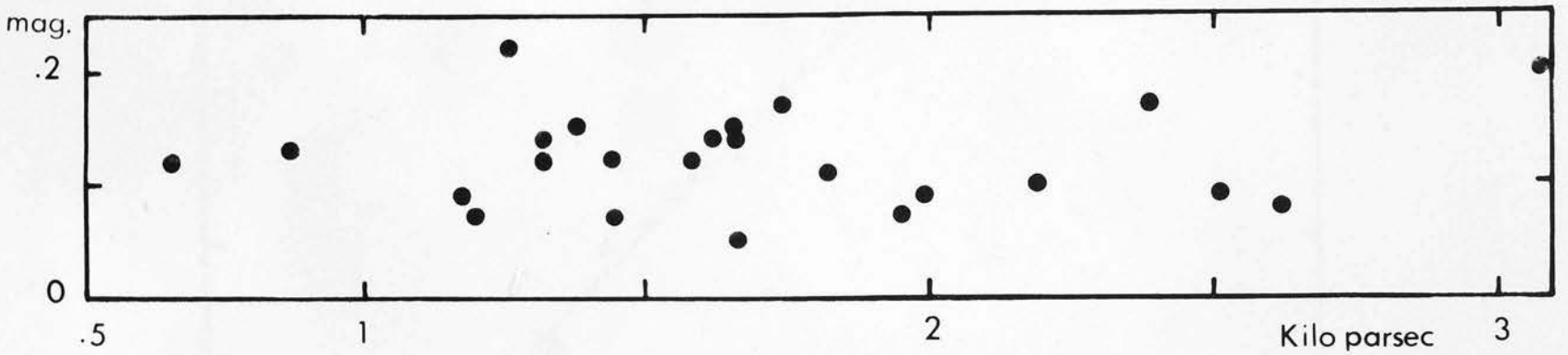

Fig. 24(a)

Mean deviation from $\frac{1}{\lambda}$ - law versus distance.

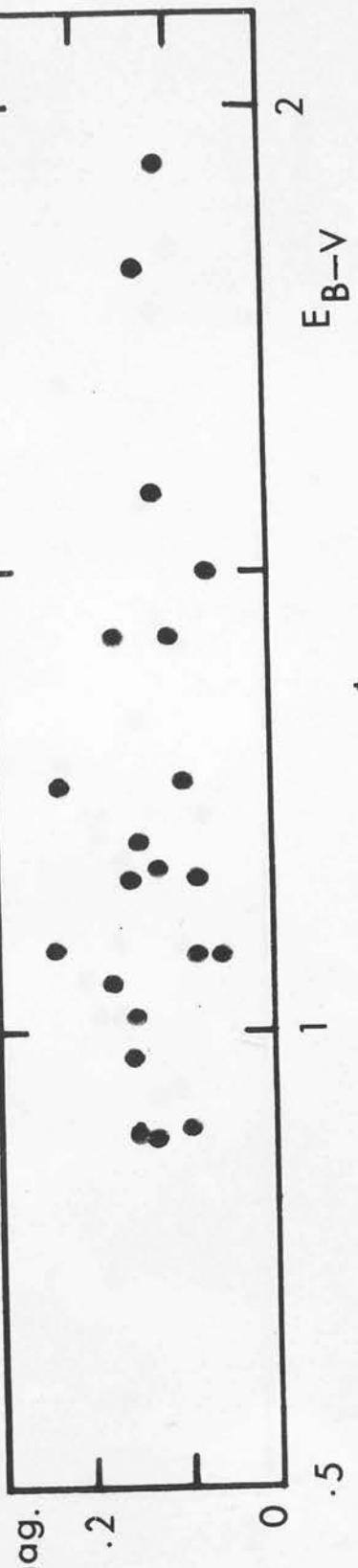

Fig. 24(b) Mean deviation from $\frac{1}{\lambda}$ - law versus colour-excess

TABLE 12

Comparison of the r.m.s. dispersion about mean Δm_λ with standard error of observation

λ	8000A	7000A	5000A	4500A	4220A	4030A	3858A	3670A	3450A
Standard errors of observations (ref. Sec. 3.5)	±.05	.07	.06	.05	.06	.07	.08	.08	.13
r.m.s. dispersion	±.03	.07	.07	.05	.06	.06	.08	.09	.13
Mean square difference (observed minus errors)	-.16	0	+.13	0	0	-.13	0	.17	0

TABLE 13

GROUP A Normalised interstellar absorption values for the stars of Group A (c.f. Fig. 21) derived from the data of different sources.

$1/\lambda$	Edinburgh $\Delta m\rangle$ 15 stars	Schalen $\Delta m\rangle$ 2 stars	Divan $\Delta m\rangle$ 3 stars	Rodgers $\Delta m\rangle$ 3 stars	Johnson & Borgman $\Delta m\rangle$ 4 stars	Stebbins & Whitford $\Delta m\rangle$ 2 stars
.99						-.26
1.19					-.02	
1.24		.03				
1.25	.02					
1.35	.12					
1.43	.22					.20
1.47		.23				
1.54	.33					
1.56					.31	
1.57		.31				
1.62		.39				
1.64			.41			
1.66			.44			
1.67	.50					
1.70		.43	.47			
1.71				.50		
1.74				.52		
1.75	.51	.50				
1.76			.54			
1.77				.55		

TABLE 13 (Contd.)

$1/\lambda$	Edinburgh Δm_λ	Schalén Δm_λ	Divan Δm_λ	Rodgers Δm_λ	Johnson & Borgman Δm_λ	Stebbins & Whitford Δm_λ
1.79		.54				.60
1.80				.57		
1.82	.59	.60	.61			
1.83				.60	.66	
1.87		.66		.65		
1.88			.66			
1.90		.69		.70		
1.92	.68					
1.94		.75	.75	.73		
1.97		.76				
1.98				.79		
1.99			.80			
2.0	.77	.81				
2.02				.83		
2.03		.86				
2.04						
2.05			.84			
2.06				.87		
2.08		.91				
2.09						.89

TABLE 13 (Contd.)

$1/\lambda$	Edinburgh Δm_λ	Schalén Δm_λ	Divan Δm_λ	Rodgers Δm_λ	Johnson & Borgman Δm_λ	Stebbins & Whitford Δm_λ
2.10			.90	.92		
2.12		.96				
2.15			.93			
2.17		.99				
2.20	.95		.96	.98		
2.21		1.0				
2.22	1.0					
2.24		1.03				
2.25			1.02	1.02		
2.26	1.06					
2.27		1.05				
2.30			1.07	1.06	1.07	
2.32		1.09				
2.35			1.12	1.10		
2.36		1.12				
2.37	1.15					
2.40		1.16	1.16			1.13
2.41	1.17			1.14		
2.44			1.20			
2.46		1.20				

TABLE 13 (Contd.)

$1/\lambda$	Edinburgh Δm_λ	Schalén Δm_λ	Divan Δm_λ	Rodgers Δm_λ	Johnson & Borgman Δm_λ	Stebbins & Whitford Δm_λ
2.47				1.19		
2.48	1.18					
2.49			1.22			
2.53				1.25		
2.54	1.25					
2.55		1.25				
2.59	1.28	1.25				
2.60				1.29		
2.62	1.20					
2.67	1.31			1.30		
2.70			1.36			
2.72	1.36					
2.74			1.41	1.35		
2.78	1.36		1.43			
2.82	1.40		1.46	1.38		
2.86	1.50		1.49			1.50
2.89			1.52			
2.90				1.49	1.44	
2.91	1.45					

GROUP B

TABLE 13 (Contd.)

Normalised interstellar absorption values for the stars of Group B (c.f. Fig. 21) derived from the data of different sources.

$1/\lambda$	Edinburgh Δm_λ 13 stars	Johnson & Borgman Δm_λ 3 stars	Stebbins & Whitford Δm_λ 2 stars
.99			-.27
1.19		-.03	
1.25	.02		
1.35	.13		
1.43	.22		.20
1.54	.33		
1.56		.29	
1.67	.49		
1.75	.52		
1.79			.59
1.82	.59		
1.83		.65	
1.92	.66		
2.0	.78		
2.04	.81		
2.09			.88
2.20	.92		

TABLE 13 (Contd.)

GROUP B

$1/\lambda$	Edinburgh Δm_λ	Johnson & Borgman Δm_λ	Stebbins & Whitford Δm_λ
2.22	1.0		
2.26	1.04		
2.30		1.08	
2.37	1.13		
2.40			1.15
2.41	1.17		
2.48	1.18		
2.54	1.23		
2.59	1.26		
2.62	1.26		
2.67	1.30		
2.72	1.35		
2.78	1.40		
2.82	1.38		
2.86	1.41		1.52
2.90		1.46	
2.91	1.50		

TABLE 14

Comparison between the reddening effect of highly reddened stars with respect to moderately reddened stars and the reddening effect of moderately reddened stars with respect to nearby stars.

$1/\lambda$	Group A (Highly reddened-Moderately reddened)		Group B (Highly reddened - Moderately reddened)		(Moderately reddened -Nearby stars)	
	Stebbins & Whitford	Johnson & Borgman	Stebbins & Whitford	Johnson & Borgman	Stebbins & Whitford	Johnson & Borgman
.99	-.26		-.27		-.22	
1.19		-.03		-.02		-.02
1.43	.20		.20		.21	
1.56		.31		.29		.32
1.79	.60		.59		.60	
1.83		.66		.65		.66
2.09	.89		.88		.90	
2.30		1.07		1.08		1.07
2.40	1.13		1.15		1.14	
2.86	1.50		1.52		1.42	
2.90		1.44		1.46		1.42

TABLE 15

Wavelength dependence of interstellar absorption in Cygnus region.

$1/\lambda$	Weighted Mean Δm_λ	Mean Standard Error	Standard Error of the Weighted Mean
1.19	-.03		
1.22	.0		
1.25	.023	.01	.003
1.35	.130	.01	.004
1.43	.211	.02	.007
1.47	.246	.02	.007
1.54	.314	.03	.009
1.56	.378	.03	.017
1.62	.409	.02	.006
1.64	.421	.02	.013
1.66	.451	.02	.011
1.67	.461	.02	.011
1.70	.489	.02	.008
1.71	.504	.02	.005
1.74	.529	.02	.005
1.75	.536	.02	.005
1.76	.540	.02	.006
1.77	.556	.02	.004
1.79	.575	.03	.008
1.80	.585	.02	.008
1.82	.604	.02	.011
1.83	.621	.03	.012
1.87	.655	.02	.013
1.88	.664	.02	.013
1.90	.682	.02	.011
1.92	.695	.03	.01
1.94	.726	.02	.012
1.97	.758	.02	.010
1.98	.769	.02	.010
1.99	.775	.02	.012
2.0	.785	.02	.008
2.02	.806	.02	.007
2.03	.812	.02	.008
2.04	.821	.02	.009
2.05	.835	.02	.011

TABLE 15 (Contd.)

$1/\lambda$	Weighted Mean Δm_λ	Mean Standard Error	Standard Error of the Weighted Mean
2.06	.845	.02	.011
2.08	.870	.02	.010
2.09	.879	.02	.008
2.10	.886	.02	.008
2.12	.902	.02	.011
2.15	.930	.02	.010
2.17	.949	.01	.008
2.20	.971	.01	.008
2.22	1.0		
2.25	1.03	.01	.005
2.26	1.042	.02	.004
2.30	1.071	.02	.003
2.32	1.090	.02	.005
2.35	1.111	.02	.005
2.37	1.131	.02	.007
2.40	1.146	.02	.007
2.41	1.156	.02	.007
2.44	1.171	.02	.004
2.46	1.182	.02	.006
2.48	1.190	.02	.006
2.50	1.207	.02	.005
2.53	1.234	.02	.008
2.54	1.242	.02	.005
2.55	1.248	.02	.005
2.59	1.268	.02	.007
2.60	1.277	.02	.007
2.62	1.283	.02	.009
2.67	1.315	.03	.009
2.70	1.346	.03	.010
2.72	1.356	.03	.010
2.74	1.365	.03	.013
2.78	1.384	.03	.017
2.82	1.406	.03	.016
2.86	1.444	.05	.021
2.90	1.468	.06	.022

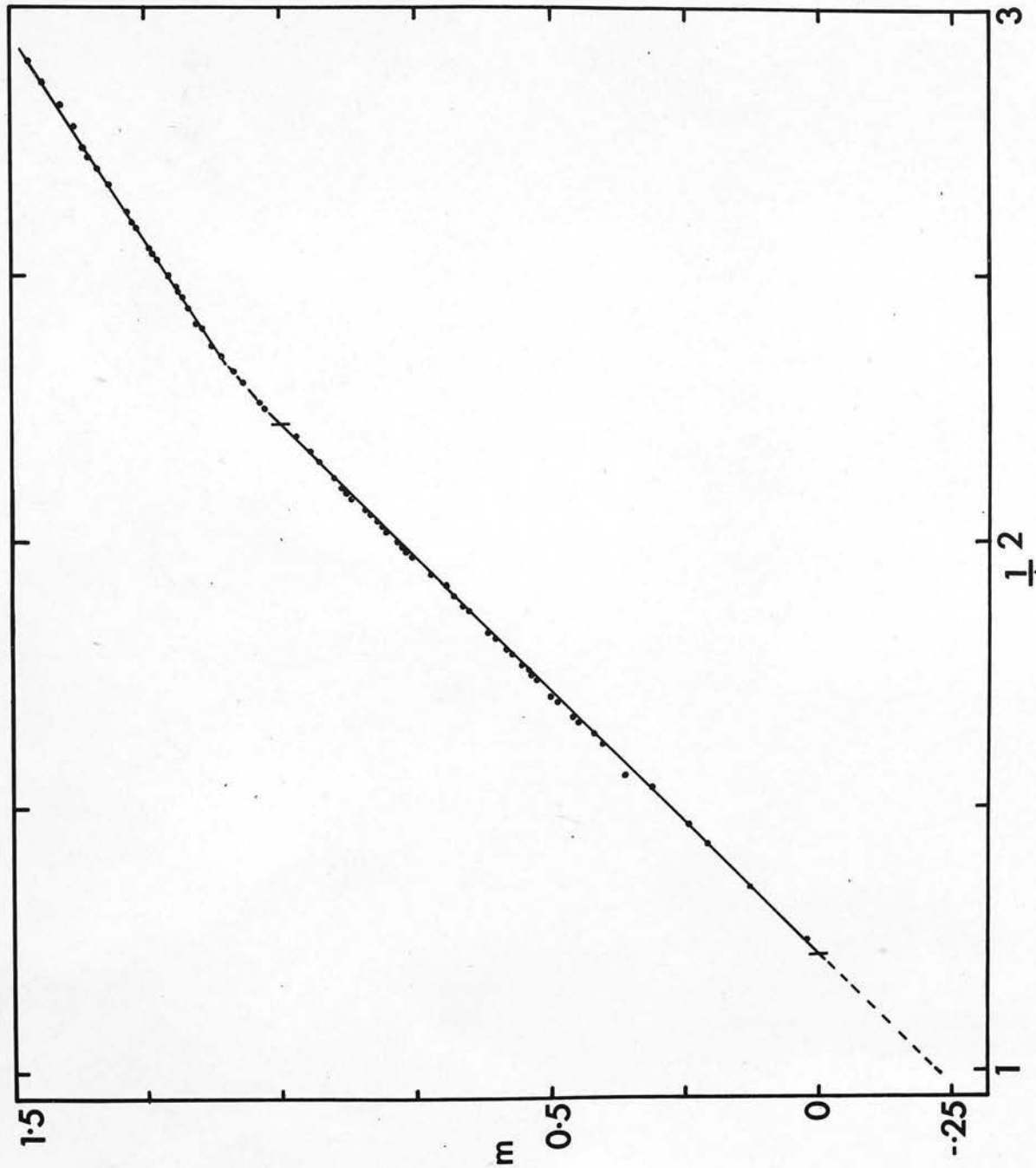

Fig. 25 The weighted mean reddening curve in the region of Cygnus

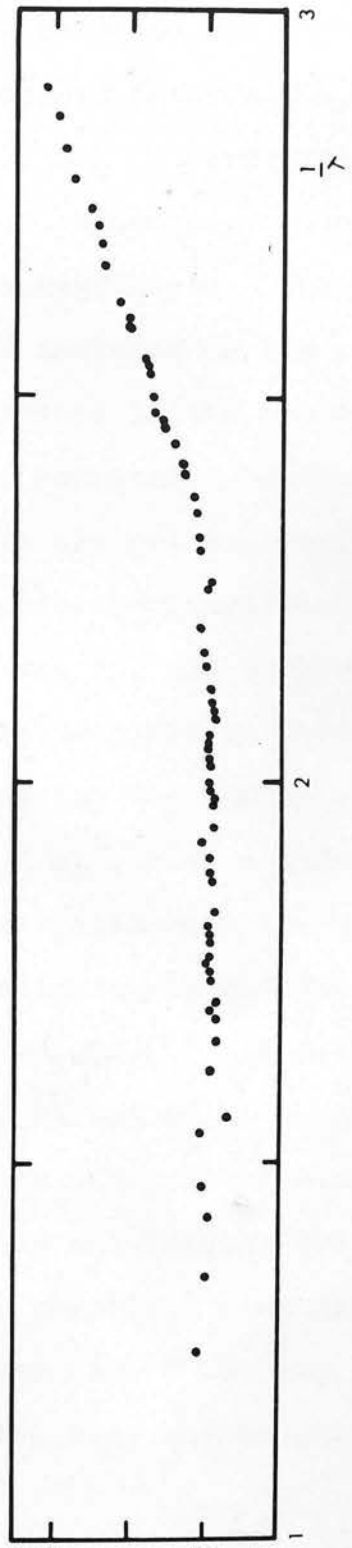

Fig. 26

Deviation from $\frac{1}{\lambda}$ - law.

4.35 Weighted mean reddening curve

Since there is no significant intrinsic dispersion, no significant distance dependence and no significant difference between the reddening curves for O- and B-stars, all the available observational data in the Cygnus region have been used to give a weighted mean reddening curve. The weight given to each individual curve included in the mean is numerically equal to the difference in the colour-excesses of the pair of stars being compared. As shown in Section 3.5 photometric errors are not important in comparison with uncertainties in spectral classification which are assumed to be about the same for all observers; and the error of the mean reddening curve is therefore substantially reduced by increasing the number of reddened stars. Weighted mean Δm_λ, mean standard error and standard error of the weighted mean are given in Table 15. The mean reddening curve and its deviation from a $1/\lambda$ -law fitted at $\frac{1}{\lambda} = 1.22\mu^{-1}$ and $2.22\mu^{-1}$ is shown in Figs. 25 and 26.

As a result of measures of a large number of stars at many wavelengths the error in the mean reddening curve resulting from different sources of error is not greater than $0^m.03$ mag. in the ultra-violet, $0^m.02$ mag. for the blue and longer wavelengths. Within these

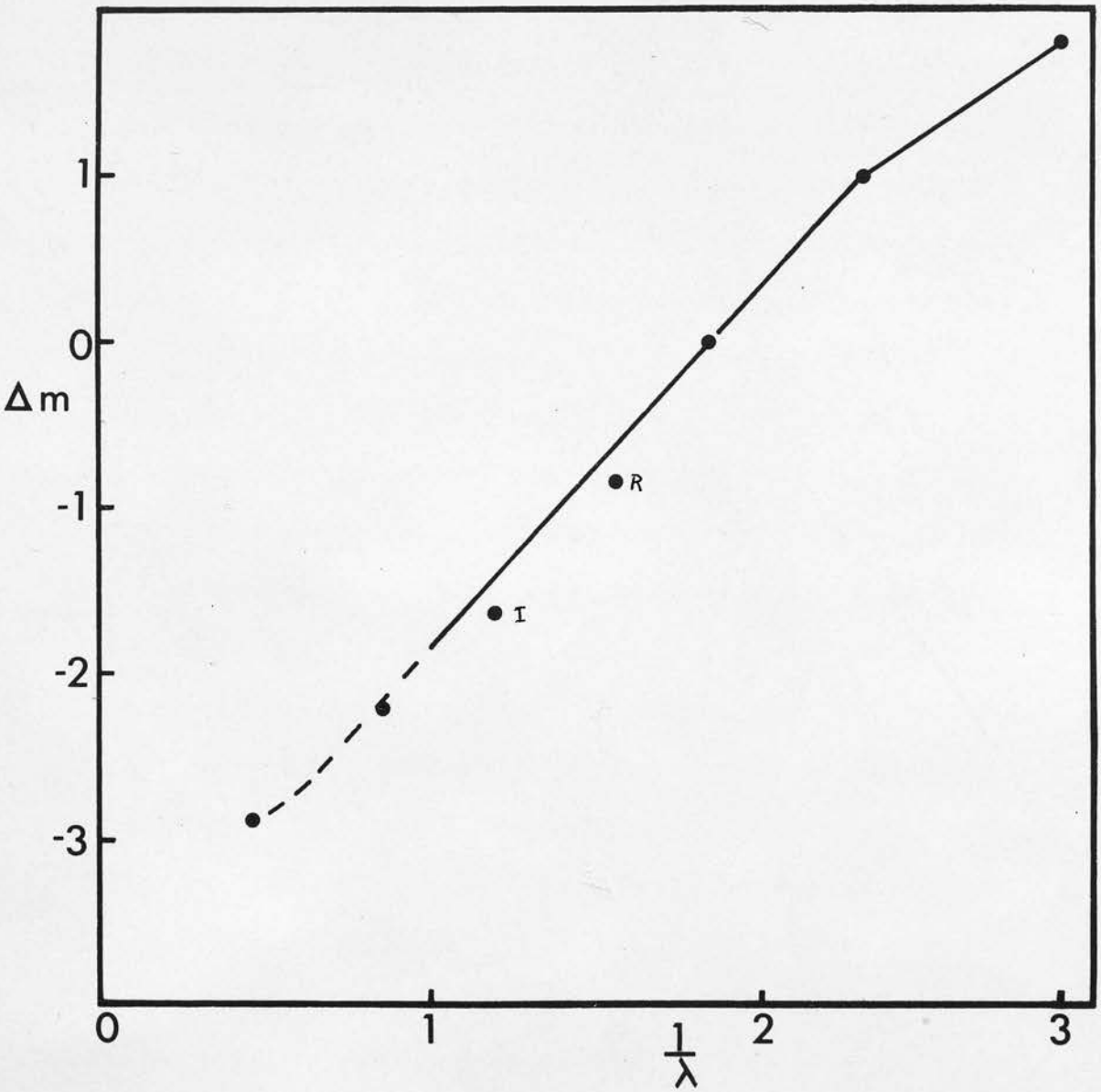

Fig. 27 The reddening curve in the Cygnus region after Johnson and Borgman, 1963 (denoted by circles). The solid line represents the weighted mean reddening curve (c.f. Fig. 25) normalised to $E_{B-V} = 1^m.0$ and $A_V = 0^m.0$.

errors the observed curve can be represented by two straight lines:

$$\Delta m_\lambda = 1/\lambda - 1.22, \quad 1.0 \leq 1/\lambda < 2.30$$
$$\Delta m_\lambda = 0.64\, 1/\lambda - 0.39, \quad 2.30 < 1/\lambda \leq 2.90 \qquad (41)$$

The change in the slope of the reddening curve occurs in a narrow wavelength range.

The result of the present work is in agreement with the conclusion of Whitford (1958). The ratio of the slope of the two linear parts from Whitford's curve is .61, which is approximately the same as found here. Whitford estimated that the change in the slope of the reddening curve occurs at $1/\lambda = 2.2\,\mu^{-1}$, while in the present investigation the slope is found to change at about $1/\lambda = 2.3\,\mu^{-1}$.

The extinction curve derived by Johnson and Borgman (1963) for Cygnus stars from colour-excess ratios (reproduced in Fig. 27) shows that the points corresponding to inverse effective wavelengths of the filters R and I do not lie on the straight line fitted at $1/\lambda = 1.80\,\mu^{-1}$ and $1/\lambda = 2.3\,\mu^{-1}$. But a shift of the assigned effective wavelengths of the R and I filters towards longer wavelengths by an amount of 300A and 500A respectively brings Johnson and Borgman's curve into good agreement with the present result. It seems that some zero-point corrections are necessary

for the red filters of Johnson and Borgman's photometry.

The colour-excess ratios calculated from the weighted mean curve for the effective wavelengths of U, B, V and J filters and for corrected effective wavelengths of R and I filters are given in Table 16.

TABLE 16

Colour-excess ratio	Edinburgh	Johnson and Borgman	
		Weighted Mean	Adopted
$\frac{E_{U-V}}{E_{B-V}}$	1.88	1.83	1.90
$\frac{E_{V-R}}{E_{B-V}}$	.80	.86	.80
$\frac{E_{V-I}}{E_{B-V}}$	1.60	1.65	1.70
$\frac{E_{V-J}}{E_{B-V}}$	2.17	2.25	2.20

Table 16 shows that the colour-excess ratios determined from the mean reddening curve agrees with Johnson and Borgman's result. An extrapolation on the basis of

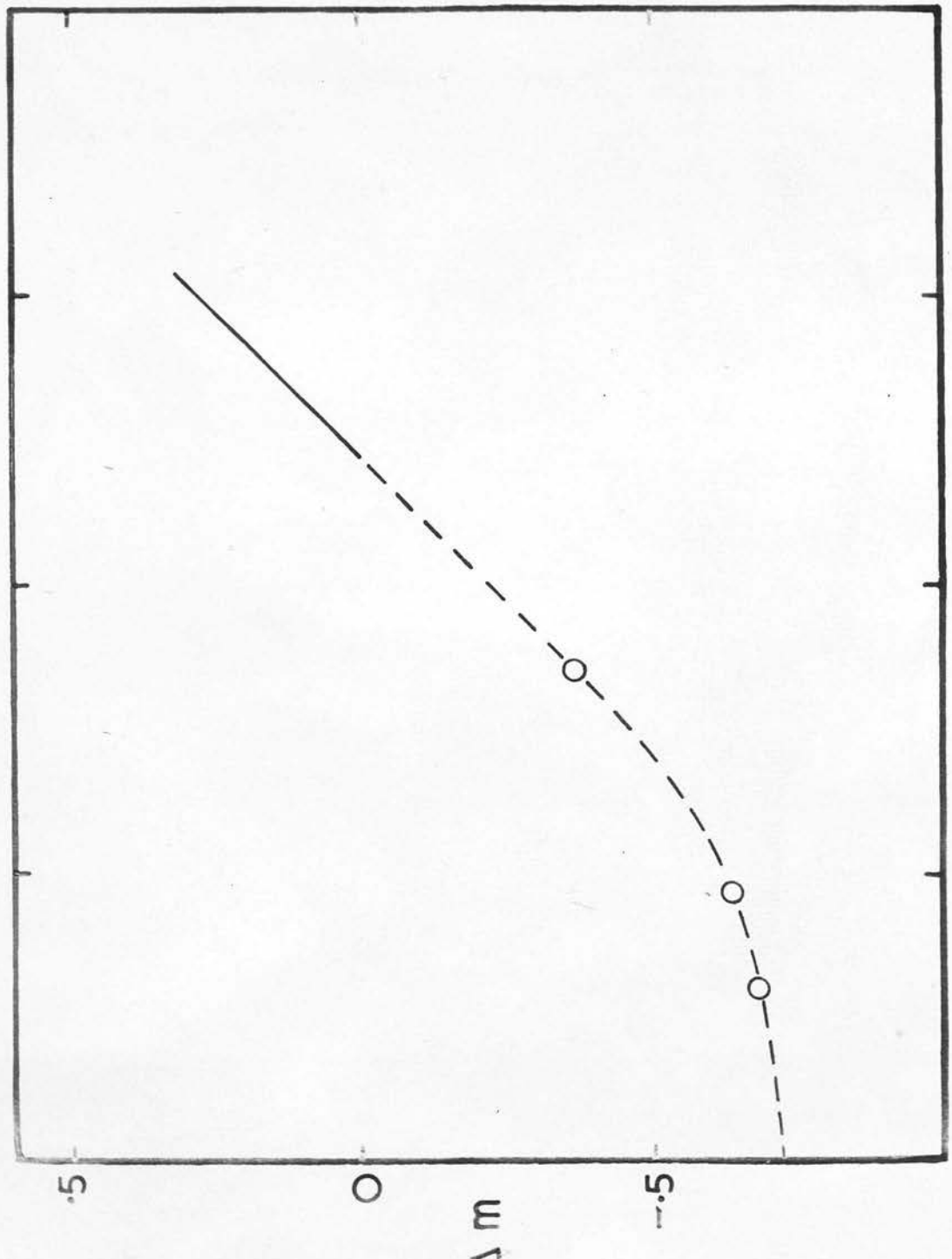

Fig. 28 Extrapolation of the weighted mean reddening curve (c.f. Fig. 25).

their adopted colour-excess ratios $\frac{E_{V-K}}{E_{B-V}}$ and $\frac{E_{V-L}}{E_{B-V}}$ gives:

TABLE 17

$\frac{1}{\lambda}(\mu^{-1})$	Δm_{λ}
.47	-.64
.30	-.68

The extrapolated part of the reddening curve has been shown by the dotted segment in Fig. 28.

The comparison of the weighted mean reddening curve with different theoretical solutions of van de Hulst (1949) has been shown in Figs. 29(a), 29(b) and 29(c). Over the wavelength range studied in the present work none of these solutions is in exact agreement with the observed curve. Curve No. 15 which has been preferred by van de Hulst deviates in the ultra-violet in the same sense as found by Divan (1954). Curve No. 8 seems to be nearest although even then absorption at $1/\lambda = 2.5\mu^{-1}$ and $2.6\mu^{-1}$ are 3 per cent higher than the observed values.

Neither Curve No. 15 nor Curve No. 8 provides the exact fit with the extrapolated part of the reddening curve, the residual without any regard to sign in each case being about $0^{m}.04$. The reality of the difference

between the theoretical solution and the extrapolated reddening curve depends on the accuracy of the infra-red colour-excess ratios and of the adopted effective wavelengths of the infra-red filter. Curve No. 8 gives the value of R = 2.8 while the extrapolation of the observed reddening curve between $1/\lambda = 1.0$ and $1/\lambda = 0$ by colour-excess ratios $\frac{E_{V-K}}{E_{B-V}}$ and $\frac{E_{V-L}}{E_{B-V}}$ gives R = 3.10

Comparison of the observed reddening curve in the Cygnus region with different theoretical solutions of van de Hulst. The solid line represents the observed curve; the points denote the theoretical solutions.

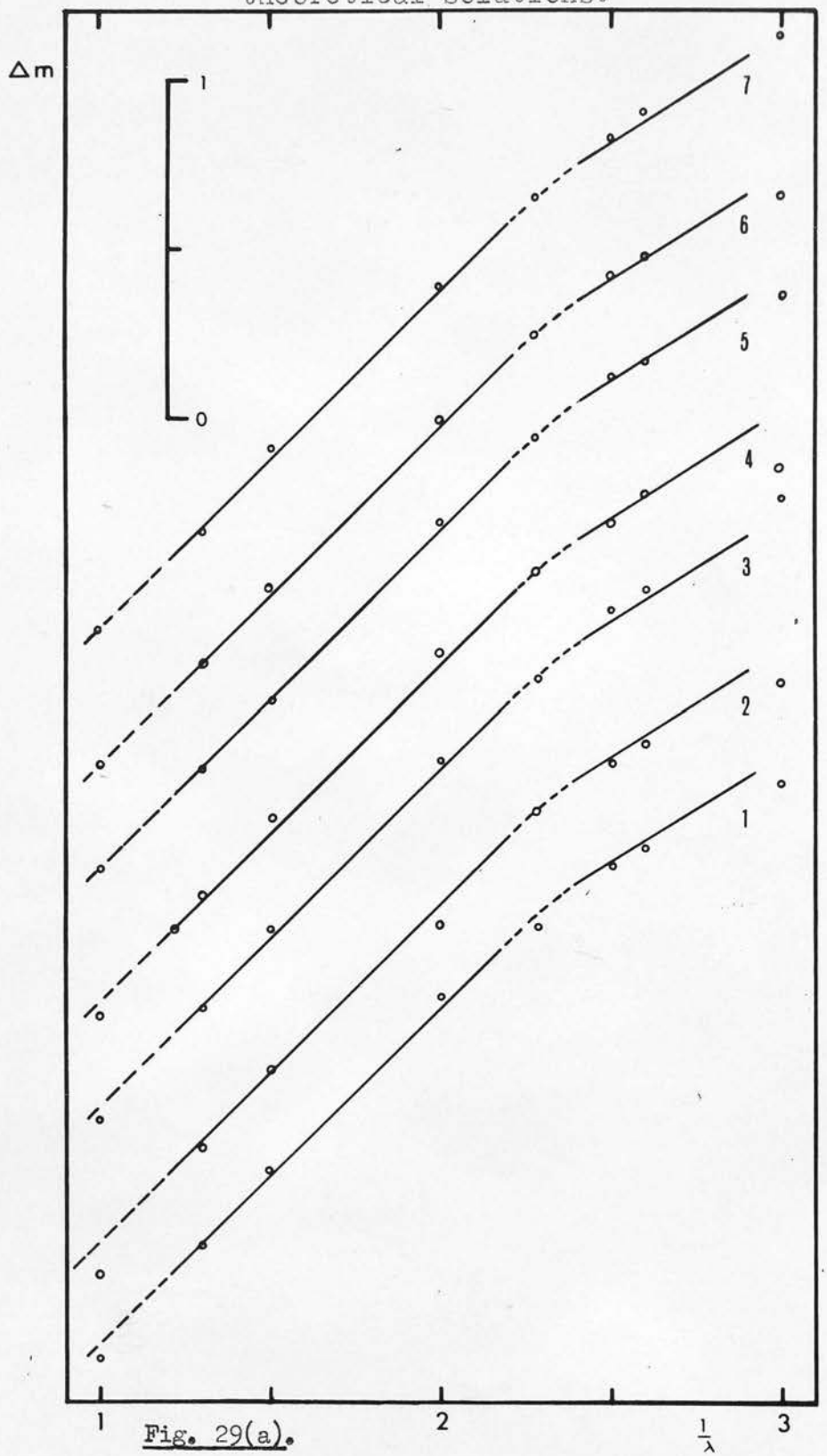

Fig. 29(a).

Comparison of the observed reddening curve in the Cygnus region with different theoretical solutions of van de Hulst. The solid line represents the observed curve; the points denote the theoretical solutions.

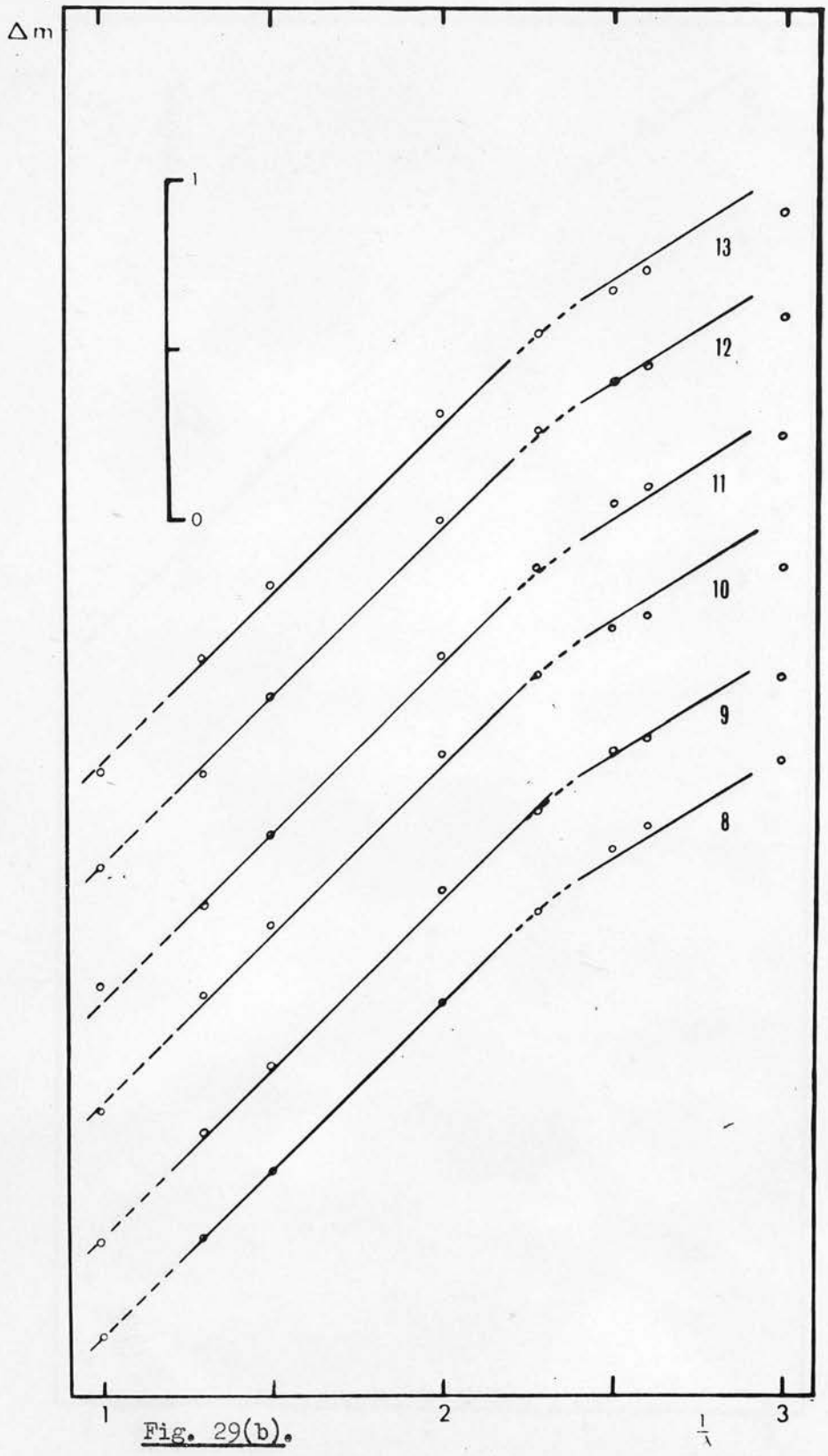

Fig. 29(b).

Fig. 29(c)

Comparison of the observed reddening curve in the Cygnus region with different theoretical solutions of van de Hulst. The solid line represents the observed curve; the points denote the theoretical solutions.

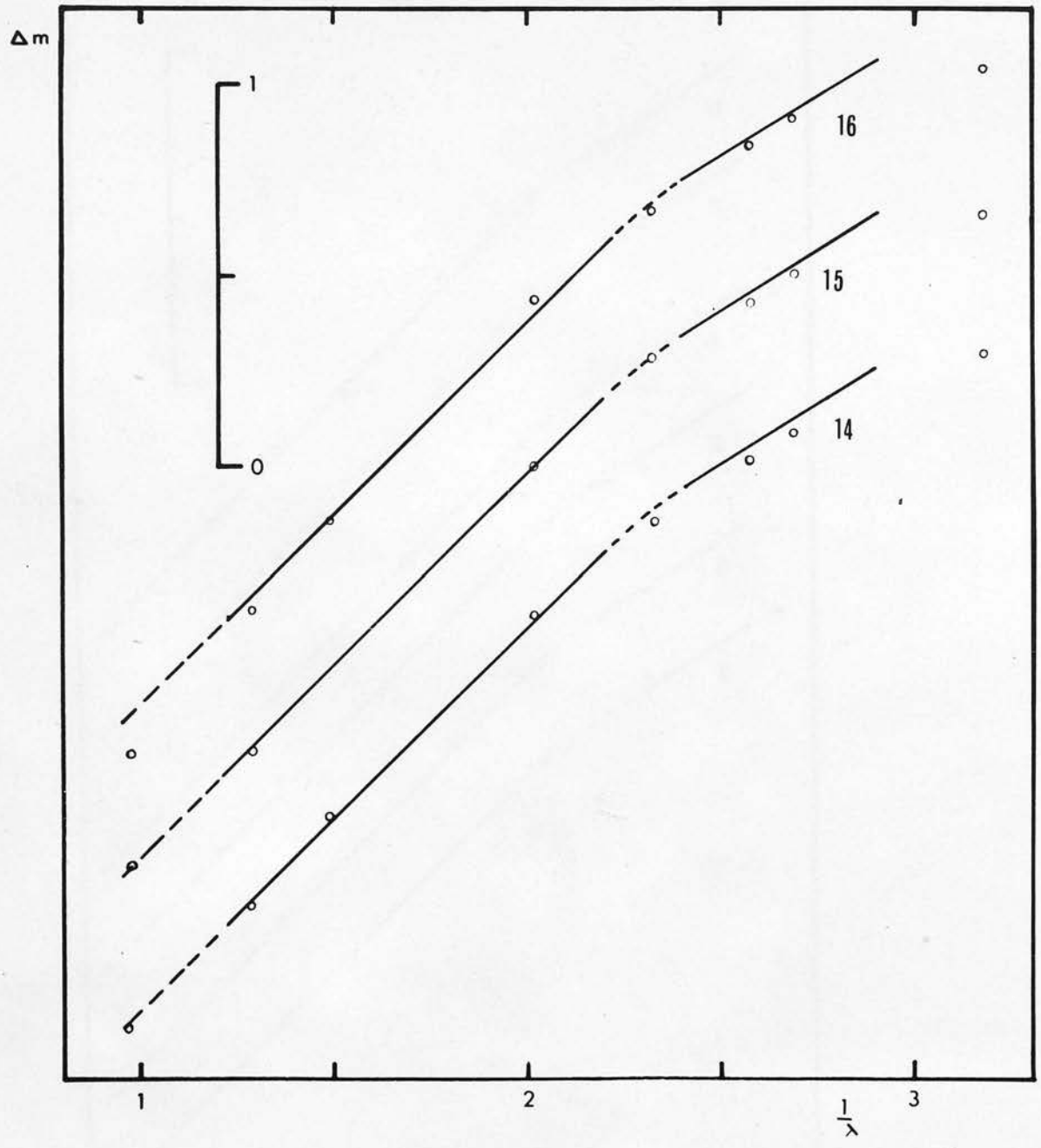

Conclusions

The mean reddening curve for Cygnus stars over the wavelength range from 8000A to 3400A consists of two linear parts, a change of slope occurring in a narrow wavelength range between 4400A and 4330A.

The dispersion in the observed reddening curves can be accounted for by errors of observation and there is no intrinsic r.m.s. dispersion in the reddening curves larger than 3 per cent.

The difference in mean reddening curves derived separately from O- and B-type stars is not greater than 5 per cent.

The fact that reddening curves derived from two groups of stars situated at average distances of 1.2 kpc. and 2 kpc. differ by not more than 3 per cent signifies that in the direction of Cygnus the reddening law is independent of distance out to at least 2 kpc.

The weighted mean-reddening curve derived by combining all the available observations in the Cygnus region is accurate to 0.8 per cent.

Acknowledgement

I am grateful to Professor H. A. Brück and Dr. V. C. Reddish for valuable suggestions and to Dr. M. J. Smyth and Mr. B. N. G. Guthrie for useful discussions. My thanks are due to Dr. Reddish, Mr. Guthrie, Mr. L. Lawrence and Mr. N. Pratt for taking some of the plates, and to Miss S. McCrea, Mr. N. G. Campbell and Mrs. Y. Slater for assistance with the reduction. I also wish to thank the Royal Society of Edinburgh for a Cormack Bequest Fellowship.

REFERENCES

Baade, W. and Minkowski, R. 1937, Ap.J., 86, 123.

Baker, E.A. 1949, Pub. Roy. Obs. Edin., 1, 15.

Barbier, M. 1962, J. Obs., 45, 57.

Blanco, V.M. 1956, Ap.J., 123, 64.

Borgman, J. 1954, B.A.N., 12, 201.
1961, B.A.N., 16, 99.

Cayrel, R. and Schatzman, E. 1954, Ann.Ap., 17, 555.

Chalonge, D. and Divan, L. 1952, Ann.Ap., 15, 201

Chandrasekhar, S. and Fermi , E. 1953, Ap.J., 118, 113.

Code, A.D. 1954, Quoted by Whitford in A.J., 63, 201 (1958)

Davis , L., Jr. 1955, Vistas in Astronomy, 1, 336
1960, Lowell Obs. Bull., 4, 266.

Davis , L., Jr., and Greenstein, J.L. 1951, Ap.J., 114, 206

Divan, L . 1954, Ann.Ap., 17, 456

Donn, B. 1955, Les Part.Sol. dans les Astres, Liege Symp., 571

1960, Lowell Obs. Bull., 4, 273.

Edlén, B. 1956, Vistas in Astronomy, 2, 1456.

Gold, T. 1952, M.N.R.A.S., 112, 215.

Greenberg, J.M. 1960, J.A.P., 31, 82.

1960a, Lowell Obs. Bull. 4, 285.

Greenberg, J.M., Pedersen, N.E. and Pedersen, J.C. 1961, J.A.P., 32, 233.

Greenberg, J.M. and Meltzer, A.S. 1960, Ap.J., 132, 667

Greenstein, J.L. 1938, Ap.J., 87, 151

Güttler, A. 1952, Z.Ap., 31, 1

Hall, J.S. 1937, Ap.J., 85, 145

1958, Pub. U.S. Naval Obs. 17, 271

Halm, J. 1917, M.N.R.A.S., 77, 243

Hallam, K.L. 1959, Quoted by Sharpless in Strand K.Aa : Basic Astronomical Data (Stars and Stellar Systems Vol.III) Univ. of Chicago Press, 1963.

Henyey, L.G. and Greenstein, J.L. 1941, Ap.J., 93, 70

Henry, J. 1958, Ap.J., 128, 497

Herbig, G.H. 1958, Stellar Population, Proc. Vatican Conference (1957), p. 135

Hiltner, W.A. 1956, Ap.J., Suppl.2, p.389

Hiltner, W.A. and Johnson, H.L. 1956, Ap.J., 124, 367

Houck, T.E. 1956, Quoted by Walker in Observatory, 82, 52, 1962

Hoyle, F. and Wickramasinghe, N.C. 1962, M.N.R.A.S., 124, 417

Johnson, H.L. and Borgman, J. 1963, B.A.N. 17, 115

Johnson, H.L. and Morgan, W.W. 1953, Ap.J., 117, 313

Johnson, H.L. and Morgan, W.W. 1955, Ap.J., 122, 142

Kahn, F.D. 1952, M.N.R.A.S., 112, 518

Kienle, H. 1937, Handbuch der Exp. Physik, 26, 647

King, I. 1952, A.J., 57, 253

Kopylov, I.M. 1958, Sov.Astr. A.J.2, 359

Lawrence, L. and Reddish, V.C. 1964, Pub.Roy.Obs. Edin. 5, (in preparation)

Lindbald, B. 1935, Nature, 135, 133

Lindholm, E.H. 1957, Ap.J., 126, 588

Menon, T.K. 1958, Ap.J., 127, 28

Mie, G. 1908, Ann. d'Physik, 25, 377 [Quoted by van de Hulst (1949)].

Morgan, W.W., Code, A.D. and Whitford, A.E.	1955, Ap.J., Suppl. II, p.41
Morgan, W.W., Whitford, A.E. and Code, A.D.	1953, Ap.J., 118, 318
Oort, J.H. and van de Hulst, H.C.	1946, B.A.N. 10, 187
Platt, J.R.	1956, Ap.J., 123, 486
Platt, J.R. and Donn, B.	1956, A.J., 61, 11
Reddish, V.C.	1961, M.N.R.A.S., 123, 27
Risley, A. M.	1943, Ap.J., 97, 277.
Rodgers, A.W.	1961, M.N.R.A.S., 122, 413
Rozi-Saulgeot, A.M.	1956, Ann.Ap., 19, 274
Rudnick, J.	1936, Ap.J., 83, 394
Russell, H.N.	1919, Proc.Nat.Acad.Sc. (Washington), 5, 398
Schalén, C.	1936, Uppsala Medd. No. 64
	1939, Uppsala Ann.1, No.2
	1952, Ann.Uppsala Obs.3, No.5
	1957, Lund Obs.Medd.Ser.II No. 135
	1959, Arkiv for Astronomi 2, No. 33, p. 359
	1961, Annales Academie Scientiarum Fennicae Series A, III Geologica-Geographica, 61
	1964, Pub.Roy.Obs.Edin. 4, 47

Schmidt-Kaler, Th. — 1962, Quoted by Voigt, H.H. in Mitt.Astr.Ges. 1962, p. 30

Schulte, D.H. — 1958, Ap.J., 128, 41

Serkowski, K. — 1963, Ap.J., 138, 1035

Sharpless, S. — 1952, Ap.J., 116, 251

1956, Quoted by Sharpless in Strand K.Aa: Basic Astronomical Data (Stars and Stellar Systems, Vol. III), University of Chicago Press, 1963.

Spitzer, L.,Jr. and Tukey, J.W. — 1951, Ap.J., 114, 187

Stebbins, J., Huffer, C.M. and Whitford, A.E. — 1939, Ap.J., 90, 209

Stebbins, J. and Kron, G.E. — 1956, Ap.J., 123, 440

Stebbins, J. and Whitford, A.E. — 1943, Ap.J., 98, 20

1945, Ap.J., 102, 318

Struve, O. — 1926, Ast. Nach, 227, 377

Struve, O., Keenan, A.C. and Hynek, J.A. — 1934, Ap.J., 79, 1

Trumpler, R.J. — 1930a, Lick.Obs.Bull.14, 154

1930b, Pub. P.A.S.P.42, 214

1930c, Ibid., p.267

Underhill, A.B. — 1959, Pub. Dominion Ap.Obs. 11, 209

1964, Observatory, 84, 35

van de Hulst, H.C. — 1949, Rech.Ast.Obs. Utrecht 11, part 2

1955, Mem.Soc.Roy. Liege, 15, 393

1964, Pub.Roy.Obs. Edin.4, 13

van Rhijn, P.J. — 1953, B.A.N., No. 441

Walker, G.A.H. — 1962, Observatory, 82, 52

Wampler, E.J. — 1961, Ap.J., 134, 861

1962, Ap.J., 136, 100

Washington, — 1908, Ann. Smithsonian Ap. Obs. II, p. 113

Wickramsinghe, N.C. — 1962, M.N.R.A.S., 125, 87

1963, M.N.R.A.S., 126, 99

Wilson, R. — 1960, M.N.R.A.S., 120, 51

Whitford, A.E. — 1948, Ap.J., 107, 102

1958, A.J., 63, 201

APPENDIX

Monochromatic Magnitudes

Relative monochromatic magnitudes for stars have been determined from the measurements on the tracings of the spectra. The wavelengths at which the magnitudes have been obtained correspond to those measured for the study of interstellar reddening. Using equation (31) the measurements of all stars have been reduced to the zero-point of one plate system. In Table 18 the monochromatic magnitude for each wavelength has been given relative to a zero-point defined by the mean magnitudes at the respective wavelengths of the following stars:

BD	HD	Sp. Type
$37^{\circ}3900$	193890	B9.5 V
$37^{\circ}3904$	193984	Ao V
$37^{\circ}3819$	228263	B1 V
$37^{\circ}3785$	227902	B1 V
$36^{\circ}3948$	228456	B2 IV
$36^{\circ}3927$	228199	B0.5 V
$35^{\circ}4019$	228326	B2 IV

Relative monochromatic magnitudes have been corrected for atmospheric extinction with the help of equation (24).

While the average standard error of a single measurement of monochromatic magnitude is of the order of $\pm 0^{m}.06$, an additional error has been introduced by the conversion

of one plate system to a standard system. The mean error in the transformation equation (20) is of the order of $\pm 0^m.03$ mag. The resulting uncertainty in relative magnitudes measured from one plate amounts to $\pm 0^m.07$. The number of measures for each star is given in the fourth column of Table 18.

TABLE 18

(Relative Monochromatic Magnitudes)

				λ	8000	7400	7000	6500	6000	5700
				$\frac{1}{\lambda}$	1.25	1.35	1.43	1.54	1.67	1.75

(Contd.

Ser. No.	Star	Sp. Type	(n)						
1	HD 190864	O6	1	-1.47					
2	190919	B1 Ib	1	-1.94					
3	190967	B1 Ib-II	1	-1.66					
4	191139	B0.5 II	2	-1.29					
5	191158		2	-1.93					
6	191201	B0 III	2	-1.86					
7	191225	A0 V	2	- .57	- .56	- .56			
8	191243	B5 Ib	1	-3.22					
9	191290		2	-1.69	-1.54	-1.59	-1.45		
10	191291		1	- .83					
11	191396	B0.5 II	1	-1.36					
12	191456	B0.5 III	3	-1.51	-1.51	-1.61	-1.85		
13	191611	B0.5 III	2	-1.11					
14	191612	O8	2	-1.30	-1.23	-1.37			
15	191703		2	-2.04					
16	191720	B9 V	2	-1.22					
17	191897		1				-1.82		
18	191917	B1 III	2	-1.36	-1.36	-1.34			
19	192003	B2 1V	2	- .41	- .36	- .37	- .36	-.39	-.41

λ	5500	5200	5000	4900	4500	4430	4220	4150	4035
$\frac{1}{\lambda}$	1.82	1.92	2.0	2.04	2.22	2.26	2.37	2.41	2.48

(Contd.)

Ser. No.									
1					-1.54	-1.05	-1.54	-1.63	-1.52
2					-2.04	-2.04			
3							-1.21		-1.05
4					-1.35	-1.42	-1.30	-1.38	-1.25
5					-2.48	-2.52	-2.37	-2.50	-2.36
6					-2.12	-2.16	-2.09	-2.18	-2.04
7					-1.01	-1.04	-1.03	-1.04	- .95
8									
9					-1.04	- .82	- .40	- .51	- .25
10					-1.51	-1.57	-1.51		-1.45
11									
12					-2.0	-2.04	-1.96	-2.06	-1.90
13					-1.00	- .97	- .94	- .94	- .88
14					-1.41	-1.38	-1.33	-1.40	-1.27
15					-2.18	-2.15	-2.05		-2.06
16					-1.78	-1.78	-1.73	-1.80	-1.74
17					-1.37	-1.18	- .87		
18					-1.62	-1.60	-1.54	-1.52	-1.50
19	-.33	-.36	-.42	-.47	- .51	- .51	- .49	- .49	- .50

λ	3930	3858	3820	3750	3670	3600	3540	3500	3440
$\frac{1}{\lambda}$	2.54	2.58	2.62	2.66	2.72	2.78	2.82	2.86	2.91
Ser. No.									
1	-1.60	-1.61	-1.67	-1.81	-1.79	-1.90	-1.91	-1.98	
2	-1.94	-1.93	-1.93	-2.05	-2.05	-2.19			
3	-1.14	- .98	-1.03	- .96	- .89				
4	-1.35	-1.27							
5	-2.0	-2.12							
6	-2.09	-2.08	-2.09	-2.18	-2.28	-2.36	-2.36	-2.33	-2.25
7	- .96	- .87	- .74	- .49					
8									
9	- .35	- .22							
10	-1.46			-1.68					
11									
12	-2.0	-1.99	-1.95	-2.08	-2.12	-2.06	-2.10	-2.14	
13	- .97	- .93	- .95	-1.09	-1.05	- .99	-1.02	-1.04	-1.05
14	-1.39	-1.37	-1.36	-1.35	-1.51	-1.51		-1.48	-1.51
15									
16	-1.72	-1.59	-1.49						
17									
18	-1.54	-1.55	-1.51	-1.56	-1.65	-1.65	-1.66	-1.71	
19	- .45	- .45	- .45	- .44	- .51	- .50	- .45	- .50	- .50

				λ 8000	7400	7000	6500	6000	5700
				$\frac{1}{\lambda}$ 1.25	1.35	1.43	1.54	1.67	1.75

(Contd.

Ser. No.	Star	Sp. Type	(n)						
20	192021		1	-2.66					
21	192078		1	-2.29	-2.22	-2.31			
22	192079	B2 III	2	- .73				-.66	-.66
23	192102		1	- .89	- .65	- .56			
24	192124		1	-1.90					
25	192182		1	-2.22	-2.26	-2.33			
26	192283	B9.5 V	2	- .79	- .73	- .56			
27	192303	B1 III	2	- .65	- .65	- .55		-.49	-.53
28	192321		1	-3.04					
29	192361		1	- .25	- .30	- .37	- .38	-.38	-.46
30	192422	B0.5 Ib	2	-2.29	-2.18	-2.21	-2.13	-2.07	-2.10
31	192445	B0.5 III	3	-1.64	-1.52				
32	192537	B8 V	1	- .12	- .17	- .25		-.12	-.11
33	192536		1						
34	192538		1	-2.27					
35	192556		1	-2.17	-2.08	-2.05			
36	192603		1	-2.11	-2.01	-2.02			
37	192604	B7 III	1	- .06					
38	192639	O8 f	2	-2.04	-1.92	-1.95	-1.75	-2.17	-2.14

	λ 5500	5200	5000	4900	4500	4430	4220	4150	4035 (Cont.
	1/λ 1.82	1.92	2.0	2.04	2.22	2.26	2.37	2.41	2.48
Ser. No.									
20									
21					- .69	- .45	- .13		
22	- .61	- .47	- .60	- .62	- .51	- .46	- .41	- .43	- .40
23					-1.33	-1.30			
24					-2.17	-2.22			-1.96
25					-1.52	-1.38	- .98	- .75	- .75
26					-1.12	-1.20	-1.18		-1.14
27	- .45	- .40	- .45	- .51	- .33	- .32	- .36	- .36	- .31
28					-2.99		-2.90		-2.72
29	- .47	- .48	- .66	- .67					
30	-2.06	-2.06	-2.04	-2.03	-1.93	-1.88	-1.85	-1.86	-1.71
31					-2.28	-2.40	-2.34	-2.44	-2.35
32	- .18	- .27	- .41	- .41	- .47	- .44	- .48		- .46
33					-1.28	-1.23	-1.17		-1.07
34									
35					- .50	- .30			
36									
37					- .29		- .43		- .35
38	-2.14	-2.05	-2.13	-2.11	-2.10	-2.06	-2.01	-2.04	-1.90

λ	3930	3858	3820	3750	3670	3600	3540	3500	3440
$\frac{1}{\lambda}$	2.54	2.58	2.62	2.66	2.72	2.78	2.82	2.86	2.91
Ser. No.									
20									
21									
22	- .40	- .38	- .42	- .49	- .49	- .43	- .45	- .47	- .29
23									
24		-1.71			-1.68				
25	- .05								
26	-1.17	- .92							
27	- .24	- .22	- .30	- .43	- .46	- .37	- .42	- .40	- .36
28	-2.34	-2.25	-2.04						
29									
30	-1.71	-1.71	-1.79	-1.85	-1.85	-1.81	-1.78	-1.83	-1.85
31	-2.38	-2.36	-2.34	-2.36	-2.50	-2.51	-2.54	-2.50	-2.50
32	- .46	- .34	- .30						
33									
34									
35									
36									
37	- .39	- .39	- .27						
38	-1.91	-1.95	-1.99	-2.06	-2.12	-2.19	-2.19		

				λ 8000	7400	7000	6500	6000	5700 (Contd
				1/λ 1.25	1.35	1.43	1.54	1.67	1.75
Ser. No.	Star	Sp. Type	(n)						
39	192660	B 0 Ia	1	-1.97	-1.95	-1.91	-1.82		
40	192744		1	-1.81					
41	192745		1	-1.03	- .85	- .78			
42	192766		2	-1.05	- .95	- .92	-1.23	-1.26	-1.28
43	192987		1	-2.21					
44	192988		1	-1.11	- .87	- .77			
45	192989		2	-2.24	-2.32				
46	192990		1	-1.75					
47	193007	B0.5 II	1	-1.56					
48	193032	B0 II	2	- .92	- .99	-1.03	- .96	-1.04	-1.01
49	193063		1					-1.37	-1.48
50	193064	B9	2	-1.20					
51	193076	B0.5 II	2	-1.66	-1.70	-1.69	-	-1.70	-1.73
52	193159		1	-1.69			-1.72	-1.91	-1.96
53	193183	B1.5 Ib	2	-2.36	-2.26	-2.26	-2.18	-2.35	-2.38
54	193184		1	-1.18	-1.05	- .79			
55	193204		1	-1.26	-1.22	-1.03			
56	193328		1	- .88				- .38	- .43
57	193344	B9	2	-1.29					

λ	5500	5200	5000	4900	4500	4430	4220	4150	4035 (Cont.
1/λ	1.82	1.92	2.0	2.04	2.22	2.26	2.37	2.41	2.48
Ser. No.									
39					-1.33	-1.39	-1.42		-1.21
40					-1.83	-1.78	-1.70		
41	-1.18	-1.24	-1.24	-1.29	-1.38	-1.35	-1.35		-1.37
42	-1.28	-1.24	-1.46	-1.43	-1.47	-1.46	-1.52	-1.55	-1.47
43									
44	- .57	- .46	- .53						
45	-1.64	-1.46	-1.02	- .73	- .67				
46	-2.54	-2.62	-2.51		-2.52		-2.40		
47	-1.54	-1.55	-1.43	-1.52	-1.50	-1.44	-1.44	-1.50	-1.52
48	- .96	- .89	- .98	- .93	- .79	- .82	- .90	- .81	- .77
49	-1.49	-1.52	-1.68	-1.70	-1.63	-1.79	-1.96		-1.88
50					-1.87	-1.89	-1.85		-1.88
51	-1.60	-1.53	-1.65	-	-1.62	-1.60	-1.55	-1.60	-1.60
52	-1.97	-2.00	-2.16	-2.17	-2.27				
53	-2.30	-2.21	-2.25	-2.33	-2.20	-2.14	-2.04	-2.02	-1.87
54					- .74	- .62	- .70		- .47
55					- .73	- .71	- .72		- .44
56	- .42	- .45	- .67	- .69	- .76	- .81	- .87		- .88
57					-1.87	-1.92	-1.87	-1.97	-1.90

λ	3930	3850	3820	3750	3670	3600	3540	3500	3440
$\frac{1}{\lambda}$	2.54	2.58	2.62	2.66	2.72	2.78	2.82	2.86	2.91
Ser. No.									
39	-1.16	-1.11	-1.15						
40									
41	-1.30								
42	-1.42	-1.36							
43									
44									
45									
46									
47									
48	- .78	- .79	- .88	- .92	-1.07	- .98			
49									
50	-1.86	-1.84							
51	-1.59	-1.55	-1.50	-1.60	-1.59	-1.55	-1.60	-1.58	-1.57
52									
53	-1.94	-1.87	-1.87	-1.93	-1.93	-1.78	-1.77	-1.80	-1.80
54	- .17								
55		- .27							
56	- .88								
57	-1.92	-1.88	-1.89						

				λ	8000	7400	7000	6500	6000	5700
				$\frac{1}{\lambda}$	1.25	1.35	1.43	1.54	1.67	1.75
Ser. No.	Star	Sp. Type	(n)							
58	193369		1		-1.39	-1.44	-1.25			
59	193426	B9 Ia	1		-1.57	-1.38	-1.24	-1.15	-1.03	- .94
60	193443	09 III			-2.04	-1.91	-1.93		-2.08	-2.08
61	193487		1		-1.78	-1.63	-1.84			
62	193537	B9.5 IV			- .47	- .22	- .02		- .31	- .41
63	193550				-2.13	-2.08	-2.15	-1.91		
64	193576	B2: II			-1.20	-1.11	- .96		- .86	- .78
65	193595	07	2		- .65	- .65	- .59	- .48	- .62	- .61
66	193611	B0 Vp			-1.06	-1.0	- .84		- .78	- .77
67	193612	Ao III			- .30	- .31	- .16		- .43	- .56
68	193621		1		-2.20					
69	193634	B3 III			-1.76				-1.87	-1.92
70	193636		1		-1.20					
71	193681		1		- .66					
72	193682	05			-1.0	- .99	-1.05		-1.06	- .93
73	193794	B0 V	2		- .83	- .71	- .67	- .58	- .42	- .39
74	193889		1		- .62	- .82	- .72	- .65	- .66	- .71
75	193890	B9.5 V			- .32	- .23	- .15	- .22	- .37	- .46
76	193908				-1.12	- .98	-1.02	-1.01	-1.22	-1.21
77										

(Cont.)

λ	5500	5200	5000	4900	4500	4430	4220	4150	4035
$\frac{1}{\lambda}$	1.82	1.92	2.0	2.04	2.22	2.26	2.37	2.41	2.48
Ser. No.									
58									
59	- .75				- .54	- .54	- .47		
60	-2.02	-1.88	-2.03	-2.03	-1.98	-1.90	-1.86	-1.88	-1.90
61					-1.87	-1.83	-1.68	-1.76	-1.62
62	- .41	- .47	- .45	- .45	- .75	- .77	- .78	- .72	- .72
63					-1.28	-1.11	- .70	- .75	- .54
64	- .75	- .58	- .62	- .61	- .39	- .36	- .33	- .25	- .10
65	- .57	- .57	- .52	- .56	- .37	- .36	- .41		- .24
66	- .68	- .53	- .60	- .59	- .33	- .30	- .31	- .30	- .11
67	- .53	- .51	- .79	- .82	- .86	- .82	- .89	- .93	- .83
68					-3.05	-3.06	-3.00	-3.13	-3.17
69	-1.87	-1.80	-1.94	-2.02	-1.91	-1.88	-1.82	-1.95	-1.82
70					-1.92	-1.97	-1.82		-1.87
71									
72	- .90	- .78	- .80	- .77	- .65	- .56	- .55	- .46	- .37
73	- .28	- .11	- .11	- .01	.04	.21	.13	.31	.32
74	- .62	- .51	- .67	- .66	- .56	- .63	- .44		- .38
75	- .44	- .51	- .71	- .71	- .37	- .42	- .53	- .62	- .66
76	-1.22	-1.26	-1.36	-1.44					

λ	3930	3850	3820	3750	3670	3600	3540	3500	3440
1/λ	2.54	2.58	2.62	2.66	2.72	2.78	2.82	2.86	2.91
Ser. No.									
58									
59	- .21	- .21	- .29	- .29	- .11	.23	.30	.31	.45
60	-1.83	-1.83	-1.79	-1.90	-1.91	-1.88	-1.90	-1.88	-1.90
61		-1.44	-1.29		-1.30				
62	- .69	- .63	- .51	- .09	.05	.06	.10	.15	.16
63	- .05			- .44					
64	- .15	- .14	- .20	- .23	- .13	- .15	- .11	- .14	- .12
65	- .30	- .32	- .40	- .51	- .56	- .54	- .48	- .49	- .46
66	- .12	- .13	- .20	- .27	- .28	- .28	- .19	- .18	- .20
67	- .88	- .85	- .83	- .76	- .63	- .62	- .52	- .44	- .43
68		-2.91							
69	-1.74	-1.76	-1.70	-1.71	-1.59				
70		-1.84							
71									
72	- .38	- .43	- .57	- .66	- .69	- .63	- .60	- .53	- .43
73	.37	.26	.19	.21	.23	.20	.29	.37	
74									
75	- .61	- .57	- .51	- .23	- .07	- .06	- .03	- .01	- .01
76									

Ser. No.	Star	Sp. Type	(n)	λ 8000	7400	7000	6500	6000	5700 (Cont'd)
				1/λ 1.25	1.35	1.43	1.54	1.67	1.75
77	193945	B0 Vm	2	-1.45	-1.35			- .96	- .90
78	193984	A0 V		- .05	- .05	- .03	- .01	- .55	- .43
79	194008			- .10	- .17			- .01	- .01
80	194092	B0.5III	2	- .84	- .79	- .73	- .81	- .98	- .97
81	194094	09 III	2	- .63	- .55	- .45	- .32	- .40	- .33
82	194194	B2 III	1						
83	194205		1	- .59	- .57	- .50	- .39	- .28	- .30
84	194279					-2.97			
85	194334	07.5 V	1					- .93	- .74
86	194649	06.5	1	(-1.15)	-1.05	-1.02	- .64		
87	194779		2	-1.51	-1.42	-1.32		-1.47	-1.48
88	194839	B0.5 Ia	2	-2.62	-2.58	-2.37		-2.01	-1.93
89	195150		2	- .79	- .81			-1.07	-1.11
90	195213	07	2	-1.24	-1.11	-1.01		- .73	- .74
91	195230		2						
92	195339		2						
93	227545		2	- .31					
94	227670		1	.20					
95	227689	B9.5 V	1	.50	.43	.35	.39		

Å	5500	5200	5000	4900	4500	4430	4220	4150	4035
ν	1.82	1.92	2.0	2.04	2.22	2.26	2.37	2.41	2.48

(Cont.)

Ser. No.									
77	- .85	- .71			- .48	- .38	- .38	- .37	- .21
78	- .31	.01	.11	.22	- .33	- .37	- .43	- .32	- .41
79	- .05	- .08	- .24	- .39		- .49	- .41		- .43
80	- .95	- .96	-1.06		-1.06	-1.17	-1.19	-1.29	-1.29
81	- .25	- .23	- .13	- .16	- .11	.12	.13		.28
82						.59	.70	.70	.73
83	- .20	- .07	- .09	- .12	.02	.04	.12	.13	.20
84					-1.13	-1.28	-1.23	-1.34	-1.29
85	- .51	- .35	- .37	- .31	- .05	- .03	.06	.11	.25
86			- .19	- .22	.27	.30	.32		.43
87	-1.46	-1.39	-1.45		-1.11	-1.16	-1.30	-1.38	-1.46
88	-1.82	-1.61	-1.56		-1.33	-1.24	-1.02	-1.09	- .82
89	-1.16	-1.20	-1.34	-1.38			-1.36		-1.63
90	- .61	- .58	- .49	- .41	.02	.20	.26		.49
91						-1.30	-1.41		-1.64
92							- .53		- .83
93									
94									
95					.38	.33	.40	.35	.36

λ	3930	3850	3820	3750	3670	3600	3540	3500	3440
$\frac{1}{\lambda}$	2.54	2.58	2.62	2.66	2.72	2.78	2.82	2.86	2.91
Ser. No.									
77	- .16	- .11	- .17	- .30	- .02	- .10	.09		.12
78	- .39	- .28	- .23	.07	.17	.17	.14	- .07	.10
79	- .41	- .17	- .21						
80	-1.27	-1.23	-1.29	-1.48					
81	.26	.27	.19	.16	.15				
82	.81	.82	.85	.81	.67	.65	.67	.70	.67
83	.18	.25	.21	.22	.23	.24	.32	.33	.29
84	-1.25	-1.19	-1.31						
85	.33	.35	.28	.22	.24	.28	.41	.35	.52
86	.57	.50	.49	.33	.25	.28	.34	.39	.40
87	-1.41	-1.46							
88	- .87	- .75	- .78	- .87	- .89	- .68	- .67		
89									
90	.49	.48	.39	.31	.31				
91	-1.35	-1.10							
92	- .61	- .49							
93									
94									
95	.48	.61	.71	.88	.89				

				λ 8000	7400	7000	6500	6000	5700 (Contd
				$\frac{1}{\lambda}$ 1.25	1.35	1.43	1.54	1.67	1.75
Ser. No.	Star	Sp. Type	(n)						
96	227691		1	-1.05					
97	227696		1	-2.18					
98	227708		1	- .80					
99	227739		1	- .52					
100	227749	B8 V	1	.18	.25	.19	.13		
101	227764		1	.10					
102	227791		1	- .69					
103	227818	B3 III	2	.46	.42	.31	.23		
104	227846		1	- .62					
105	227902	B1 V	2	.10	.08	.08	.06	.12	.04
106	227912		1	- .87	- .67	- .32			
107	227958	B8 V	1	.41				.39	.40
108	227966		1	- .09	.06	.01	.11		
109	227977	B2 III	2	.25	.26	.16	.26	.21	.19
110	227990		2	.29	.40	.34	.24		
111	228018		1	.61	.59	.47			
112	228019		1	- .91					
113	228068		2	.79	.73	.61			
114	228069	Ao V	1	- .45	- .15	- .18			

λ	5500	5200	5000	4900	4500	4430	4220	4150	4035
$\frac{1}{\lambda}$	1.82	1.92	2.0	2.04	2.22	2.26	2.37	2.41	2.48

(Con

Ser. No.									
96									
97							-2.63	-2.66	-2.52
98									
99									
100					- .05	- .09	- .08	- .08	- .07
101									
102									
103					.32	.47	.46	.43	.45
104	.06	.05	.04	.03	.01	.02	.06	.07	.13
105									
106									
107	.45	.27	.24		.52	.51	.48	.49	.50
108					.26	.27	.47	.38	.57
109	.20				.38	.41	.44	.35	.42
110					.17	.13	.21	.16	.25
111					.68	.64	.71	.56	.75
112									
113					.87	.85	.84	.84	.84
114					- .45		- .45		- .20

λ	3930	3858	3820	3750	3670	3600	3540	3500	3440
$\frac{1}{\lambda}$	2.54	2.58	2.62	2.66	2.72	2.78	2.82	2.86	2.91
Ser. No.									
96									
97	-2.42								
98									
99									
100	- .08	0	.12						
101									
102									
103	.34	.37	.27	.30	.33	.31	.30	.35	
104	.07	.06	.06	.08	.06	.07	.05	.03	.10
105									
106									
107	.57	.64	.78	1.02					
108	.77	.67	.73	.52	.56	.58			
109	.42	.42	.37						
110	.30	.41	.50	.61	.69	.62			
111	.82	.92	1.01	1.05	1.20				
112									
113	1.0								
114									

Ser. No.	Star	Sp. Type	(n)	λ 8000	7400	7000	6500	6000	5700 (Cont
				1/λ 1.25	1.35	1.43	1.54	1.67	1.75
115	228114	B8 IV	2	- .34	- .27	- .29	- .24	- .34	- .41
116	228128	B8 IV	2	-1.22					
117	228140	Ao V	2	.18	.13	.09			.15
118	228163	Ao IV	2	.22	.21	.15	.13	.16	
119	228171	B9 V	2	- .07	- .11	- .04	- .07	- .15	- .12
120	228187		2	.32	.34	.38	.33	.37	.30
121	228188		1	-1.22	-1.57	-1.58			
122	228199	B0.5 V	2	- .05	- .22	- .15	- .12	.12	.06
123	228206	B9.5 V	2	.69	.64	.57		.60	.55
124	228214		1	.82	.76				
125	228243	A5 IV	2	.16	.18	.16	.19	.35	.30
126	228244		1	- .56					
127	228263	B IV	2	.09	.10	.08	.04	.16	.19
128	228290		2	- .06	- .05	.01	.02		
129	228293	B6 III	2	.57	.48	.45	.41		
130	228304		1	-1.81	-1.57	-1.64			
131	228324		1	.12	.17	.23	.24		
132	228326	B2 IV	2	.03	.05	.01	- .07	.16	.19
133	228437	B2 II	2	-.39	- .38	- .36			

λ	5500	5200	5000	4900	4500	4430	4220	4150	4035 (Con
$\frac{1}{\lambda}$	1.82	1.92	2.0	2.04	2.22	2.26	2.37	2.41	2.48
Ser. No.									
115	- .37	- .35	- .38	- .42	- .41	- .38	- .46	- .45	- .40
116									
117	.15	.12	.13	.11	.14	.12	.18	.16	.17
118	.12	.01	- .08	- .11	- .06	- .06	- .10	- .07	- .07
119	- .15	- .13	- .28	- .34	- .32	- .29	- .36	- .37	- .32
120	.28	.16	.14	.34	.30	.27	.25	.31	.34
121									
122	.05	- .03	- .08	- .15	- .08	- .12	- .15	- .17	- .08
123	.52	.35	.31		.79	.76	.78	.78	.78
124					.83	.80	.82	.76	.76
125	.35	.29	.19		.38	.36	.37	.22	.44
126									
127	.17	.12	.11	.13	.06	.11	.14	.07	.15
128					.21	.18	.26	.18	.32
129					.70	.69	.72	.66	.65
130					- .70	- .74	- .40	- .42	- .44
131					.30	.32	.36	.33	.42
132	.16	.09	.09	.06	.19	.16	.21	.23	.24
133					.11	.15	.21		

λ	3930	3858	3820	3750	3670	3600	3540	3500	3440
$\frac{1}{\lambda}$	2.54	2.58	2.62	2.66	2.72	2.78	2.82	2.86	2.91
Ser. No.									
115	- .42	- .38	- .40						
116									
117	.25	.35	.46	.75					
118	- .02	.06	.20	.45	.74	.70	.69	.71	.61
119		- .28	- .31						
120		.30	.30	.27	.31				
121									
122	- .10	- .10	- .09	- .26	- .23	- .26	- .24	- .24	- .26
123	.93	.96	1.05						
124	.81	.80	.85						
125	.66	.66	.74	.70	.62	.71			
126									
127	.13	.11	.13	.04	- .11	- .05	- .12	.02	- .07
128	.18	.27	.32	.13	.14	.12			
129	.62	.63	.63	.52	.48	.50	.52		
130									
131	.73	.62	.71	.76					
132	.21	.17	.20	.14	.04	.10	.12	.21	.24
133									

Ser. No.	Star	Sp. Type	(n)	λ 8000	7400	7000	6500	6000	5700
				$\frac{1}{\lambda}$ 1.25	1.35	1.43	1.54	1.67	1.75 (contd.)
134	228356		1	- .78	- .66	- .49			
135	228403	A7 III	2	- .46	- .42	- .49	- .55		
136	228413		1	-1.46					
137	228416		1	-1.37					
138	228438	B0.5 IV	2	- .95	- .67	- .60			
139	224839		1	-1.01					
140	228450	B0.5 p	1	- .26					
141	228456	B2 IV	2	.46	.42	.25	.29	.37	.41
142	228461	B1 II	1	- .15	- .15	- .13		- .12	
143	228462		1	- .38	- .45	- .33		.02	.06
144	228474		2	.02	.06	.02	.04		
145	228481		2	0	- .02	- .02		.15	.18
146	228483	B9 V	2	- .06	- .03	.03	.08	.03	.04
147	228490		2	- .02	.03	.03	.03	.16	.19
148	228519		2	- .03	.04	.06	.01		- .11
149	228521	B9	2	.66	.62	.55			
150	228533		1	- .22	- .30	- .23	- .08	.02	
151	228587	B1 II	2	- .01	.13	.46		.53	
152	228558		1	.45	.44	.39	.29		

λ	5500	5200	5000	4900	4500	4430	4220	4150	4035
$\frac{1}{\lambda}$	1.82	1.92	2.0	2.04	2.22	2.26	2.37	2.41	2.48

(Contd.)

Ser. No.									
134					.11	.15	.21		
135					- .28	- .23	- .30		- .08
136									
137									
138					- .46	- .46	- .50	- .51	- .36
139									
140									
141	.35	.28	.42	.46	.62	.62	.68	.69	.63
142			.11		.34	.38	.42	.44	.47
143	.15				.64	.77	1.04	1.05	1.09
144					.29	.27	.36	.31	.44
145	.17	.14	.10	.06	.16	.21	.31	.35	.34
146	.12	.12	.11	.09	.34	.37	.46	.38	.52
147	.11	.08	.04		.15	.12	.20	.12	.22
148	- .10	- .04	- .14	- .14	- .12	.10	.16	.10	.16
149					.38	.34	.29	.28	.32
150	.12		.11						
151	.56	.70			1.41	1.38	1.26	1.50	
152					.28	.19	.29	.20	

λ	3930	3858	3820	3750	3670	3600	3540	3500	3440
$\frac{1}{\lambda}$	2.54	2.58	2.62	2.66	2.72	2.78	2.82	2.86	2.91
Ser. No.									
134									
135	.18	.07	.12	.08	.24	.13			
136									
137									
138	- .35	- .49	- .44	- .52	- .59	- .55			
139									
140									
141	.67	.58	.44						
142	.44	.36	.30	.25	.25	.30	.38		
143	1.46	1.60	1.49						
144	.40	.42	.39						
145	.60	.52	.57	.56	.65	.67			
146									
147	.19	.24	.33						
148	.12	.15	.19	.12	.15	.15	.14		
149	.37	.52	.65						
150									
151	1.58	1.66	1.67	1.52	1.49	1.64	1.62	(1.	
152	.34	.35	.49	.60	.53	.55			

			λ	8000	7400	7000	6500	6000	5700 (Contd
			$\frac{1}{\lambda}$	1.25	1.35	1.43	1.54	1.67	1.75
Ser. No.	Star	Sp. Type	(n)						
153	228602		2	.06	.10	.11	.20		
154	228603		1						
155	228608		1	- .31					
156	228623		1	.81	.74				
157	228690	B0.5 V	2	- .27	- .06			.07	0
158	228705		1	.35				.55	.59
159	228715		1	-1.47	-1.49	-1.31			
160	228722		1	-1.34	-1.35	-1.07			
161	228766	06f/WR	2	- .77	- .69	- .51			- .27
162	228807		1	- .25	- .30	- .33			
163	228828		1	.12	.10	.17	.16		
164	228835		1	- .24	- .32	- .20	- .08		
165	228841	O 7.5p	2	.65	- .59	- .49	- .34	- .42	- .41
166	228845		1	- .14	- .10				
167	228854	08	2	-1.24	-1.12	- .92		- .62	- .63
168	228860	B0.5 IV	2	- .18	- .10				
169	228882	B0.5 Ia	2	-1.27	- .99	- .91	- .71		
170	228905		1	.44	.52	.49	.48		
171	228906		1	.90					

λ	5500	5200	5000	4900	4500	4430	4220	4150	4035
$\frac{1}{\lambda}$	1.82	1.92	2.0	2.04	2.22	2.26	2.37	2.41	2.48 (contd)
Ser. No.									
153					.90	.94	1.02	1.01	1.07
154					.07	.15	.0		
155									
156						.97	1.04	.99	1.03
157	- .03	0	.04	- .07	- .05	.15	.13	.23	.16
158	.67	.47	.36		.31	.29	.30		.31
159					- .38	- .08	.22		
160					- .70	- .57	- .52		- .25
161	- .20	- .22	- .02	0	.37	.42	.35		.59
162									
163					.26	.24	.32	.32	.38
164					.27	.26	.50	.36	.62
165	- .34	- .35	- .26	- .31	- .02	- .05	- .01		.15
166					- .09	- .04			
167	- .59	- .43	- .35	- .36	- .06	0	.03		.19
168					.79	.80	.92	.87	.99
169	- .16	- .11	.16	.14	.67	.75	.97		1.13
170					1.07				
171						.79	.84	.77	.80

λ	3930	3858	3820	3750	3670	3600	3540	3500	3440
1/λ	2.54	2.58	2.62	2.66	2.72	2.78	2.82	2.86	2.91
Ser. No.									
153	1.04	1.05	1.14						
154									
155									
156	1.01	1.27	1.29						
157	.12	.22	.11	.12					
158									
159									
160									
161	.55	.54	.40		.42				
162									
163	.29								
164	.96	.83	.94						
165	.12	.10	.04	- .06	- .05				
166									
167	.22	.21	.15	.08	.14	.08	.15		
168	.97	.96	.87	.81	.89				
169		1.24	1.08	1.04	1.11				
170									
171	.82	.88							

				λ 8000	7400	7000	6500	6000	5700 (Contd)
				1/λ 1.25	1.35	1.43	1.54	1.67	1.75
Ser. No.	Star	Sp. Type	(n)						
172	228919	B1 IV	2	- .25	- .10	- .07		.22	
173	228920		1	.72	.74				
174	228928	B2 Ip^{nn}	2	- .48	- .29	- .26	- .08	.09	.27
175	228929	B0.5 Ib	2	- .88	- .73	- .62	- .43		
176	228932		1	.52	.41	.37			
177	229040		1	.13					
178	228941		2	- .55	- .49	- .49	- .43		
179	228943	B0 II:	2	- .78	- .66	- .51		- .19	- .18
180	228969		2	- .42	- .34	- .32		- .02	.02
181	228979		1	.68	.60				
182	228989	09 Vnn	2	- .27	- .11	- .11	- .17	.15	.21
183	228997		1	- .10				- .08	- .16
184	229021		1	- .27	- .35	- .37	- .25	- .19	- .25
185	229027		1	.25				.36	.25
186	229033	B0 II-III	2	-1.05	- .97	- .76			- .61
187	229042		2	.26	.30	.29	.31		
188	229069		1	- .10	.01	.03	.13		
189	229096		1	.29	.36	.31	.35		
190	229108	B0.5 Ib	2	- .67	- .74	- .58		- .05	- .07

λ	5500	5200	5000	4900	4500	4430	4220	4150	4035 (Cont
$\frac{1}{\lambda}$	1.82	1.92	2.0	2.04	2.22	2.26	2.37	2.41	2.48
Ser. No.									
172	.35	.38	.46	.44	.62	.63	.71	.76	.82
173					1.03				
174	.34	.40	.55	.54	.87	1.01	1.15		1.36
175	.14	.26	.39	.38	1.0	1.16	1.23	1.18	1.40
176					.78	.81	.78	.84	.84
177									
178									
179	- .10	.17	.11		.56	.51	.72		.74
180	.05				.41		.88		.78
181						1.11	1.24	1.17	1.28
182	.33	.25	.46	.40	.97		.94		1.20
183	- .19	- .18	- .39	- .35		- .45	- .44		- .52
184	- .19	- .16	- .26	- .29	- .10	- .16	- .02	- .03	.06
185	.32	.29	.17		.07	.03	- .02		
186	- .48	- .27	- .31	- .34	.02	.02	.04	- .07	.13
187					.40	.43	.44	.54	.49
188					.95	.97	1.11	1.10	1.21
189					1.06	1.04	1.20	1.06	1.26
190	.08	.28	.40		.59	.72	.81	.87	.88

λ	3930	3858	3820	3750	3670	3600	3540	3500	3440
$\frac{1}{\lambda}$	2.54	2.58	2.62	2.66	2.72	2.78	2.82	2.86	2.91

cont

Ser. No.									
172	.89	.92	.77	.86	.84	.81	.82	.95	
173									
174	1.25	1.24							
175	1.42	1.42	1.44	1.28	1.28				
176	.78	.78							
177									
178									
179		.92		.84	.90	.96	1.04		
180	.71	.72	.73						
181									
182	1.19	1.27	1.13						
183	- .47	- .45	- .42						
184	.23	.24	.34	.26	.52	.56			
185									
186	.34	.34	.28	.18	.13	.19	.26	.27	.35
187	.66	.89	.81	.87	.74	.84	.85		
188	1.17	1.20	1.18	.94	.98	1.10			
189	1.24	1.24	1.26	.94	1.11				
190	.95								

				λ 8000	7400	7000	6500	6000	5700 (Cont
				1/λ 1.25	1.35	1.43	1.54	1.67	1.75
Ser. No.	Star	Sp. Type	(n)						
191	229119		1	- .91	- .79	- .77	- .74		
192	229151		1	.16				.42	.36
193	229196		2	-1.71	-1.63	-1.36			
194	229202	08 V	2	- .65	- .46	- .47	.12	- .02	.04
195	229232	05 f	1	- .49	- .39	- .35	- .10	- .02	- .01
196	229237		1	.08					
197	229245		1	- .83	- .69	- .74	- .63		
198	BD 35°3994		1	-1.73					
199	36°3894		1	.73	.64	.64	.52		
200	36°3950		1	- .07	.03	.01	.01		
201	36°3957		1	- .09	- .08	- .05	- .10		
202	36°3965		1	.46					
203	36°4000	B0.5 Ia	2	- .41	- .39	- .19		.12	.14
204	36°4004	B0.5 III	2	- .22	- .24	- .28	- .08	.09	.13
205	36°4007		1	-1.35	-1.32	-1.18			
206	37°3782		1	- .29	- .28	- .23	- .17		
207	38°4002		2	- .44	- .43	- .40		- .18	- .14
208	38°4004	B1 V	1					.66	.67
209	38°4054	B1 III	1						

λ	5500	5200	5000	4900	4500	4430	4220	4150	4035 (Cont
$\frac{1}{\lambda}$	1.82	1.92	2.0	2.04	2.22	2.26	2.37	2.41	2.48
Ser. No.									
191									
192	.44	.30	.28						
193									
194		.40	.29	.45	.74	.79	.91		.99
195	.16	.18	.29	.30	.64	.78	.78		1.08
196									
197									
198						-2.02	-1.89	-1.93	-1.81
199					.66	.66	.72	.69	.79
200					.10	.12	.23	.22	.33
201									
202									
203	.17	.58	.42		.91	.97	1.01	1.0	1.02
204	.21	.29	.46	.56	1.11	1.02	1.02	1.02	1.18
205					- .15	0	.22		
206					.33	.44	.77	.69	.91
207	- .18				0	.05	.07		.14
208	.67	.67	.54	.63	.97	.98	1.01	.99	1.07
209					.63	.62	.58	.62	.61

λ	3930	3858	3820	3750	3670	3600	3540	3500	3440
$\frac{1}{\lambda}$	2.54	2.58	2.62	2.66	2.72	2.78	2.82	2.86	2.91
Ser. No.									
191									
192									
193									
194	1.09	1.10	1.17		1.05	1.04	.97		
195	1.01	1.07	.90	.80	.84	.87	.86		
196									
197									
198	-1.84	-1.84	-1.81	-1.90	-2.02	-2.05	-1.98	-2.03	
199	.72	.83	.78	.77	.88	.73			
200	.50	.50	.53	.54	.64	.60			
201									
202									
203	1.10	1.19	1.18	1.21	1.08	1.24	1.28	1.20	
204	1.23	1.23	1.07	1.08	1.09	1.08			
205									
206									
207	.14	.16	.12	.12					
208	1.13	1.06	1.09	.97	.92				
209	.71	.75	.85	1.04	1.05				

Ser. No.	Star	Sp. Type	(n)	λ 8000	7400	7000	6500	6000	5700 (Contd
				$\frac{1}{\lambda}$ 1.25	1.35	1.43	1.54	1.67	1.75
210	BD38°4098	B9 Ib	1					- .56	
211	39°4117	B1 II	2	- .41	- .13	- .11			.40
212	40°4185	Bo V:	2	- .40	- .14			.29	.35
213	40°4212	09	2	-1.08	- .69	- .51			
214	40°4219	08	2	- .37	- .31				
215	40°4220	07f	1	-1.79					
216	40°4227	06f	2	-1.85	-1.62	-1.42			- .73
217	41°3804	09.5 Ia	2	-1.09	- .94	- .60			
218	41°3807	06f	1	- .90					

λ	5500	5200	5000	4900	4500	4430	4220	4150	4035
1/λ	1.82	1.92	2.0	2.04	2.22	2.36	2.37	2.41	2.48 (contd)
Ser. No.									
210		- .04			.13	.18	.37	.31	.49
211	.58	.55	.65		1.12	1.23	1.29	1.30	1.33
212	.49	.47	.58	.73	.91	1.03	1.10	1.14	1.23
213					1.90	2.10	2.30		2.44
214					1.30	1.37	1.51		1.70
215					.73	.84	1.27	1.25	1.41
216	-.66	- .45			.32	.52	.57		.70
217					1.34	1.39	1.36		1.56
218					1.52	1.68	1.83	1.85	2.00

λ	3930	3858	3820	3750	3670	3600	3540	3500	3440
1/λ	2.54	2.58	2.62	2.66	2.72	2.76	2.82	2.86	2.91
Ser. No.									
210	.62	.69	.67	.70	1.12				
211	1.37	1.46	1.38	1.35					
212	1.25	1.29	1.27	1.29	1.14				
213									
214	1.79	1.74	1.76	1.69					
215	1.61	1.63							
216	.82	.85	.82	.78	.71		1.07		
217									
218									